

ornl

ORNL/Sub/91-SG341/1

**OAK RIDGE
NATIONAL
LABORATORY**

MARTIN MARIETTA

**HIGH TEMPERATURE
HEXOLOY™ SX
SILICON CARBIDE**

FINAL REPORT

G. V. Srinivasan
S. K. Lau
R. S. Storm

CERAMIC TECHNOLOGY PROJECT

MANAGED BY
MARTIN MARIETTA ENERGY SYSTEMS, INC.
FOR THE UNITED STATES
DEPARTMENT OF ENERGY

DISTRIBUTION OF THIS DOCUMENT IS UNLIMITED

This report has been reproduced directly from the best available copy.

Available to DOE and DOE contractors from the Office of Scientific and Technical Information, P.O. Box 62, Oak Ridge, TN 37831; prices available from (615) 576-8401, FTS 626-8401.

Available to the public from the National Technical Information Service, U.S. Department of Commerce, 5285 Port Royal Rd., Springfield, VA 22161.

This report was prepared as an account of work sponsored by an agency of the United States Government. Neither the United States Government nor any agency thereof, nor any of their employees, makes any warranty, express or implied, or assumes any legal liability or responsibility for the accuracy, completeness, or usefulness of any information, apparatus, product, or process disclosed, or represents that its use would not infringe privately owned rights. Reference herein to any specific commercial product, process, or service by trade name, trademark, manufacturer, or otherwise, does not necessarily constitute or imply its endorsement, recommendation, or favoring by the United States Government or any agency thereof. The views and opinions of authors expressed herein do not necessarily state or reflect those of the United States Government or any agency thereof.

DISCLAIMER

Portions of this document may be illegible in electronic image products. Images are produced from the best available original document.

HIGH TEMPERATURE HEXOLOY™ SX SILICON CARBIDE

G. V. Srinivasan
S. K. Lau
R. S. Storm

Date Published-September 1994

FINAL REPORT

Prepared by The Carborundum Company
Niagara Falls, New York

Funded by
Propulsion System Materials Program
Office of Transportation Technologies
the Assistant Secretary for Energy Efficiency and Renewable Energy
U.S. Department of Energy
EE 51 01 00 0

Subcontract No. 62X-SG341C

for
OAK RIDGE NATIONAL LABORATORY
Oak Ridge, Tennessee 37831
managed by
MARTIN MARIETTA ENERGY SYSTEMS, INC.
for the
U.S. DEPARTMENT OF ENERGY
under Contract DE-AC05-84OR21400

MASTER

1000

ABSTRACT

HEXOLOY®¹ SX-SiC, fabricated with Y and Al containing compounds as sintering aids, has been shown to possess significantly improved strength and toughness over HEXOLOY® SA-SiC. This study was undertaken to establish and benchmark the complete mechanical property database of a first generation material, followed by a process optimization task to further improve the properties. Detailed mechanical characterizations were then conducted on the optimized material.

Mechanical characterization on the first generation material indicated that silicon-rich pools, presumably formed as a reaction product during sintering, controlled the strength from room temperature to 1232°C. At 1370°C in air, the material was failing due to a glass-phase formation at the surface. This glass-phase formation was attributed to the reaction of yttrium aluminates, which exist as a second phase in the material, with the ambient. This process was determined to be a time-dependent one that leads to slow crack growth. Fatigue experiments clearly indicated that the slow crack growth driven by the reaction occurred only at temperatures >1300°C, above the melting point of the glass phase. Experimental results also revealed that this material possesses excellent creep resistance, though the creep mechanism is not yet well understood.

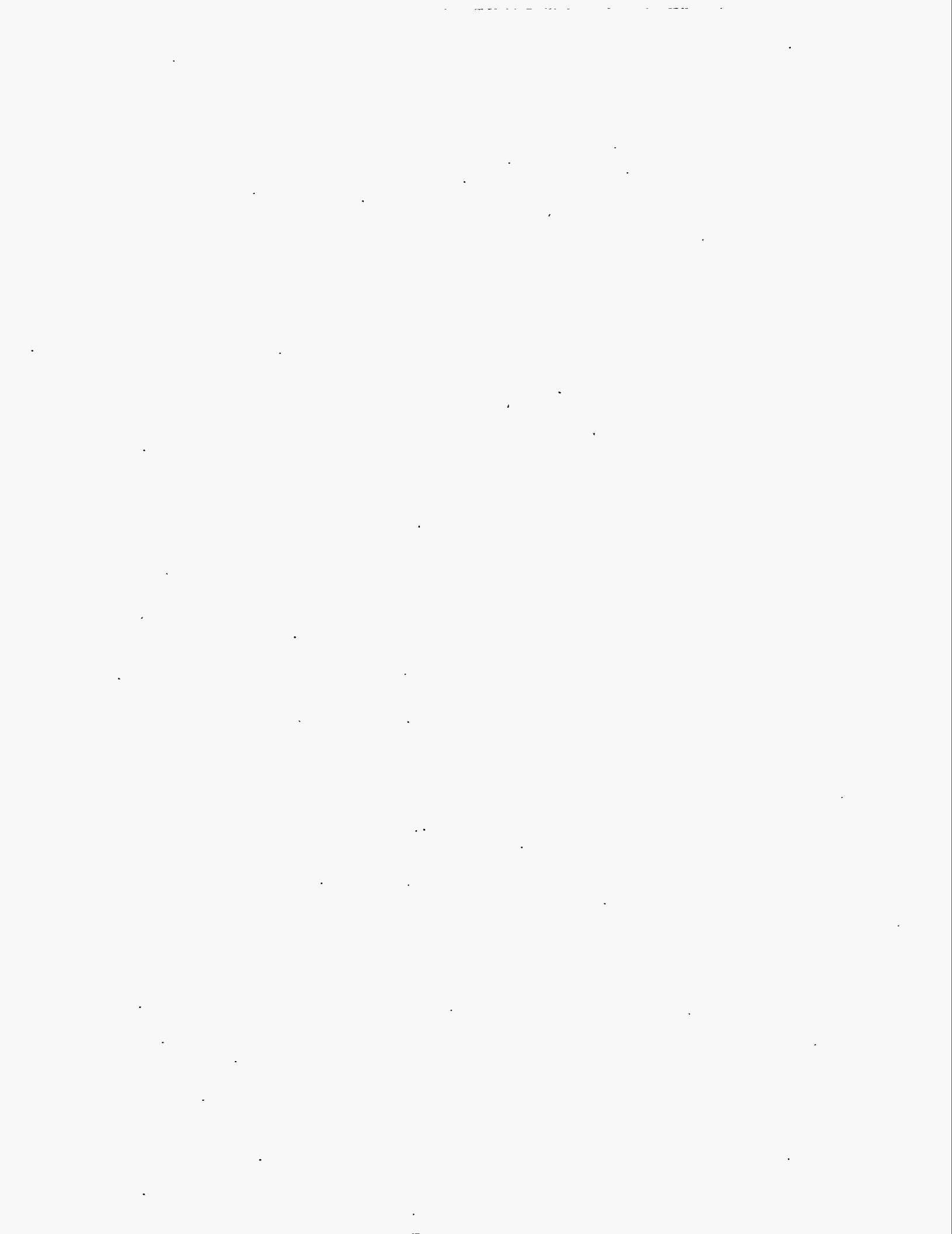
Process optimization tasks conducted included the selection of the best SiC powder source, studies on mixing/milling conditions for SiC powder with the sintering aids, and a designed experiment involving a range of sintering and post-treatment conditions. During the course of the mixing/milling study it was found that the turbomilling process provided the best room-temperature strengths ever achieved (>1 GPa) when conducted on a small batch of powders. It was, however, found that more development was needed to effectively translate the milling conditions to a larger batch.

The optimization study conducted on the densification variables indicated that lower sintering temperatures and higher post-treatment pressures reduce the Si-rich pool formation, thereby improving the room-temperature strength. In addition, it was also determined that furnacing configuration and atmosphere were critical in controlling the Si-rich formation.

¹HEXOLOY is a trademark of The Carborundum Company registered in the U.S. Patent & Trademark Office.

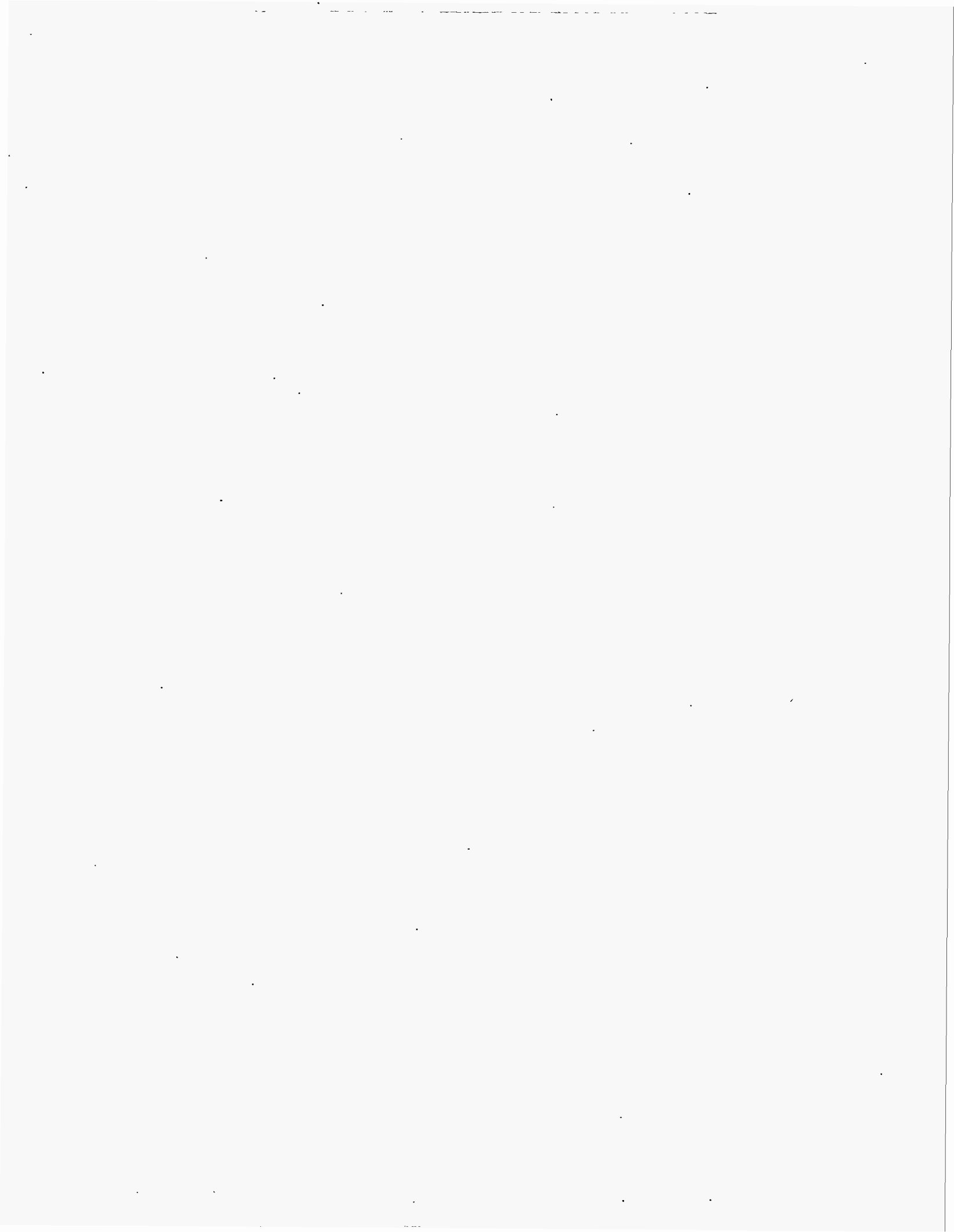
TABLE OF CONTENTS

	<u>Page</u>
Abstract	iii
Table of Contents	v
List of Tables	vii
List of Figures	ix
Introduction	1
Scope & Objective	1
Task 1: Complete Characterization of First Generation SX-SiC Material	3
Task 2: SiC Powder Selection	34
Task 3: Development of an Improved Dispersion Process	39
Task 4: Optimize the Current SX-G1 SiC Material Through an Experimental Design Methodology	42
Task 5a: Further Optimization of SX-G1	53
Task 5b: Complete Characterization of Optimized SX-G1 Composition	58
Summary	61
Conclusions	62
Acknowledgments	63
References	64



LIST OF TABLES

	<u>Page</u>
1. Flexure Test Data and Tension Test Data	20
2. Sintering Characteristics of Various SiC Powders	35
3. Mechanical Properties of SX-G1 Material Fabricated with Various SiC Powders	38
4. Turbomilling Results	41
5. Density and Mechanical Properties Determined at Specific Densification Conditions in the Experimental Design Matrix	45
6. Density and Mechanical Properties Determined at Specific Densification Conditions in the Expanded Experimental Design Matrix	55
7. Summary of Strength and Flaw Data from Tasks 1, 3, and 5b	57



LIST OF FIGURES

	<u>Page</u>
1. Microstructure of SX-G1 from a Polished Surface	6
2. Microstructure from an Etched Surface	6
3. Fracture Toughness at Various Temperatures	7
4. Flexural and Uniaxial Tensile Strength at Various Temperatures	7
5. A Typical "Silicon-Rich Pool" as a Fracture Origin in a Flexural Bar Tested at Room Temperature. The Flexural Strength = 875 MPa (127 ksi)	9
6. Elemental Mapping of a Strength-Limiting Pool from a Scanning Auger Microscope (SAM)	10
7. Similar "Silicon-Rich Pool" in a Tensile Sample Tested at Room Temperature. Tensile Strength = 411 MPa (59.6 ksi)	11
8. "Si-Rich Pool" in a High Strength Tensile Sample Tested at Room Temperature. Tensile Strength = 567 MPa (82 ksi)	12
9. Elemental Mapping of a Strength-Limiting Pool from a Sample Sintered at Higher Temperature	13
10. Fracture Origin from a Flexure Bar Tested at 1370°C. MOR = 420 MPa (61 ksi)	14
11. Elemental Mapping of the "Glassy Phase" as Observed in SAM	15
12. "Glassy Phase" as the Failure Origin in a Tensile Sample Tested at 1370°C and at a Stress Rate of 0.11 MPa/s. Tensile Strength = 279 MPa (40.4 ksi)	16
13. "Si Pool" as Strength-Limiting Defect in a Tensile Sample Tested at 1370°C and at a Stress Rate of 11 MPa/s. Tensile Strength = 309 MPa (44.8 ksi)	17
14. Stress-Strain Plot at 1370°C for Different Stress Rates	19
15. Dynamic Fatigue Response for SX-G1	21

Page

16. Stress Rupture Response for SX-G1	21
17. Creep Strain vs Time at 1260°C	23
18. Creep Strain vs Time at 1370°C	24
19. Creep Strain vs Time at 1450°C	25
20. Fracture Origin in a Tensile Sample Failed at 1370°C at a Stress of 150 MPa for 49 Hours	26
21. Fracture Origin in Tensile Sample Failed at 1450°C at a Stress of 100 MPa for 12 Hours	27
22. Transmission Electron Micrograph from Longitudinal Section	28
23. Transmission Electron Micrograph from Transverse Section	29
24. Transmission Electron Micrograph from a Pristine Sample	30
25. Fracture Surface of a Sample Loaded to Failure at 1260°C. Tensile Strength = 379 MPa. Sample was Stressed up to 250 MPa for >150 Hours at 1260°C Before Loading to Failure	31
26. Steady-State Strain Rate vs Applied Stress at 1370 and 1450°C	33
27. The As-Sintered and Post-Treated Densities as a Function of % Particles <1 μm	36
28. The As-Sintered and Post-Treated Densities as a Function of Surface Area of SiC Powders	37
29. A Schematic of the Experimental Design Matrix	43
30. "Silicon-Rich Pool" as Strength-Limiting Volume Defect. Flexural Strength = 1,020 MPa (148 ksi)	46
31. Machining Induced Surface Defect as the Fracture Origin. Flexural Strength = 938 MPa (136 ksi)	47

Page

32. Room-Temperature Flexural Strength Corresponding to Various Densification Conditions in the Experimental Matrix	48
33. Contour Map of Room-Temperature Flexural Strength as a Function of Sintering Temperature and Post-Treatment Temperature	50
34. Contour Map of Room-Temperature Flexural Strength as a Function of Sintering Temperature and Post-Treatment Pressure	51
35. Contour Map of Room-Temperature Flexural Strength as a Function of Post-Treatment Temperature and Post-Treatment Pressure	52
36. Room-Temperature Flexural Strength Corresponding to Various Densification Conditions in the Expanded Experimental Matrix	56
37. Flexural and Tensile Strength Determined in Tasks 1 and 5b at Various Temperatures	60
38. Dynamic Fatigue Response Measured from Tasks 1 and 5b	60

INTRODUCTION

HEXOLOY®¹ SA Silicon Carbide, a pressureless sintered α -SiC, has shown excellent oxidation, corrosion, erosion, and wear resistance. Its toughness and strength retention at elevated temperatures up to 1500°C in air have also been demonstrated. Powder availability, price competitiveness, and net-shape-forming capability make this SiC material an attractive candidate for many structural applications. However, relatively low strength (primarily due to its low toughness) still represents limitations for some applications involving higher stresses such as rotating components in advanced gas turbine engines. Various approaches have been considered to enhance its fracture toughness and strength. Among them the key ones are based on the modification of microstructure and fracture characteristics of the material by the incorporation of appropriate sintering additives and variation of processing conditions. Using these approaches, Carborundum recently developed an improved SiC material, namely HEXOLOY® SX SiC, which is sintered with the addition of yttrium and aluminum compounds.

HEXOLOY® SX SiC had been demonstrated to possess a higher toughness and strength than HEXOLOY® SA SiC[1]. Its toughness was about 50% to 100% higher than that of SA and its typical room-temperature MOR value ranged between 620-915 MPa (90-133 ksi). However, the available database was preliminary in nature. A detailed characterization was necessary to completely establish the mechanical property database for benchmarking and, more importantly, to understand the failure mechanisms and establish microstructure-property correlations. Using the structure-property correlation, it was believed that the mechanical properties could be further improved via proper optimization of composition and processing conditions.

SCOPE AND OBJECTIVE

The approach taken for the current work was first to establish a complete mechanical property database and conduct detailed microstructural characterization on the first generation SX material. Then a process optimization study was carried out to further enhance the high-temperature mechanical properties. Simultaneously, a Carborundum in-house sponsored program with the objective of identifying a second generation additive composition with improved high-

¹HEXOLOY is a trademark of The Carborundum Company registered in the U.S. Patent & Trademark Office.

Research sponsored by the U.S. Department of Energy, Assistant Secretary for Energy Efficiency and Renewable Energy, Office of Transportation Technologies, as part of the Ceramic Technology Project of the Propulsion System Materials Program, under contract DE-AC05-84OR21400 with Martin Marietta Energy Systems, Inc.

temperature properties was conducted. Then a second set of designed experiments was to be conducted to optimize the properties of this second generation SX material. Finally, the complete property database was to be established for the second generation composition.

The three major objectives for this program were as follows: (1) establish a property database and conduct detailed characterization for the best SX material, (2) improve the processing conditions of that material via a designed experimental method, and (3) develop a second generation SX material with superior high-temperature properties. To achieve these objectives the work was split into six tasks:

<u>Task</u>	<u>Objective</u>	<u>Duration</u>
1	Complete Characterization of First Generation SX	April '91-Dec. '91
2	Selection of SiC Powder Source	Aug. '91-Dec. '91
3	Develop Improved Dispersion Technique	Aug. '91-Dec. '91
4	Property Optimization of First Generation SX	Jan. '92-April '92
5a	Property Optimization of Second Generation SX	May '92-Aug. '92
5b	Complete Characterization of Second Generation SX	Sept. '92-Dec. '92

From previous internal work at Carborundum, a particular composition of SX, designated SX-G1, with 2 wt % total additive, had shown excellent MOR strengths. Preliminary evaluation of its creep and dynamic fatigue resistance was also encouraging. SX-G1 was, therefore, chosen as the composition for the work to be conducted in Tasks 1, 2, 3, and 4 of this contract.

Task 1: Complete Characterization of First Generation SX-SiC Material.

In this task, a complete mechanical and microstructural characterization was conducted. Mechanical characterization included MOR, tensile strength, and K_{Ic} determinations at room and elevated temperatures; stress rupture, dynamic fatigue, and creep measurements at elevated temperatures. Microstructural characterization included: X-ray diffraction; quantitative image analysis; optical, scanning electron, and Auger microscopies.

Experimental Procedure

Sample Preparation: Two 20-lb batches of a commercial SiC powder from source A were mixed with the appropriate amounts of yttrium and aluminum compound sintering additives and spray dried into soft, flowable agglomerates. The powder was compacted into 63.5-mm-square plates and subsequently isostatically pressed to 117 MPa. The green plates were pressureless sintered and post-treated at elevated temperatures and pressures to >99% theoretical density. The plates were then machined into flexural bars of 3 x 4 x 48 mm. In fabricating the tensile specimens, green rods of 216 mm in length and 21 mm in diameter were isostatically pressed to 117 MPa. They were then pressureless sintered to about 96% theoretical density, which was next enhanced to >99% by a post-treatment process. A higher sintering temperature was required to achieve this density as compared to that used for the plates. The densified rods were then machined into ORNL buttonhead-type tensile specimens.

Mechanical Properties Evaluation: A detailed microstructural and mechanical property characterization was conducted. The mechanical properties evaluated included fracture toughness, flexural strength, tensile strength, dynamic fatigue, stress rupture, and creep.

The fracture toughness (K_{Ic}) was determined by the Chevron-notch technique. Chevron notches were cut in the bars (3 x 4 x 48 mm) which were subsequently fractured at a cross-head speed of 0.5 mm/min in four-point bending. K_{Ic} was evaluated using the fracture load from five samples each at room temperature, 1000, 1232, and 1370°C.

Flexural strength was evaluated using MIL-STD-1942 on bars (3 x 4 x 48 mm) in four-point bending at a cross-head speed of 0.5 mm/min with 20- and 40-mm inner and outer spans. Flexural strength was evaluated from 20 bars each at room temperature, 1000, 1232, and 1370°C.

The strength of the SX-G1 samples was also determined in uniaxial tension. The specimens were machined according to the ORNL buttonhead tensile specimen specification. The specimens were then tested at a stressing rate of 11 MPa/s using self-aligning Instron Super Grip™ hydraulic

couples in the load train to minimize specimen bending. The uniaxial tensile strengths were determined at room temperature, 1000, 1232, and 1370°C. These tension tests were carried out at the ORNL/HTML User Facility.

Dynamic fatigue tests were conducted at 1232 and 1370°C in four-point bending using MIL-STD-1942 flexure bars. About six specimens were tested at each of three loading rates covering three orders of magnitude. Stress-rupture experiments were also conducted at 1232 and 1370°C in four-point bending. The load-point deflection of each specimen was monitored during the testing.

Creep tests were conducted in uniaxial tension at 1260, 1370, and 1450°C. Strain rates were determined using extensometers at several temperatures ranging from 1260 to 1450°C and at several stress levels ranging from 50 to 250 MPa.

Extensive microstructural and fractographic analyses were conducted using both optical and scanning electron microscopy (SEM). When needed, scanning auger microscopy (SAM) was also used to identify the chemistry of the fracture origin(s).

Results

Microstructural Characterization: The typical microstructure for a polished surface of a SX-G1 sample is shown in Figure 1. The brighter regions in the backscattered SEM image are deduced by elemental mapping to be YAG. XRD also revealed that the major second phase in the SX-G1 is YAG. An etched microstructure is shown in Figure 2. The SiC grains are equiaxed with a narrow grain-size distribution. The average grain size is estimated to be 1.5 μm .

Toughness and Strength: The fracture toughness (K_{IC}) determined as a function of temperature is shown in Figure 3. The K_{IC} of SX-G1 decreases from 4.05 $\text{MPa}\cdot\text{m}^{1/2}$ at room temperature to 2.6 $\text{MPa}\cdot\text{m}^{1/2}$ at 1370°C. The K_{IC} for single-phase α -SiC is also shown for comparison[2]. Note that the K_{IC} for α -SiC remains unchanged at all temperatures, while K_{IC} for SX-G1 decreases at elevated temperatures.

It has been proposed that the increase in toughness of SX relative to SA is related to a microcracking mechanism that resulted from residual stresses developed by the coefficient of thermal expansion (CTE) mismatch between SiC and YAG[3]. At elevated temperatures the residual stresses are reduced and a decrease in fracture toughness is expected. The observation that toughness decreases with increasing temperatures is consistent with the proposed toughening mechanism in SX-SiC materials.

The strength of SX-G1 measured from four-point bending and uniaxial tension at various temperatures is shown in Figure 4. Note that the variation in uniaxial tensile strength with temperature is similar to that of the flexural strength. However, at a given temperature the tensile strengths are consistently lower due to the larger effective volume of the buttonhead specimen. The strength decrease with an increase in temperature is consistent with the K_{Ic} reduction at high temperature.

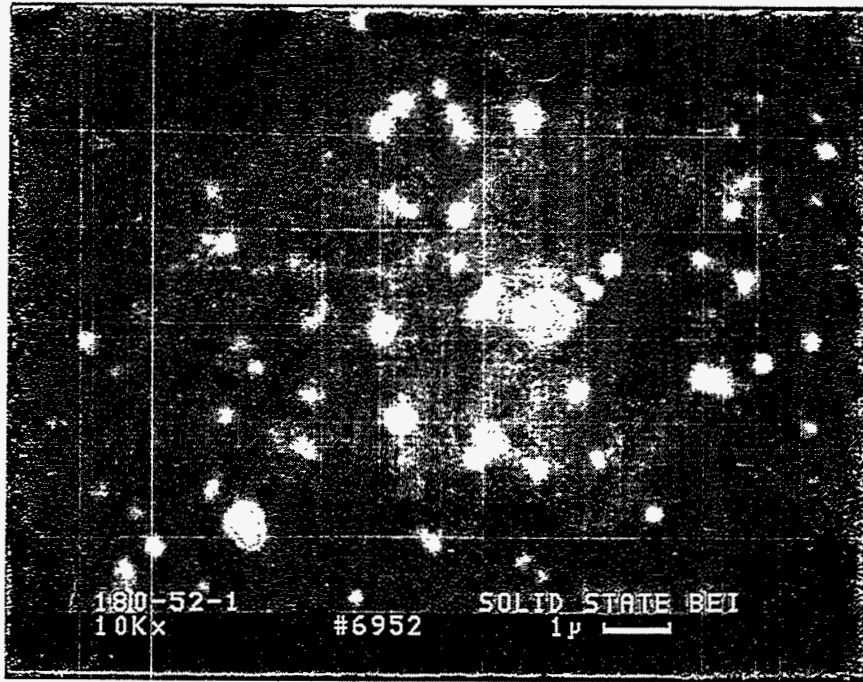


Figure 1. Microstructure of SX-GI from a Polished Surface.

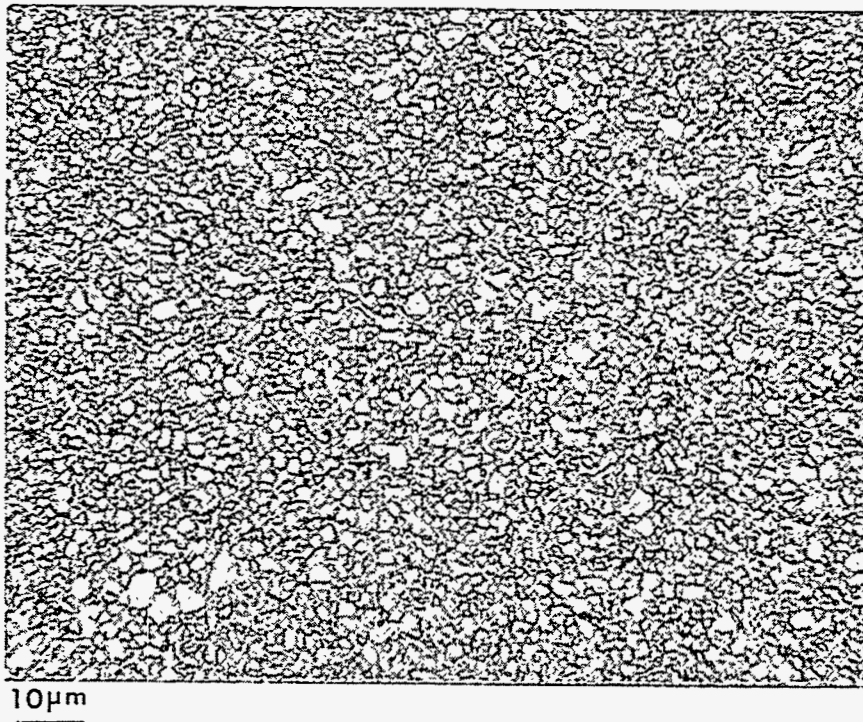


Figure 2. Microstructure from an Etched Surface.

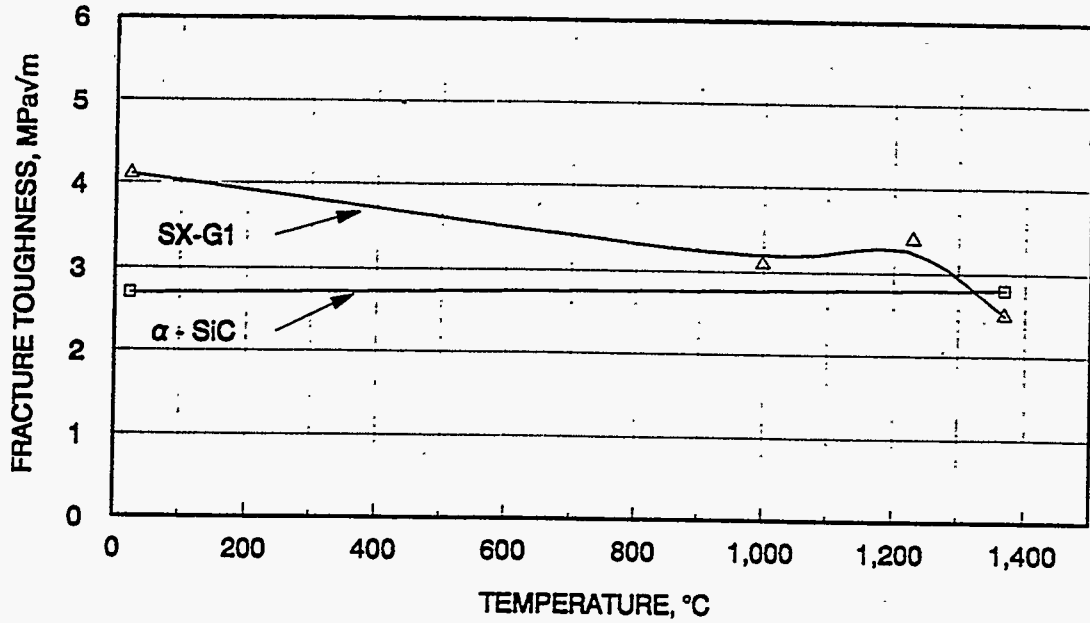


Figure 3. Fracture Toughness at Various Temperatures.

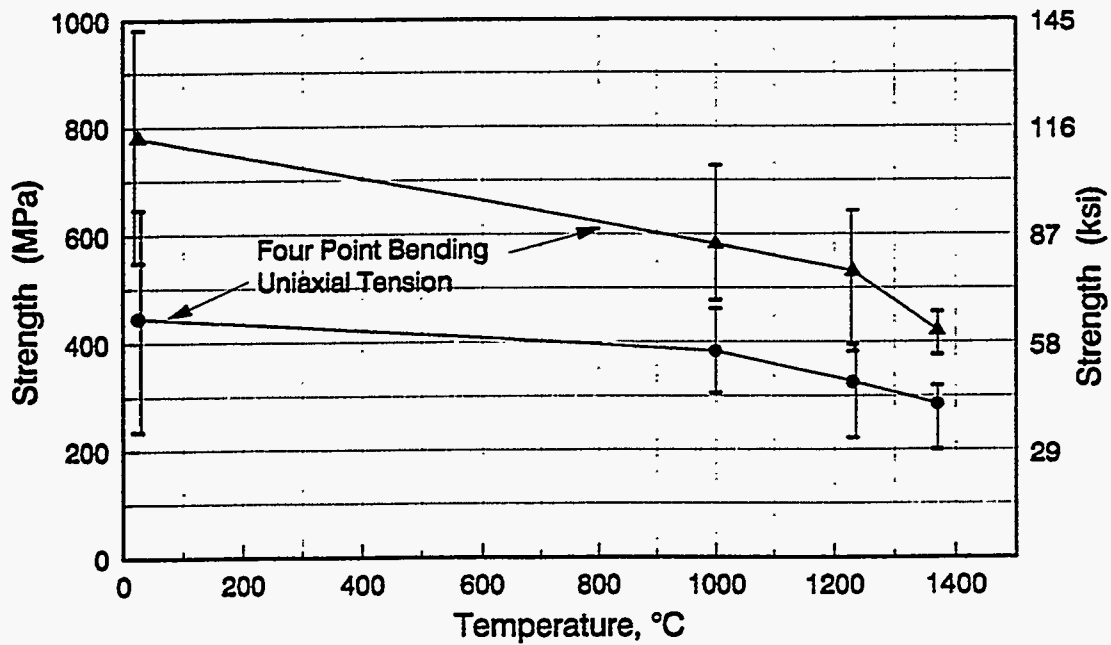
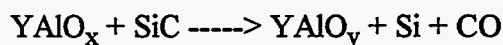


Figure 4. Flexural and Uniaxial Tensile Strength at Various Temperatures.

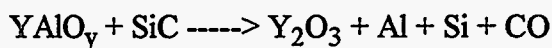
Strength-Limiting Defects: Optical fractography was performed on all of the fractured specimens. Selected specimens were analyzed using SEM and SAM. Figure 5 shows a fracture surface and failure origin from a typical flexure bar tested at room temperature. The same sample was examined in the SAM. Elemental mapping obtained from the SAM suggests that the fracture origin consisted of elemental silicon and Y-Al-O phases as seen in Figure 6.

Similar volume flaws were identified as the strength-limiting defects in all the tensile specimens tested at room temperature, 1000, and 1232°C. Figures 7 and 8 show typical fracture origins which are very similar to those observed in the flexural specimens.

Although the strength-limiting flaws are associated with the formation of elemental silicon and an associated void area, the starting powder premix does not contain any significant amount of elemental Si to explain the presence of Si in all the specimens. One possibility is, therefore, that the Si forms as a product of some reaction between the Y-Al-O secondary phase and SiC matrix as given below:



At higher temperatures, further reduction occurs to produce additional elemental Si:



The existence of these reaction products can be seen using SAM in samples sintered at higher temperatures as shown in Figure 9. Similar reactions have been reported in the system SiC-Al₂O₃-Y₂O₃ during sintering by Omori and Takei[4].

The fracture behavior at 1370°C was different from that noted above for lower temperatures. In the 1370°C flexural tests, all the specimens failed from the surface. Figure 10 shows a typical fracture surface and failure origin. Note the appearance of a "glassy phase" along the fracture origin. Elemental mapping of the "glassy phase" was conducted using SAM and is shown in Figure 11. The composition of the "glassy phase" contains Y, Al, Si, and O. This phase could be yttrium alumino silicate glass. When the tensile specimens were tested at 1370°C under a lower stress rate (0.11 MPa/s), the failure originated from the surface as shown in Figure 12. Such failure origins were very similar to those observed on the flexural specimens tested at 1370°C. Presumably the SiO₂ formed by the oxidation of SiC reacted with the Y-Al-O secondary phase to form a low-melting silicate that was responsible for the high-temperature failure origin. However, when the tensile specimens were tested at 1370°C and at higher stress rates (11 MPa/sec.), the failures were from a volume flaw as shown in Figure 13. This flaw is very similar to those shown in Figures 7 and 8 for low temperatures. It appears that the formation of this glass phase is a time-dependent phenomenon. The stress-strain plots for tension tests performed at 1370°C for

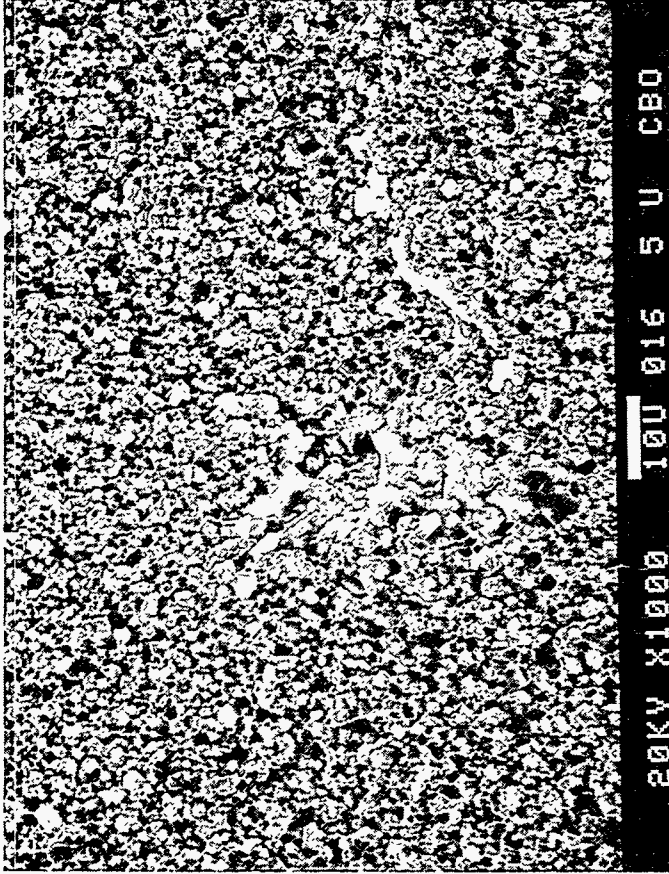
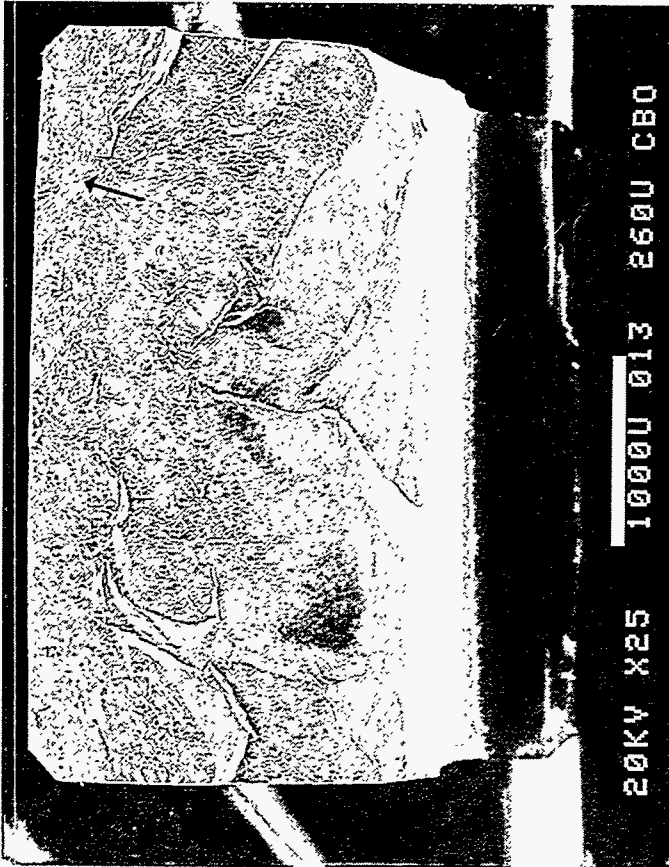


Figure 5. A Typical "Silicon-Rich Pool" as a Fracture Origin in a Flexural Bar Tested at Room Temperature.
Flexural Strength = 875 MPa (127 ksi).

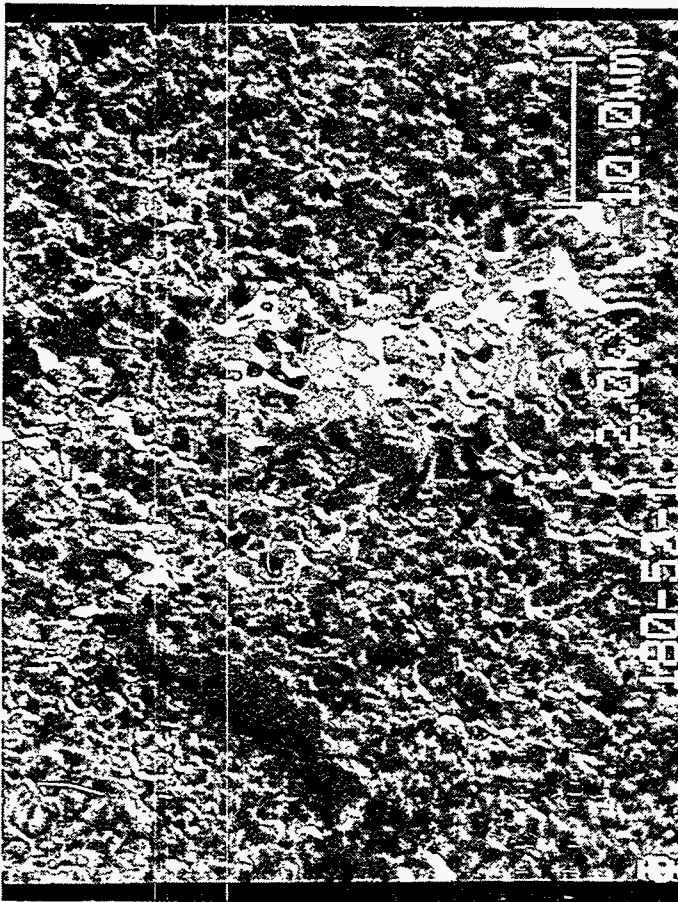
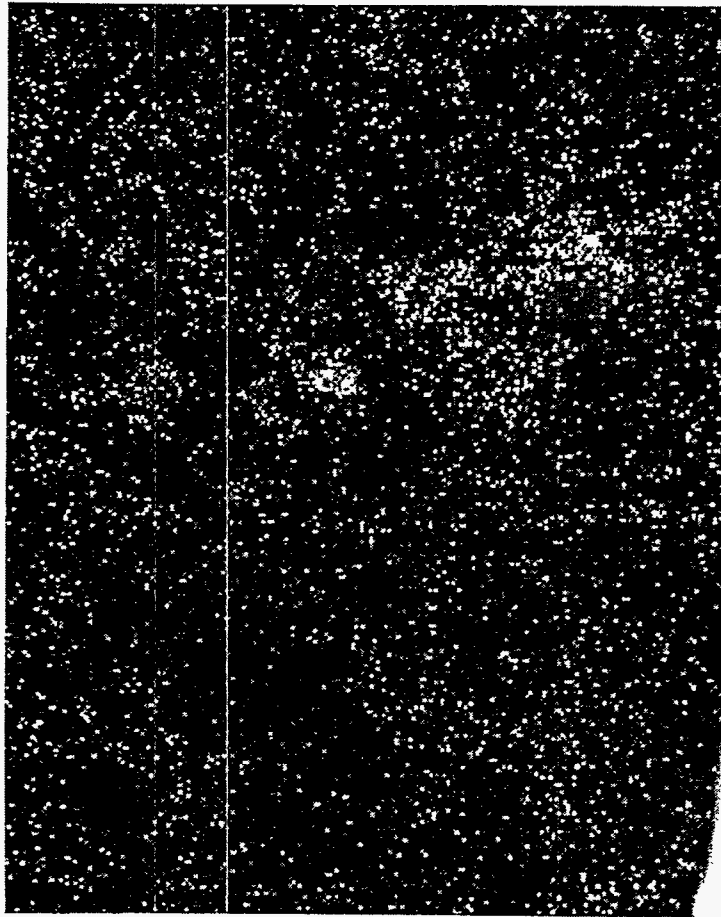


Figure 6. Elemental Mapping of a Strength-Limiting Pool from a Scanning Auger Microscope (SAM).

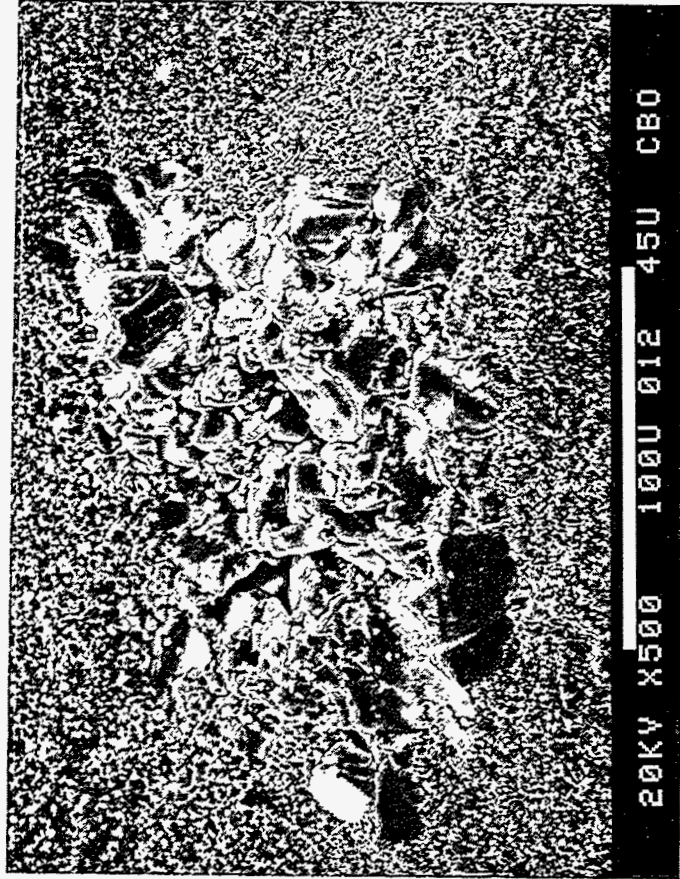
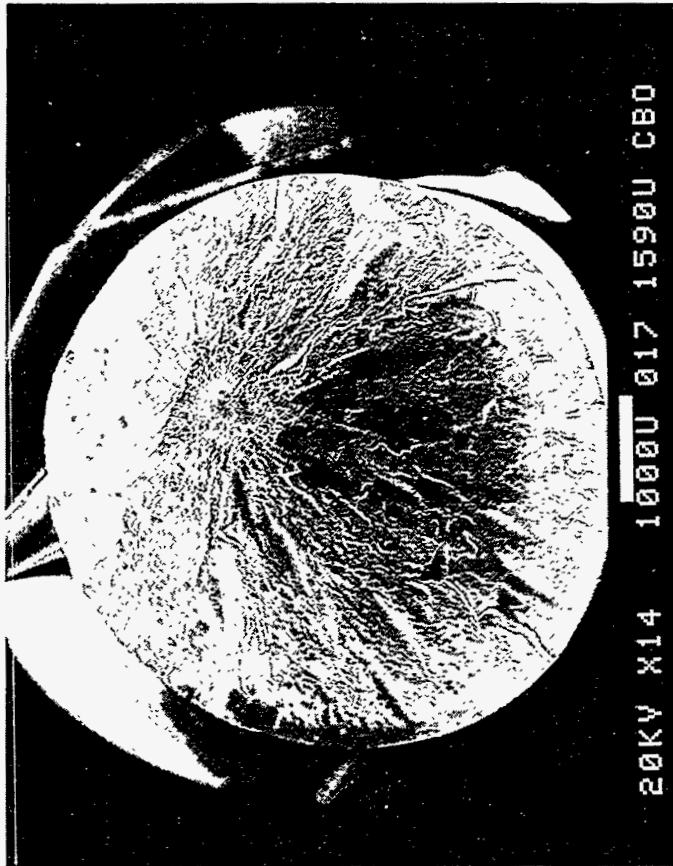


Figure 7. Similar "Silicon-Rich Pool" in a Tensile Sample Tested at Room Temperature.
Tensile Strength = 411 MPa (59.6 ksi).

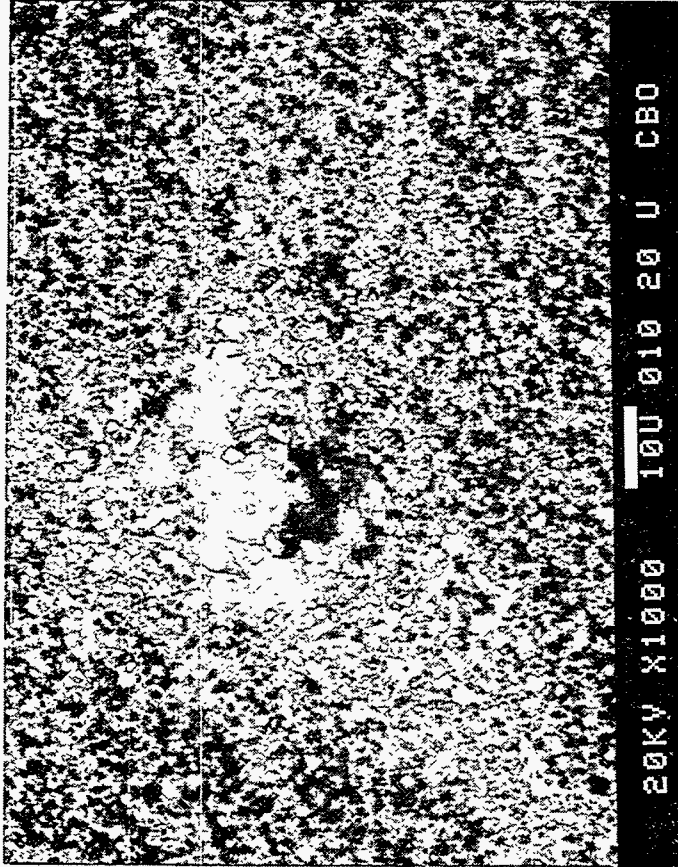
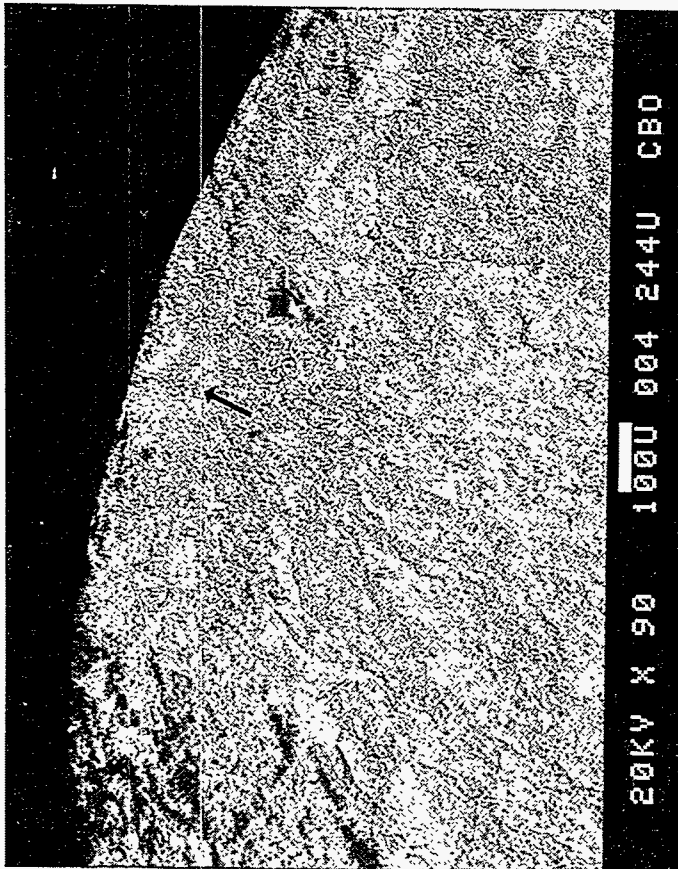


Figure 8. "Si-Rich Pool" in a High Strength Tensile Sample Tested at Room Temperature.
Tensile Strength = 567 MPa (82 ksi).

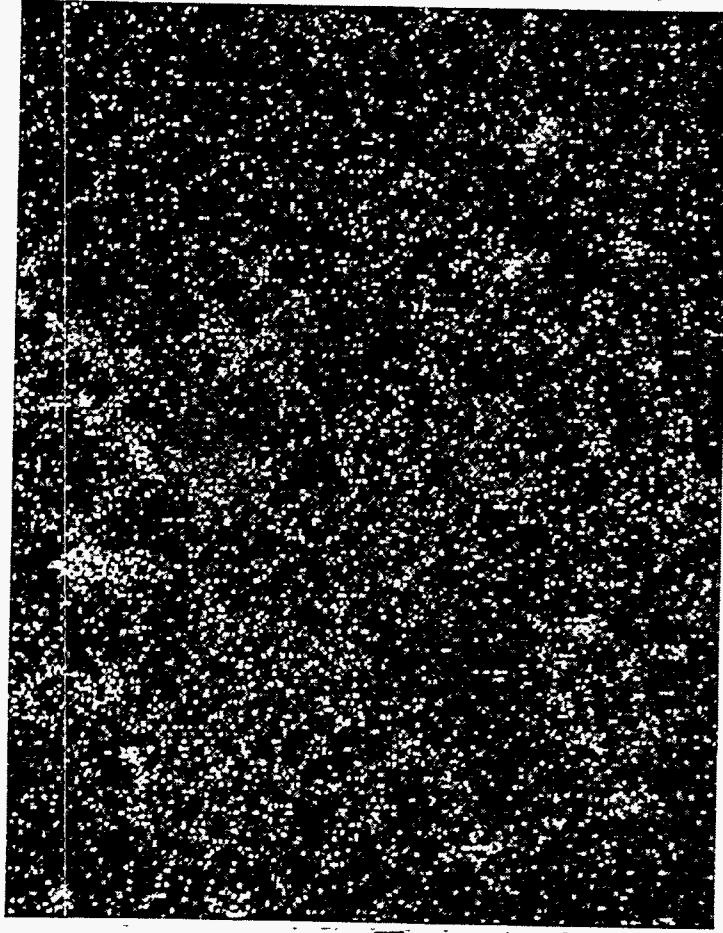


Figure 9. Elemental Mapping of a Strength-Limiting Pool from a Sample Sintered at a Higher Temperature.

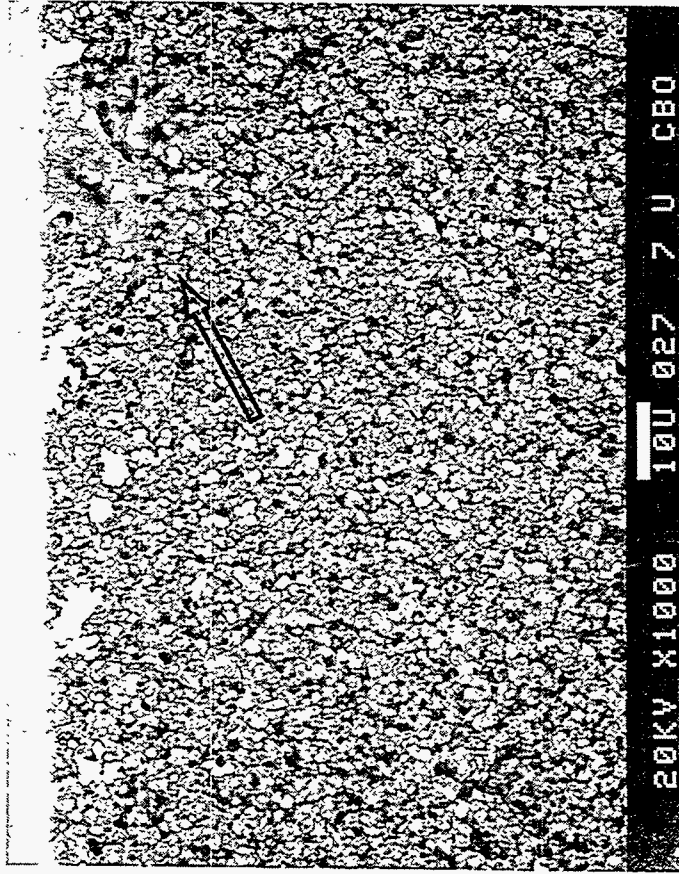
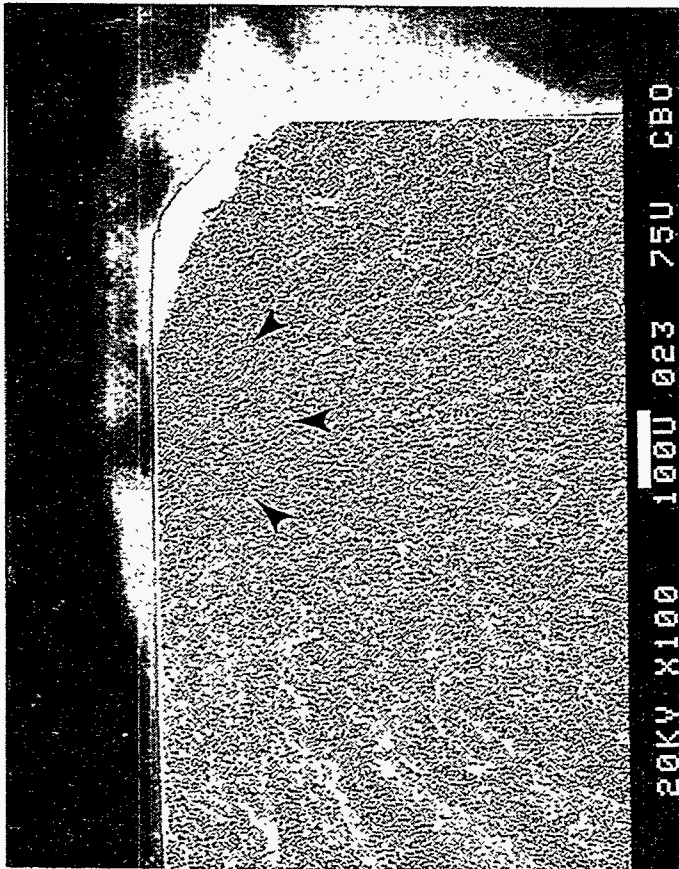
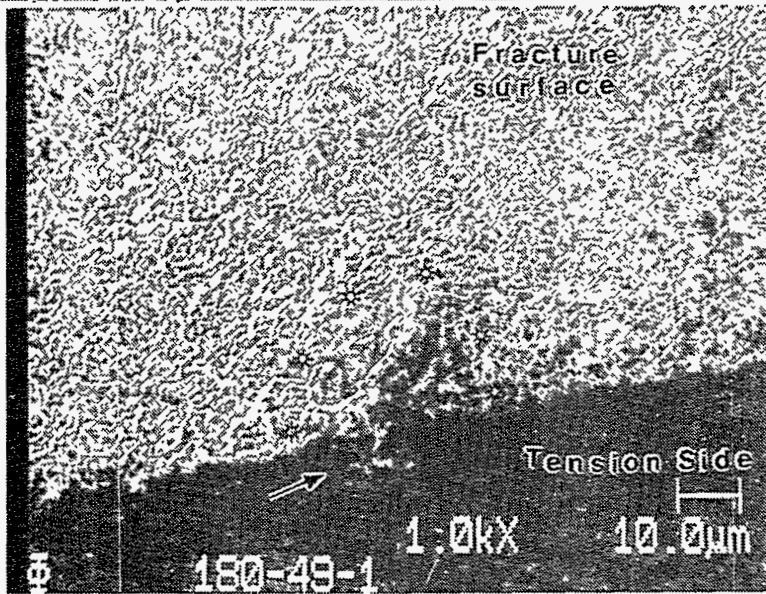
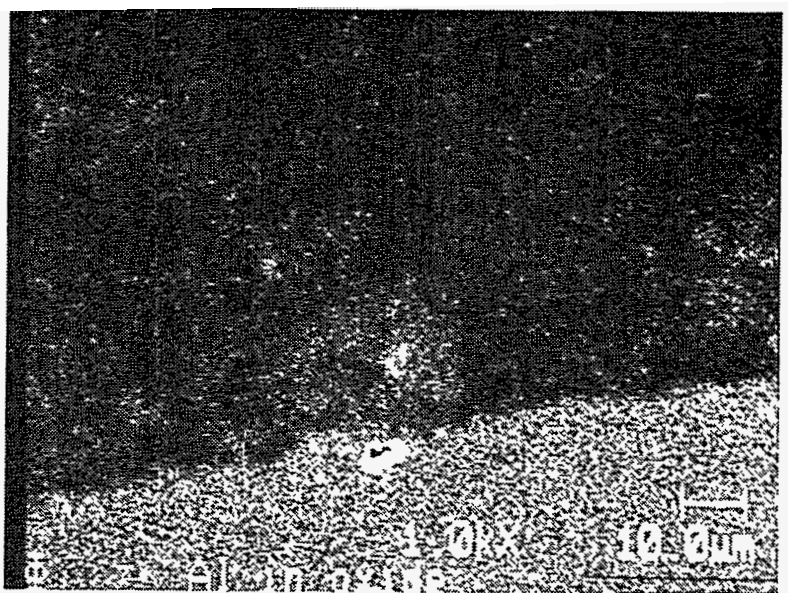
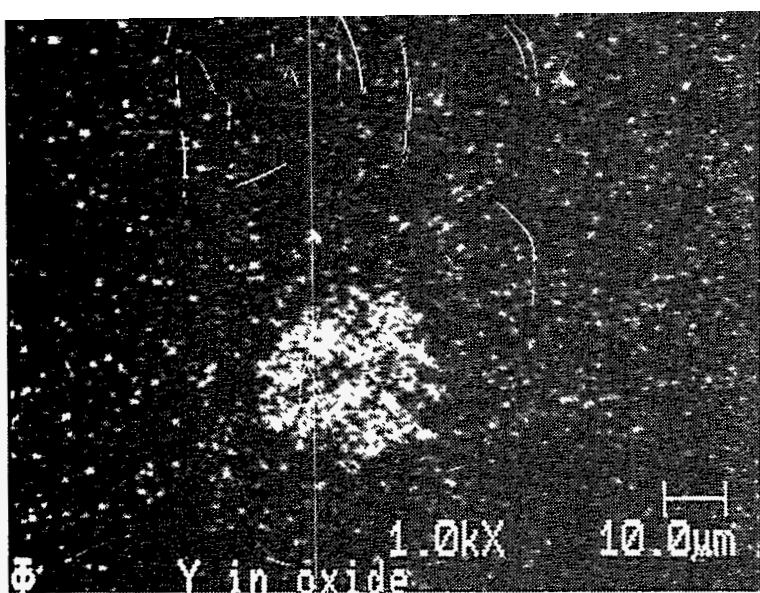


Figure 10. Fracture Origin from a Flexure Bar Tested at 1370°C.
MOR = 420 MPa (61 ksi).



SX-G1 Fractured at 1371°C
Strength Limiting Flaw is
YAlSiO₄ Glass
(Melting Point Around 1300°C)

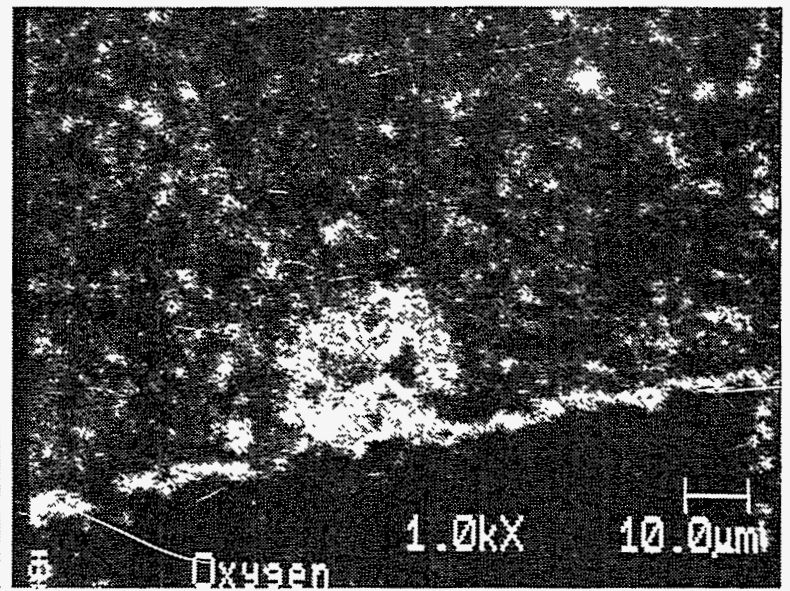
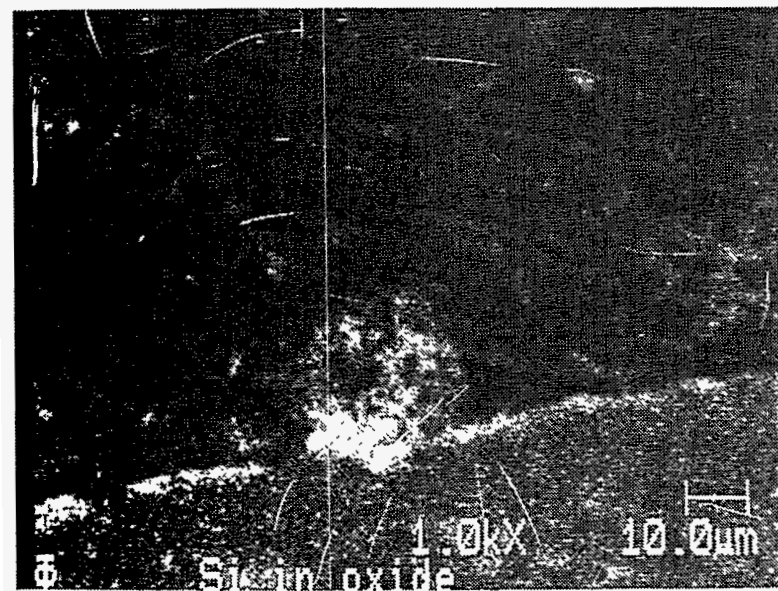


Figure 11. Elemental Mapping of the "Glassy Phase" as Observed in SAM.

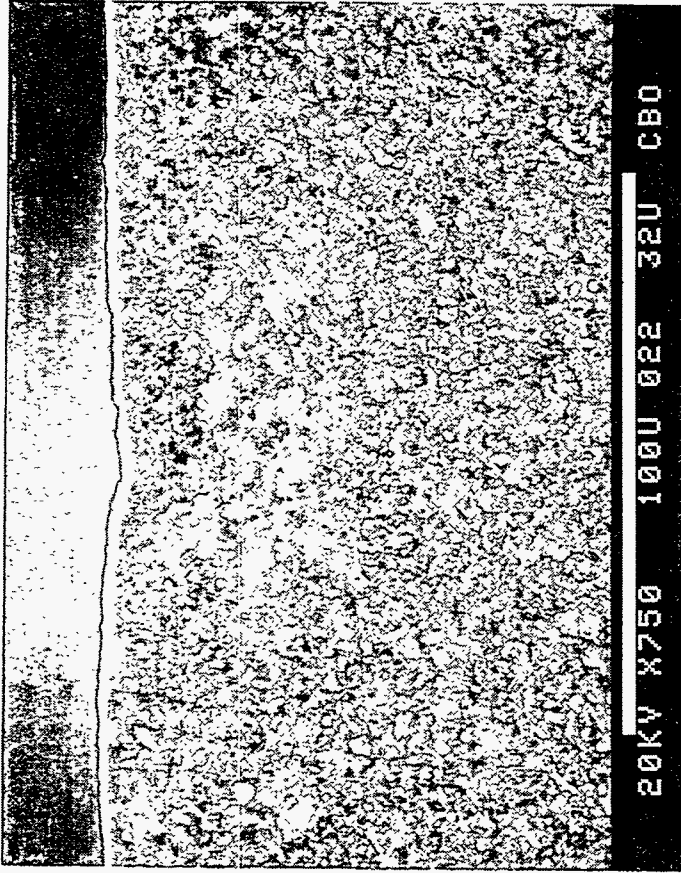
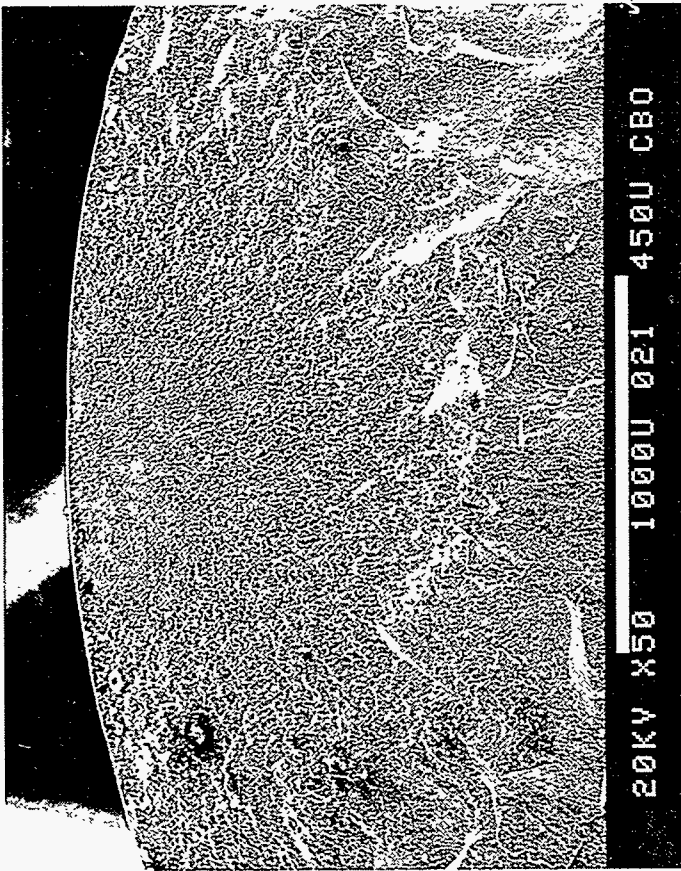


Figure 12. "Glassy Phase" as the Failure Origin in a Tensile Sample Tested at 1370°C and at a Stress Rate of 0.11 MPa/s.
Tensile Strength = 279 MPa (40.4 ksi).

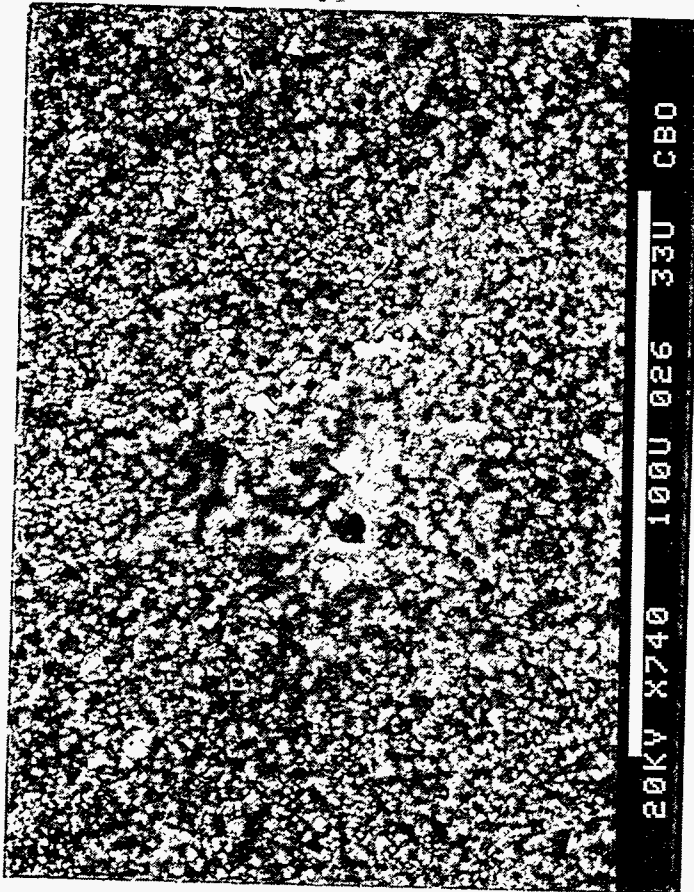


Figure 13. "Si Pool" as Strength-Limiting Defect in a Tensile Sample Tested at 1370°C and at a Stress Rate of 11 MPa/s.
Tensile Strength = 309 MPa (44.8 ksi).

various stress rates are shown in Figure 14. The nonlinear behavior at lower stressing rates with the glass-phase formation at the surface suggests probable slow crack growth. The average strengths, Weibull modulus, and the defect type obtained from flexural tests and tension tests are summarized in Tables 1a and 1b.

Fatigue Results: Dynamic fatigue experiments were carried out in four-point flexure at 1232 and 1370°C. Constant stress rates were used, which varied from 0.633 MPa/s to 63.3 MPa/s. The average strengths measured at various stress rates are shown in Figure 15. The slow crack growth parameter is calculated using the relation:

$$\sigma_f = \dot{\sigma}^{1/(N+1)}$$

where σ_f is the fracture strength, $\dot{\sigma}$ is the stressing rate, and "N" is the slow crack growth parameter. The slow crack growth parameter "N" is calculated from the slope of the best fit regression line. At 1232°C there is very little reduction in strength at lower stress rates and hence a very high slow crack growth parameter of 51.6 was obtained. Also, the failures corresponded to volume defects which were very similar to the defects observed in flexural bars used for strength evaluation as shown in Figure 5. However, at 1370°C there was a definite strength reduction at lower stress rates—indicative of slow crack growth (N=14.5). At 1370°C all the specimens failed from surface flaws. The fracture origins were very similar to the one shown in Figure 10.

Stress rupture experiments were also conducted in four-point flexure at 1232 and 1370°C. The failure time for a given stress level was recorded and the applied stress vs failure time plot is shown in Figure 16. The slow crack growth parameter was estimated using the relation

$$t_f \propto \sigma_{app}^N$$

where t_f is the failure time, σ_{app} is the constant applied stress, and "N" is the slow crack growth parameter. The slow crack growth parameter was estimated as 75 at 1232°C. Again, a high value of "N" at 1232°C suggests very little or negligible slow crack growth or fatigue behavior. However, the fact that "N" decreased to 16.9 at 1370°C indicates that significant slow crack growth occurred at this temperature. These results are in good agreement with those obtained from the dynamic fatigue flexural results.

The slow crack growth here appears to be associated with the glass-phase formation at the surface. As discussed above, the glass phase, $YAlSiO_x$, might have formed from the reaction of

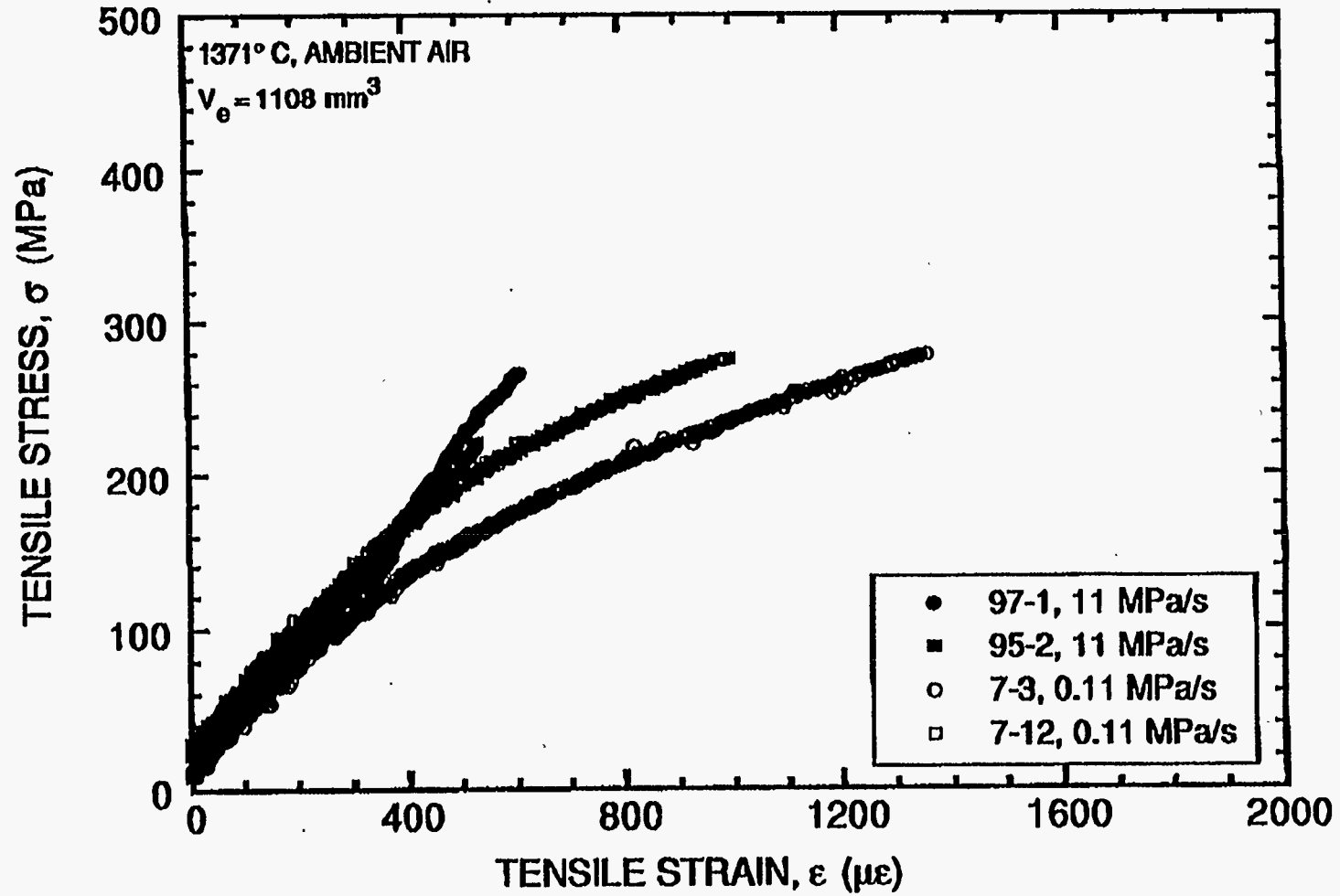


Figure 14. Stress-Strain Plot at 1370°C for Different Stress Rates

TABLE 1a**Flexure Test Data**

Temp °C	MOR MPa (ksi)	Weibull Modulus	Flaw
RT	780 (113)	5.3	Volume defects, Si containing region
1000	580 (84)	8.2	"
1232	531 (77)	5.8	"
1370	421 (61)	10.3	Surface, glassy phase formation

TABLE 1b**Tension Test Data**

Temp	# of Specimens	Stress Rate MPa/sec	Ultimate Tensile Strength MPa (ksi)	Weibull Modulus	Flaw
RT	15	11	446 (64.7)	3.0	Volume defects, Si containing region
1000	8	11	384 (55.7)	6.5	"
1232	8	11	325 (47.2)	4.3	"
1370	6	11	286 (41.5)	4.5	"
	2	0.11	281 (40.8)	-	Surface, glassy phase formation

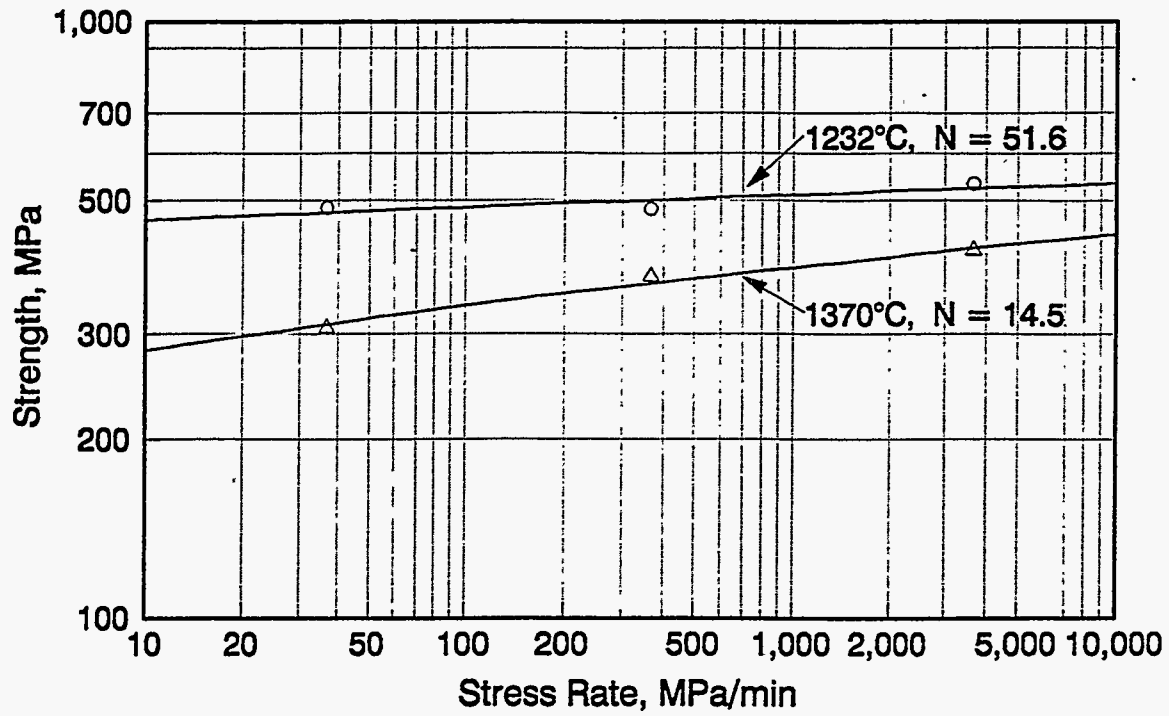


Figure 15. Dynamic Fatigue Response for SX-G1.

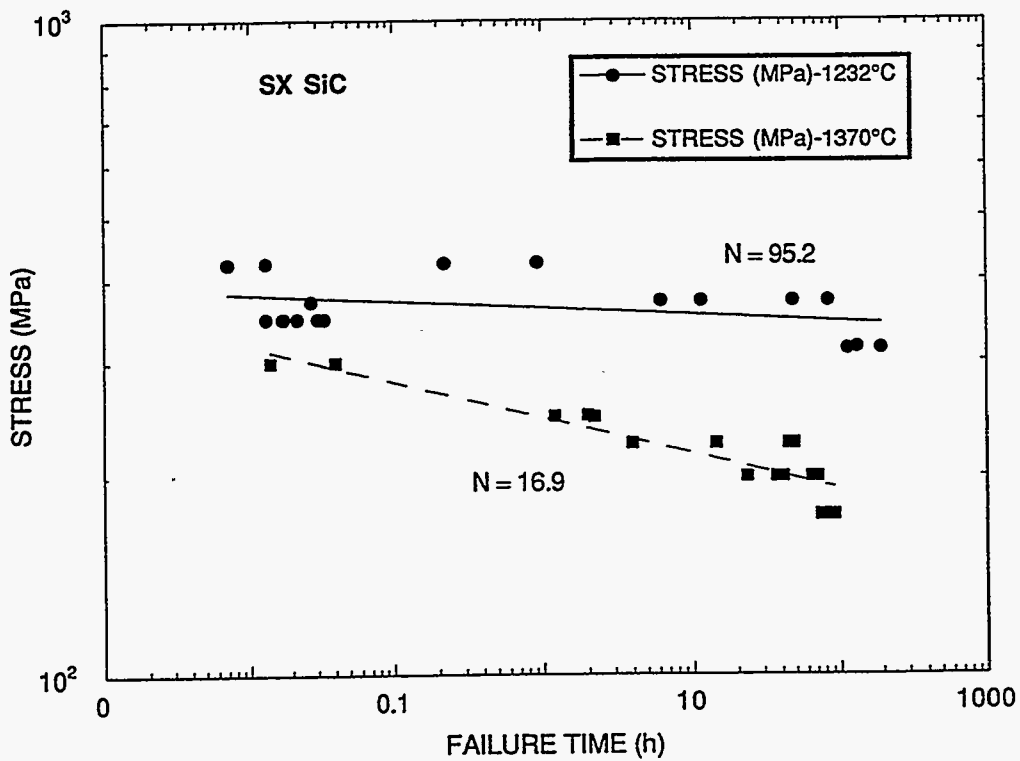


Figure 16. Stress Rupture Response for SX-G1.

yttrium aluminate with the SiO₂ layer which forms on SiC due to oxidation at elevated temperatures. The slow crack growth can occur as the reaction progresses from the tensile surface to the bulk of the sample. The failure origins for such samples always occur from the tensile surface when tested in air. Moreover, dynamic fatigue experiments conducted at 1400°C in argon indicated no glass phase formation and hence no slow crack growth was observed at 1400°C[5]. Therefore, the mechanism of slow crack growth can be classified as "Environmentally Induced Slow Crack Growth." Since a chemical reaction at the surface is involved which promotes slow crack growth, it can also be called "Stress Corrosion Cracking."

Creep: Creep tests were carried out in uniaxial tension at 1260, 1370, and 1450°C with stresses varying from 50 to 300 MPa. The creep strain vs time plots at these temperatures are shown in Figures 17-19. Very little or negligible deflection was recorded at 1260°C at stresses varying between 200 and 250 MPa. At 1370 and 1450°C measurable steady-state strain rates were obtained. However, samples failed in relatively shorter time periods at temperatures of 1370 and 1450°C. As seen from the creep plots, no tertiary creep was observed before failure. The fracture surface of the sample failed at 1370°C under a stress of 150 MPa is shown in Figure 20. A clear oxidation layer and a slow crack growth area were observed. The oxidation layer was large and the severity of slow crack growth was greater at 1450°C as seen in Figure 21. The oxidation layer and the fracture initiation sites appear "glassy" as seen in Figures 20 and 21.

A transmission electron microscopic (TEM) investigation was conducted on samples that failed in a creep test as well as on a pristine sintered sample. Samples were prepared from surfaces parallel and perpendicular to the tensile stress axis. Typical TEM micrographs from longitudinal and transverse sections of the sample subjected to creep are shown in Figures 22 and 23, respectively. A microstructure from a pristine sample is shown in Figure 24 for comparison. No cracking along grain boundaries and cavitation at triple junctions could be seen from the material subjected to creep. The microstructure appears to be unchanged compared to the pristine sample. It appears that microstructural damage due to creep has not occurred.

Appearance of an oxidation layer and slow crack growth regime associated with a glassy fracture origin from the surface of samples subjected to tensile creep suggest that the failure is attributed to slow crack growth due to glass phase formation by oxidation, rather than creep induced failure.

However, samples tested for creep at 1260°C did not show any observable creep strain at the various stress levels and did not fail even after a cumulative time of 160 hours. One of those samples was then loaded to failure. The sample failed because of a volume flaw as shown in Figure 25 at a stress of 379 MPa. This flaw was similar to those observed in tensile samples and

CARBORUNDUM HEXOLOY SX TENSILE CREEP
1260° C, AMBIENT AIR

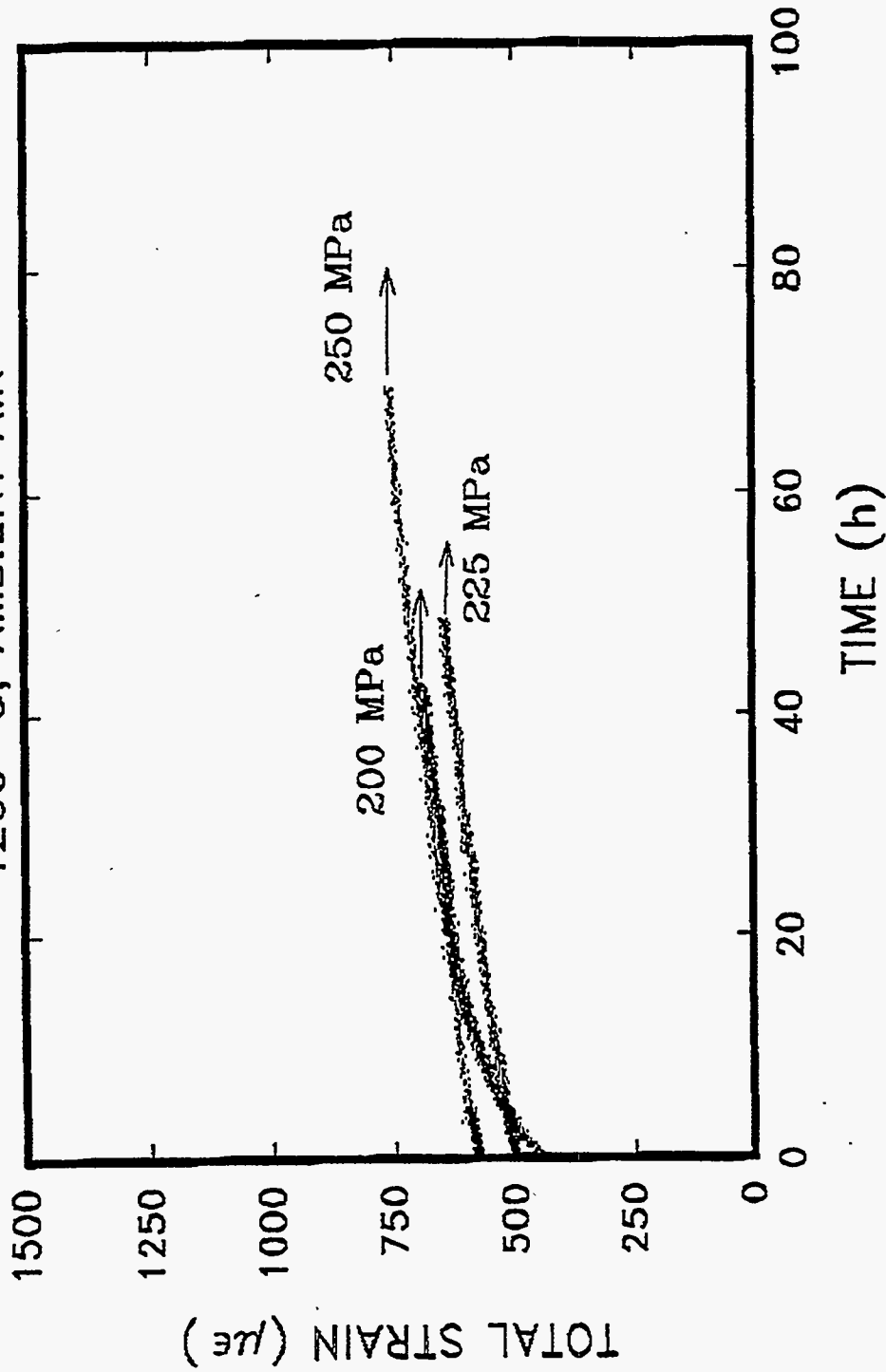


Figure 17. Creep Strain vs Time at 1260°C.

CARBORUNDUM HEXOLOYS SX TENSILE CREEP
1371° C, AMBIENT AIR

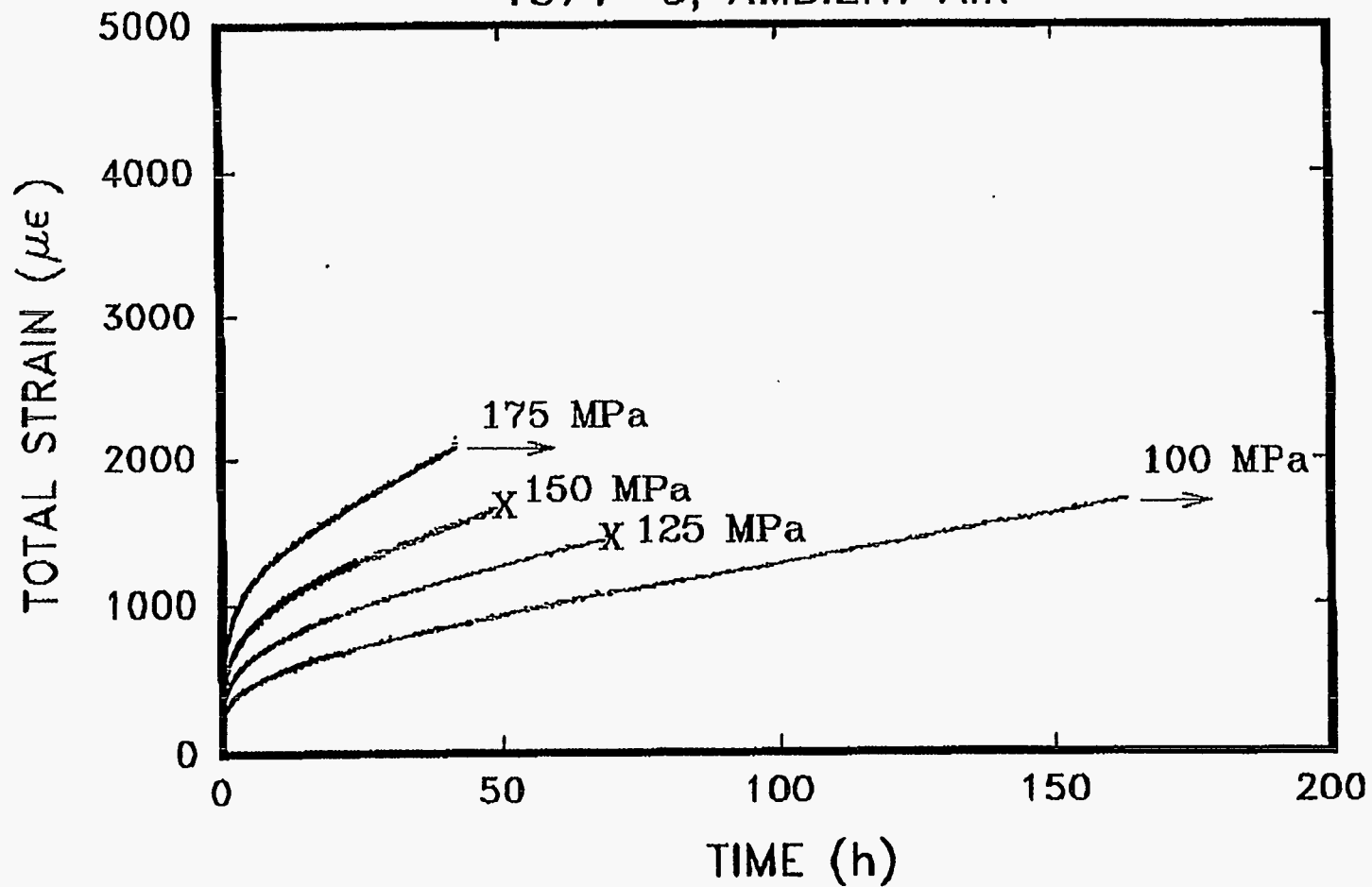


Figure 18. Creep Strain vs Time at 1370°C.

CARBORUNDUM HEXOLOY SX TENSILE CREEP
1450° C, AMBIENT AIR

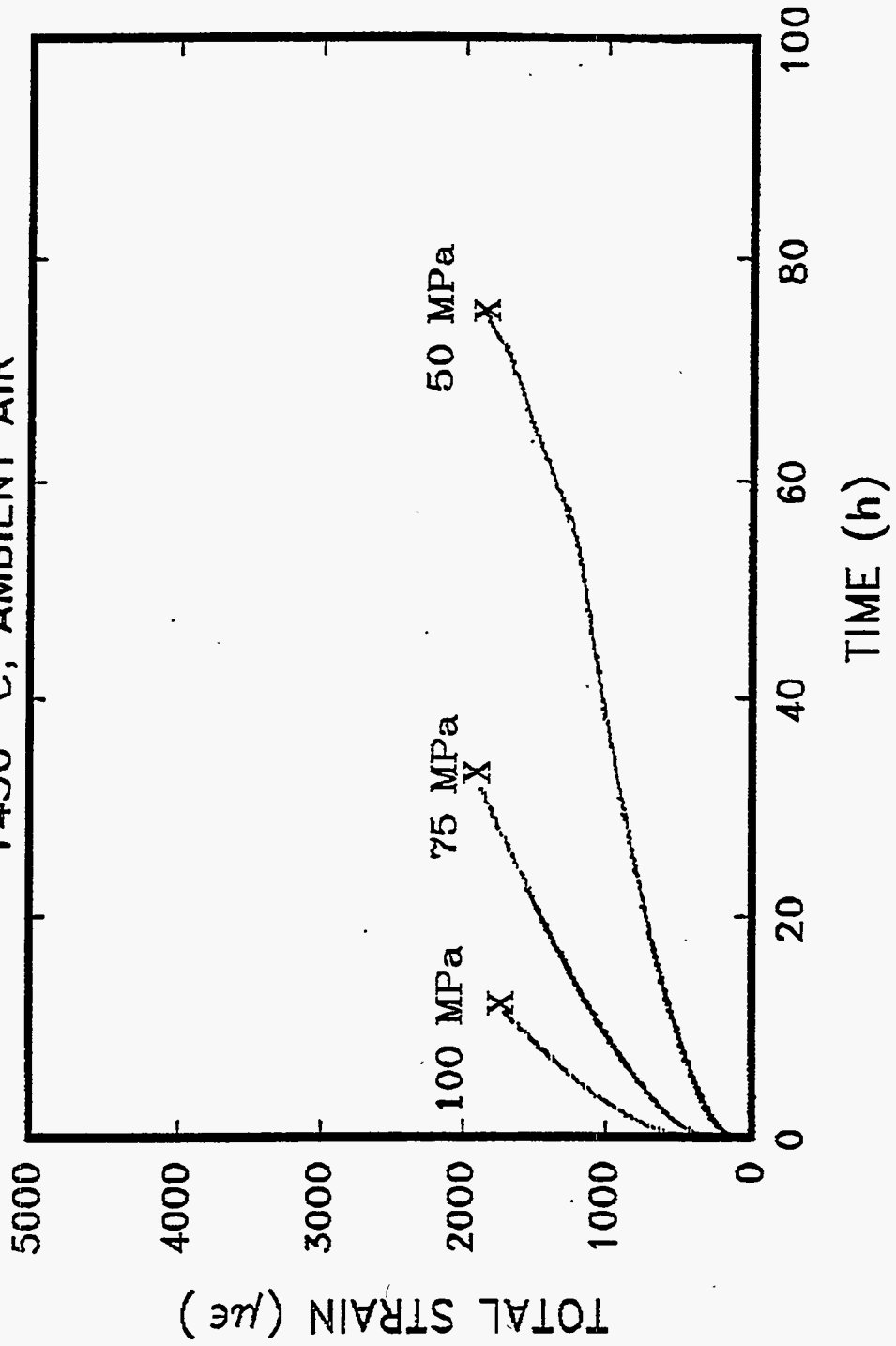


Figure 19. Creep Strain vs Time at 1450°C.

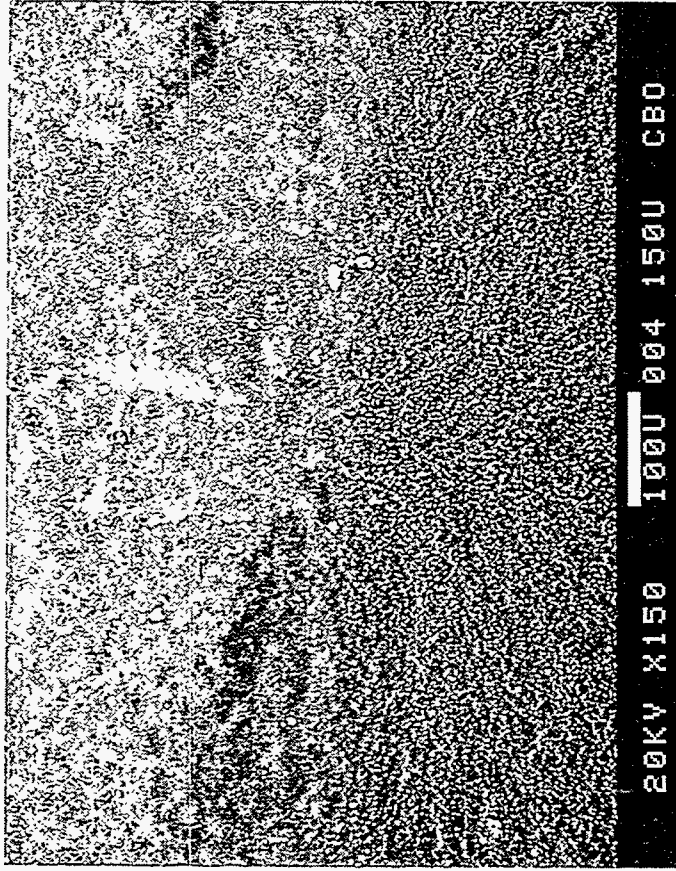
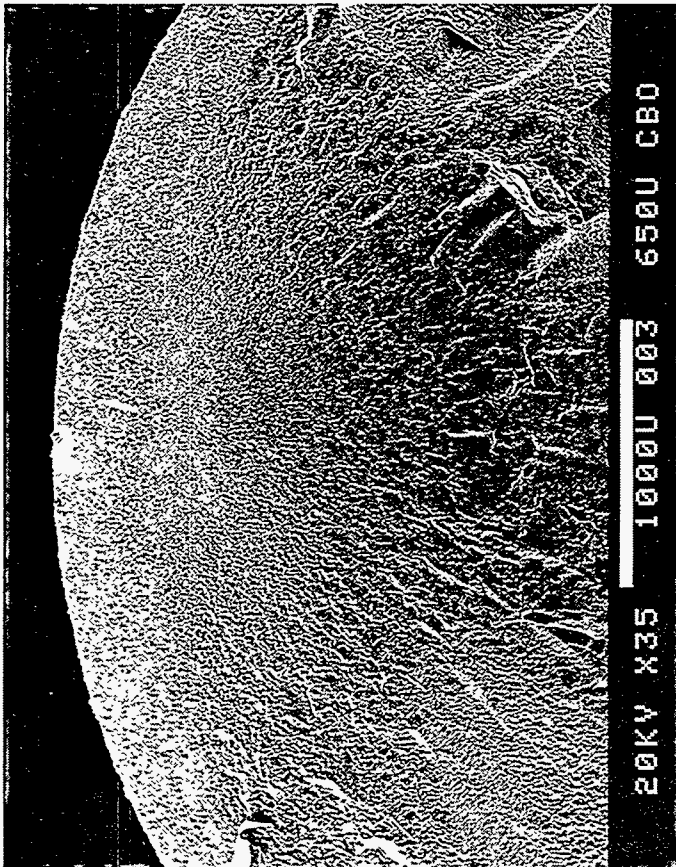


Figure 20. Fracture Origin in a Tensile Sample Failed at 1370°C at a Stress of 150 MPa for 49 Hours.

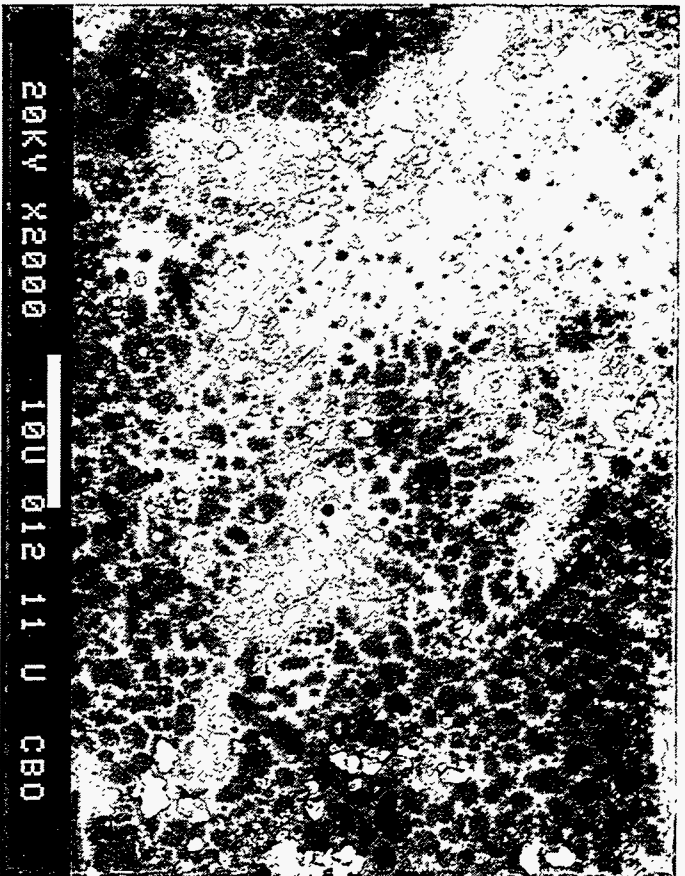
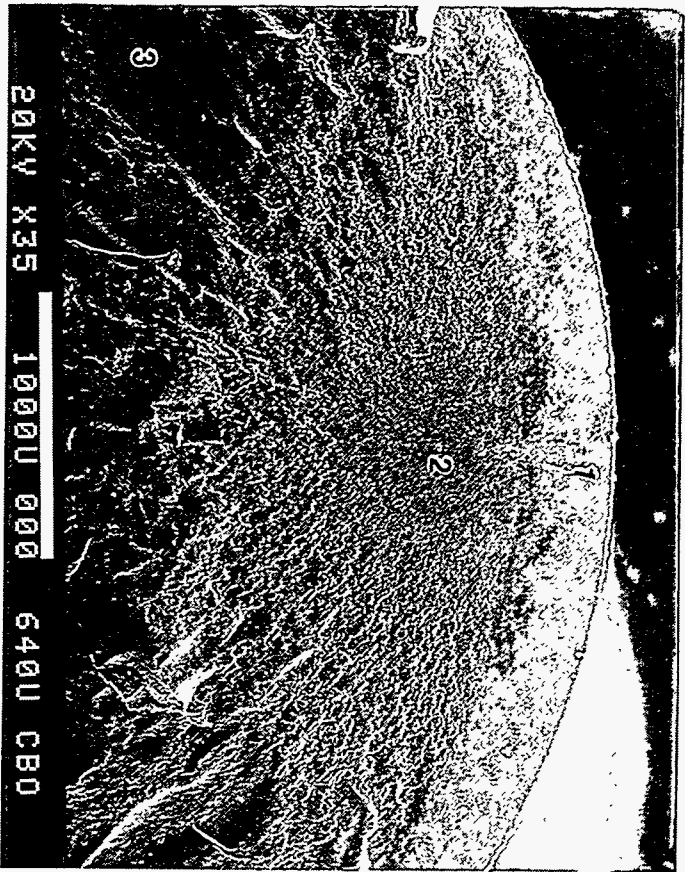
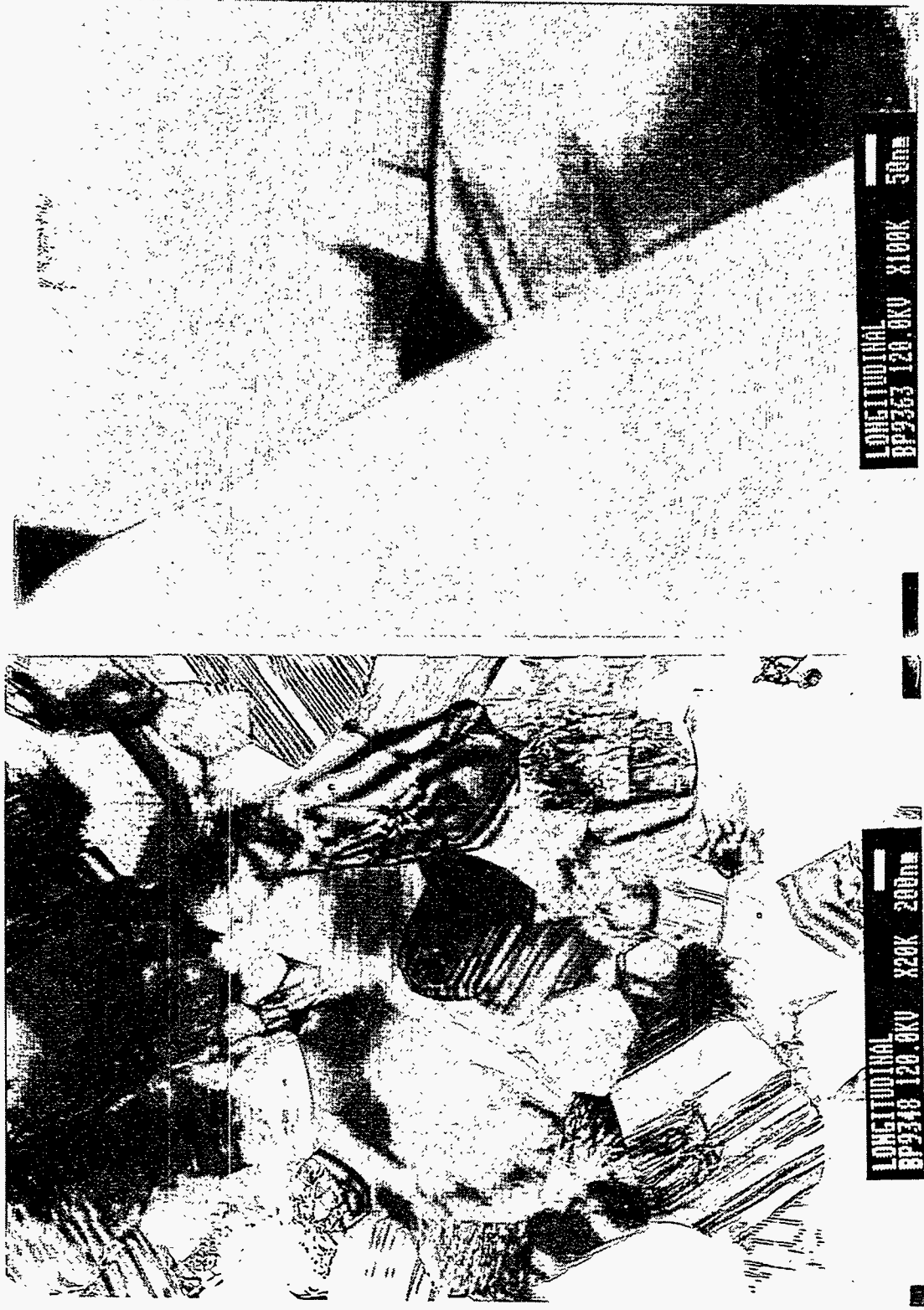


Figure 21. Fracture Origin in Tensile Sample Failed at 1450°C at a Stress of 100 MPa for 12 Hours.



a

b

Figure 22. Transmission Electron Micrograph from Longitudinal Section.



a
Figure 23. Transmission Electron Micrograph from Transverse Section.



Figure 24. Transmission Electron Micrograph from a Pristine Sample.

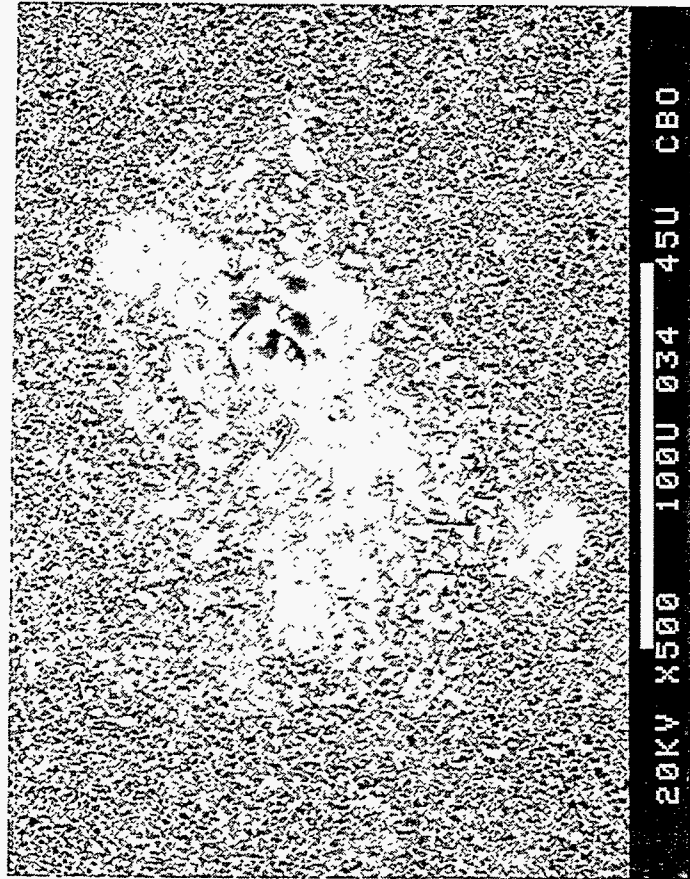
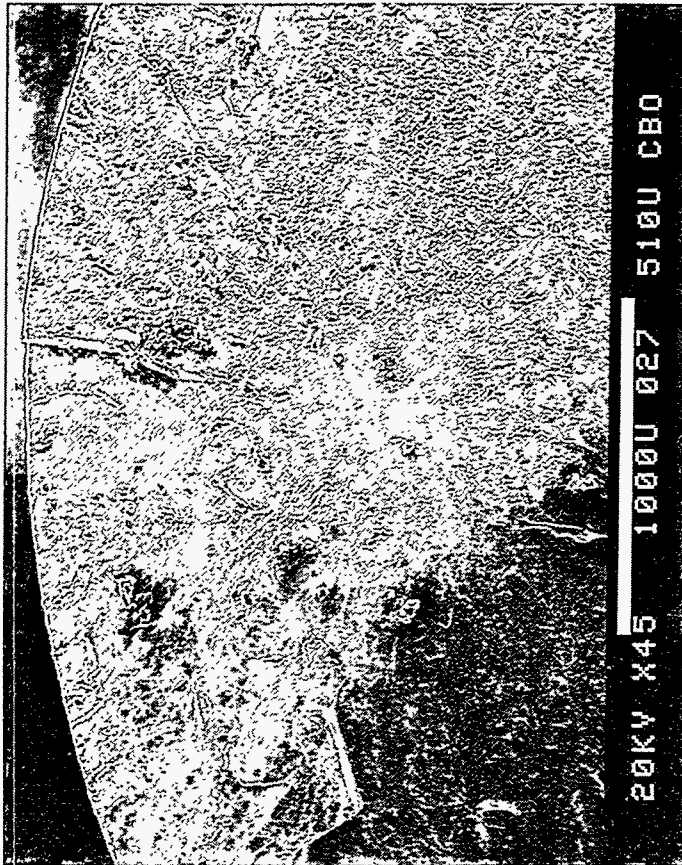


Figure 25. Fracture Surface of a Sample Loaded to Failure at 1260°C. Tensile Strength = 379 MPa. Sample was Stressed up to 250 MPa for >150 Hours at 1260°C before Loading to Failure.

MOR bars tested at 1232°C. The oxidation layer and the glass phase were not observed in this sample. This observation was another verification that slow crack growth due to glass phase formation does not occur up to a temperature of at least 1260°C. The slow crack growth becomes pronounced only at temperatures above 1300°C since the glass phase melting temperature is about 1300°C.

Figure 26 shows a plot of steady-state strain rate vs applied stress at 1370 and 1450°C. It can be observed that the steady-state strain rates were between 1×10^{-9} and 2×10^{-8} /sec. A multiple line regression analysis was used to determine the creep parameters from the generalized creep relation

$$\dot{\epsilon} = A \sigma^n \exp(-Q/RT)$$

where $\dot{\epsilon}$ is the steady-state strain rate, A is a constant, σ is the stress, "n" is the stress exponent, Q is the activation energy, R is the gas constant, and T is the absolute temperature. The values of "n" and "Q" were estimated as 2.4 and 720 kJ/mol, respectively. These creep parameters do not agree with the parameters determined for monolithic sintered SiC materials[6]. The mechanism of creep in the temperature and stress regime explored, if any, was not obvious in this material.

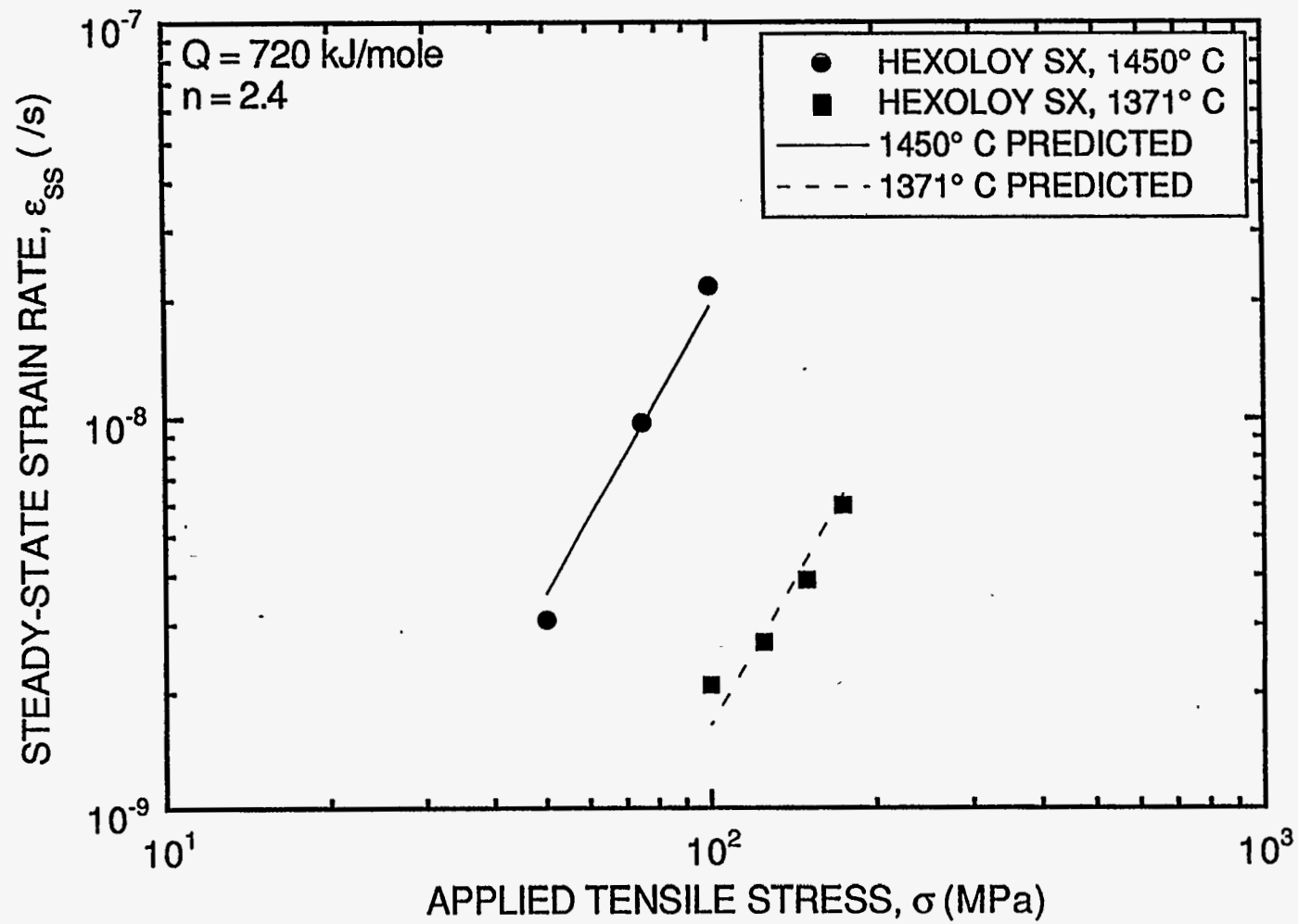


Figure 26. Steady-State Strain Rate vs Applied Stress at 1370 and 1450°C.

Task 2: SiC Powder Selection.

In this task the effect of starting SiC powder characteristics on densification and mechanical properties was explored. Powder availability and cost were also considered.

Experimental Procedure

Six different sources of commercially available SiC powder were chosen for this study. The greenforming process and densification conditions were the same for all powders. The powders were characterized for particle size distribution and surface area. The six different SiC powders were Sweco™ milled with sintering aid additives and spray dried into soft flowable agglomerates. The powders were isostatically pressed into 65-mm-square plates. The plates were pressureless sintered and later post-treated at a slightly higher temperature and pressure. Densities were measured by immersion techniques. The densified plate samples were machined into MIL-STD-1942 "B" (3 x 4 x 45 mm) MOR bars. Chevron notches were cut in the bars for fracture toughness (K_{IC}) evaluation. Mechanical characterization included flexural strength and K_{IC} at room temperature and dynamic fatigue at 1370°C. About 20 samples were used for the flexural strength evaluation and five Chevron-notched samples were used for the K_{IC} evaluation of each powder. Six samples were tested per stress rate at three stress rates differing by an order of magnitude for the slow crack growth parameter evaluation (dynamic fatigue). Fractographic investigation was also conducted to establish the flaw population.

Results

The powder characteristics and the densities obtained after pressureless sintering and post-treating are listed in Table 2. The median particle size for all the SiC powders is approximately the same. However, noticeable differences are observed in the particle size distribution and surface area of the powders, leading to differences in densification. The as-sintered and post-treated densities as a function of cumulative percentage of particles <1 μm in the distribution are shown in Figure 27. The densities as a function of surface area are shown in Figure 28. It appears from Figures 27 and 28 that there is a sharp cut-off limit in the particle size distribution and surface area beyond which densification is facilitated.

The results of the mechanical property evaluation for different powder sources are listed in Table 3. Mechanical property evaluation from materials fabricated from SiC powder "E" was not attempted due to inadequate densification. The fracture toughness (K_{IC}) evaluated from Chevron-notched bars fabricated from different SiC powder sources are not significantly different.

TABLE 2
Sintering Characteristics of Various SiC Powders

SiC Powder Source	Surface Area sq:m/gm	Median Particle Size μm	% Particles $\leq 1 \mu\text{m}$	% Theoretical Density Pressureless Sintered	Post Treatment Density
A	17.1	0.45	99.3	96.0	99.8
B	9.3	0.45	78.1	91.3	95.2
C	16.3	0.44	92.2	94.0	99.0
D	11.7	0.43	82.0	91.3	95.8
E	8.2	0.48	70.9	78.5	86.4
F	32.0	0.44	99.9	97.0	99.8

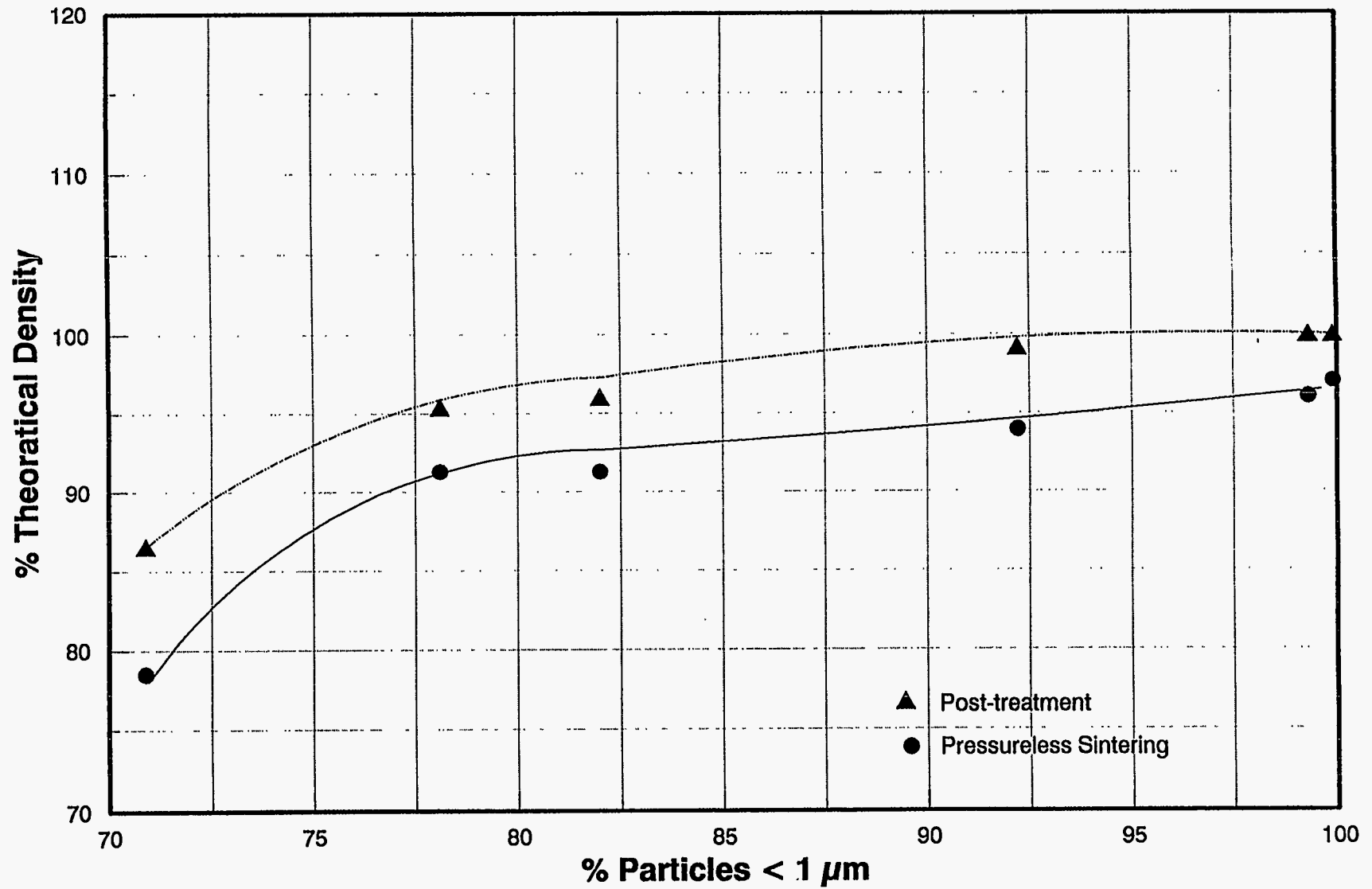


Figure 27. The As-Sintered and Post-Treated Densities as a Function of % Particles <1 μm.

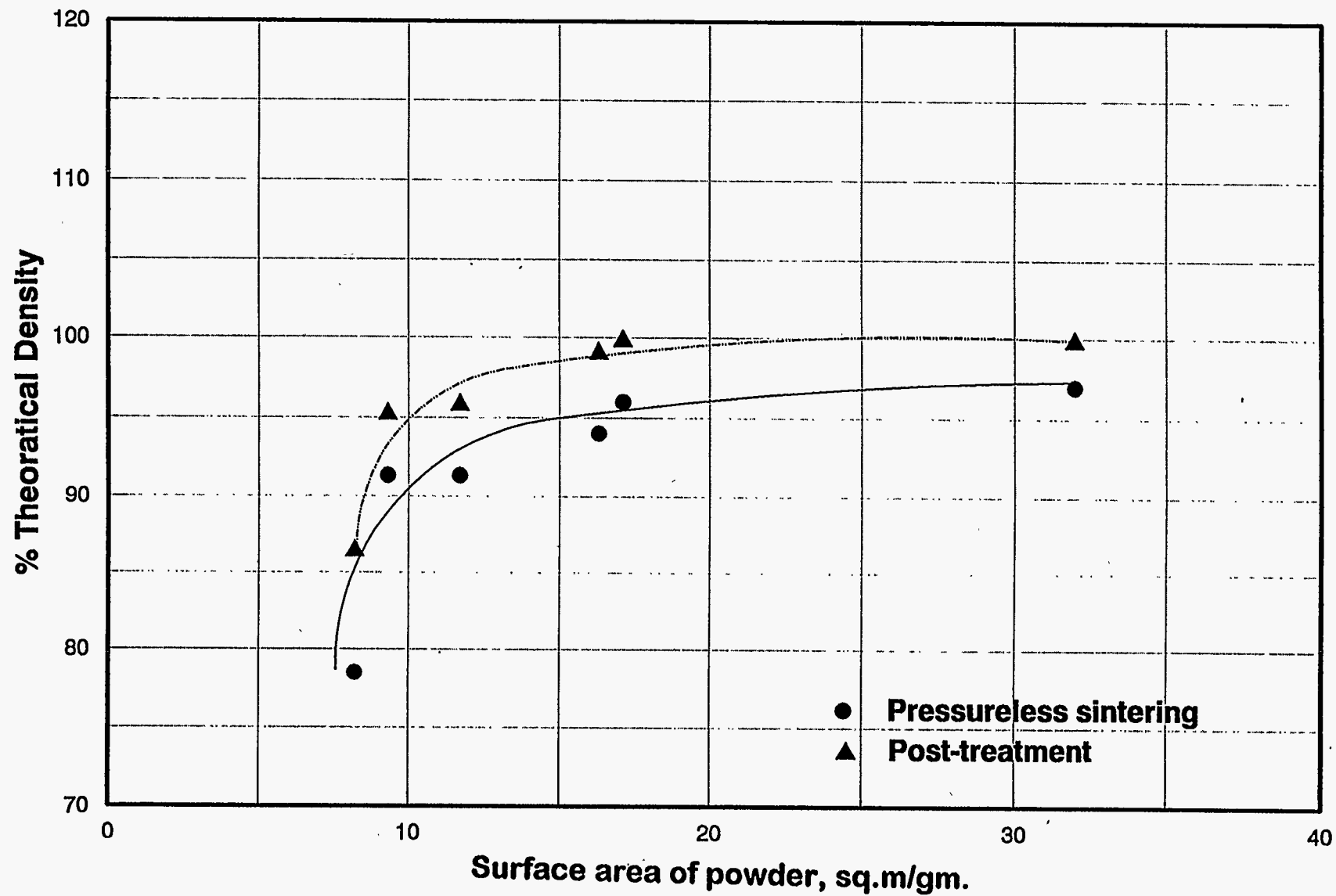


Figure 28. The As-Sintered and Post-Treated Densities as a Function of Surface Area of SiC Powders.

Mechanical Properties of SX-GI Material Fabricated with Various SiC Powders

TABLE 3

		Room Temperature						1371°C	
Powder Source	Toughness MPa.m ^{1/2}	MOR MPa	Weibull Modulus	Flaw	MOR MPa	Weibull Modulus	Flaw	SCG ^a Parameter	
A	4.05	779	5.3	Volume, Pools	420	10.3	SCG	14.5	
B	4.43	627	4.5	Volume, Pools	365	12.6	SCG	35.0	
C	3.77	724	2.6	Volume, Agglom. Surface, Mach.	352	2.9	SCG	17.3	
D	3.87	796	6.3	Volume, Voids	269	7.2	SCG	9.0	
E	-	-	-	-	-	-	-	-	
F	4.25	648	4.0	Volume, Pools	338	15.4	SCG	63.0	

*SCG - slow crack growth

However, the average room-temperature flexure strengths varied from 496 to 779 MPa. In almost all cases, the strength-limiting defects were identified to be "pools" of second phase clusters. The origination of such "pools" was related to the reaction of SiC with the second phase and was reported in detail in Task 1. The flexural strength at 1370°C appeared to be proportional to flexural strength at room temperature. Slow crack growth accompanied by glass phase formation has been determined to be the failure mechanism at 1370°C for samples fabricated from each of the powder sources. The slow crack growth mechanism was explained under Task 1. Though the slow crack growth parameter appeared to be high for powders "B" and "F," the strength levels were low. Actually, significant slow crack growth occurred even at higher stress rates for these materials as evidenced from optical fractography.

Samples fabricated from SiC powder source "A" yielded the best properties in terms of densification behavior and flexural strengths at room temperature and 1232°C. The other responses such as K_{IC} and slow crack growth exhibited only minor variations. Moreover, the SiC powder from source "A" was commercially available and the cost was the second lowest among the six powders considered. Based on these considerations, SiC powder from source "A" was selected for further optimization studies.

Task 3: Development of an Improved Dispersion Process.

The objective of this task was to improve the mixing and dispersion of the sintering aids. Three approaches were explored and are discussed below.

Experimental Procedure and Results

The first approach was to use chemical precursor sintering aids such as soluble nitrides and butoxides, rather than ceramic powders. Three mixes were prepared with additives from the chemical precursors. The total additive levels were 2 wt %, 2.5 wt %, and 3.0 wt %. Sintered densities of 70%, 88%, and 81% T.D., respectively, were obtained. These values were considerably lower than those with the control mix (95.5% T.D.). Chemical analysis for these three mixes showed relatively high free carbon contents (1.20 wt %, 1.15 wt %, and 1.12 wt %). This was believed to cause the low sintered density.

The second approach focused on improving premix uniformity by intensive grinding of sintering additives. Using a lab-size attrition mill, the sintering additives were ground to a median size of 0.50 to 0.55 μm from an as-received size of between 3.0 and 4.9 μm . With these ground sintering additives, three mixes were prepared with total additives of 2 wt %, 2.5 wt %, and 3.0 wt %.

Densities of 72%, 90%, and 93% T.D., respectively, were obtained for these three mixes, again lower than the control mix.

High-energy turbomilling of the sintering-aid powder was the third technique investigated. Professor Dale Wittmer of Southern Illinois University was retained as a consultant for this task. Using the turbomill in his laboratory, high-surface-area mixes (up to $22.8 \text{ m}^2/\text{gm}$) were obtained. More significantly, green densities as high as 66% were achieved. These samples were sintered and post-treated to high densities, with the exception of the samples from mix WR5 (Table 4) which were milled with sintered ZrO_2 (Y_2O_3) grinding media. It was suspected that contamination from ZrO_2 (Y_2O_3) media wear was responsible for the poor sintering in that sample. It should also be noted that all the green samples were prepared by a filter-pressing technique without the use of a binder. As a result the samples showed numerous cracks after sintering.

Because of this cracking problem, only a limited number of samples were obtained for MOR evaluation. These results are listed in Table 4. It can be seen that on the average turbomilled SX samples showed higher MOR strengths than those of the traditionally prepared samples. A high single-sample value of 1,227 MPa was obtained. To eliminate the cracking problem, a sixth turbomilled batch duplicating mix WR4 was prepared. Instead of using the filter-cake approach with no binder, spray drying with an added binder was used. With the later technique, the cracking problem was resolved. The average strength of the samples fabricated from spray drying was 903 MPa, with a highest single value of 1,172 MPa. Nevertheless, the sinterability was not consistent. A second plate processed the same way was found to exhibit a low density (<95% T.D.). However, based on the exceptional mechanical properties potentially achievable, turbomilling was chosen as the processing technique to be used for the next task.

TABLE 4**Turbomilling Results**

	Milled Time (hour)	Grind Media	Surface Area m ² /g	Postsinter Density g/cc	MOR R.T. MPa	No. of Samples
WR1	2	SiC	22.0	3.224	804	2
WR2	2	SiC	20.5	cracked	NA	
WR3	1	SiC	18.6	3.226	969	3
WR4	4	SiC	22.8	3.226	1231	1
WR5	0.5	Y-ZrO ₂	NM*	cannot be densified	NM	
WR6	4	SiC	NM	3.220	903**	4
SX-G1+	NA***	SiC	16.0	3.220	779	20

*Not measured

**Average strength 903 MPa, highest individual strength is 1,172 MPa

***Not applied

+Conventional process

Task 4: Optimize the Current SX-G1 SiC Material Through an Experimental Design Methodology.

Experimental Procedure

The objective of Task 4 was to optimize SX-G1 properties using a designed experiment approach by varying the three most influential processing parameters, namely, the sintering temperature, post-treatment temperature, and post-treatment pressure. The upper and lower limits for each of these factors are listed below:

Sinter Temperature: ST1 and ST2

Post-Treat Temperature: PT1 and PT2

Post-Treat Pressure: P1 and P2

A main factor plus interaction model was used to design this series of experiments[7]. The upper and lower limits of these three factors form a design experiment cube. Totally, there were ten sets of experimental conditions, with eight at the corners of the cube and two at the center of the cube as shown in Figure 29. The responses used to monitor these experiments included MOR and toughness at room temperature and 1232°C, and dynamic fatigue at 1232°C.

Results

Five powder mixes were prepared by turbomilling at Southern Illinois University using a new batch of SiC grit as grinding media. Sintered densities for these five mixes were between 90 and 94% T.D., as compared to >95% for the earlier turbomilled samples. After post-treatment the densities were in the range of 92 to 97%; however, they were still below full density. To understand the reason for this low density, particle size analyses for these five mixes were conducted. Larger particles (>1 mm) were detected with a Horiba analyzer. BET surface area measurements of these turbomilled mixes were between 16.0 and 17.2 m²/g as compared to >20 m²/g obtained on earlier turbomilled samples. Both results indicated the presence of large particles which are believed to be from the wear of SiC grit grinding media. A review of powder processing data also confirmed that there was about 250 grams of media wear from the grinding grit for each 1,500 gm batch mix. This excessive wear of grinding media was expected to have a significant effect on retarding the sintering kinetics.

The fracture surfaces of the Task 3 turbomilled sintered samples were also reviewed in light of this information. In one set of samples that densified poorly, excess grit concentration was observed on both the etched microstructure and the fracture surfaces. In another set that

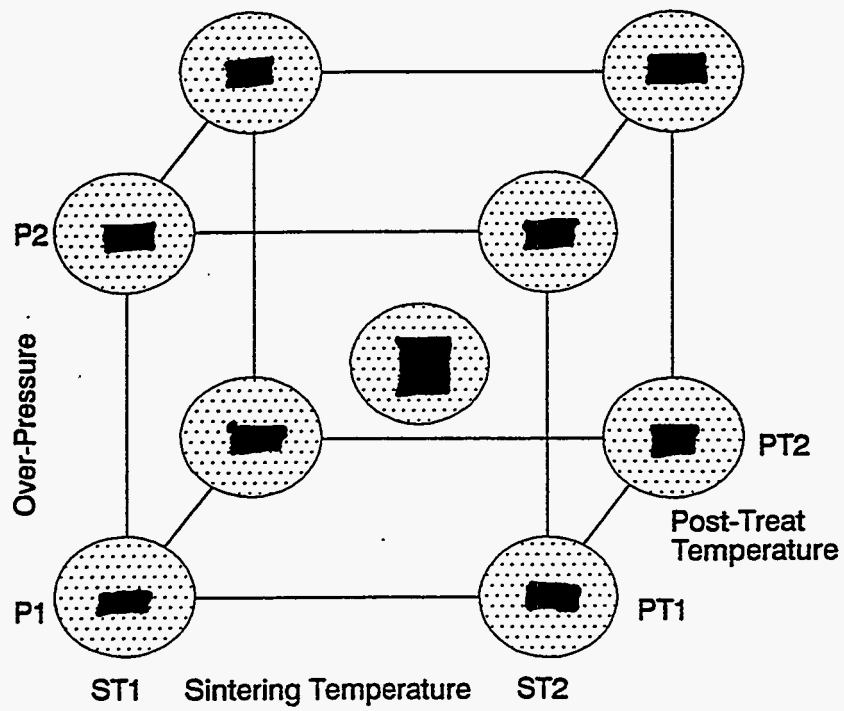


Figure 29. A Schematic of the Experimental Design Matrix.

achieved high densities and exhibited strengths in excess of 896 MPa (as high as 1,227 MPa), the fracture analysis revealed no obvious fracture origin. In other plates that also densified well but with somewhat lower strengths (ranging from 620 to 896 MPa), occasional grits were found and were determined to be the strength-limiting defects.

These results reveal that although turbomilling had shown the potential of achieving exceptionally high mechanical properties, processing reproducibility was a major issue. It was concluded that more effort was required to overcome this problem. It was therefore decided to utilize the traditional milling process as in Task 1 to complete the remaining Task 3 work.

A new SX-G1 mix was then prepared. All of the ten experiments were conducted successfully. The final densities obtained were between 97.7% and 100.0% T.D. with six out of ten conditions showing densities over 99.3% T.D. The appropriate mechanical testing and microstructural characterization were then conducted.

The mechanical properties determined at different combinations of the densification conditions are listed in Table 5. The upper limit of each processing parameter is denoted as +1 and the lower limit as -1. The toughness (K_{IC}) does not change appreciably as a function of densification parameters. However, the average flexure strength varies from 580 MPa (84 ksi) to 965 MPa (140 ksi) at room temperature.

Two types of strength limiting defects at room temperature were observed. One was a volume defect containing "pools" of second phase reaction product clusters. The other type of defect was surface defects induced by machining. Samples failing from the machining defects have a relatively high strength in excess of about 800 MPa (116 ksi). The flexure strength varied anywhere from about 345 MPa (50 ksi) to 900 MPa (130 ksi) for the volume defects, depending upon the location and size of the flaw. A typical volume defect (i.e., "pool") is shown in Figure 30, while a machining-induced surface failure is shown in Figure 31. Table 3 also lists the fraction of failures due to "pools." It can be seen that a higher mean flexure strength corresponds to fewer "pools" observed.

The strength at 1232°C appears to be directly related to the strength at room temperature. Moreover, no slow crack growth was evidenced at 1232°C since no strength drop at lower stress rates was observed. This observation is consistent with the earlier results observed in Task 1. Hence, the room-temperature flexural strength (MOR) was considered to be the primary response for different densification conditions. The room-temperature flexure strength response is shown schematically in Figure 32 corresponding to different densification conditions explored in the

TABLE 5

Density and Mechanical Properties Determined at Specific Densification Conditions in the Experimental Design Matrix

Sin. Temp	PT* Temp	PT Pressure	PT Density %	MOR, ksi		Fraction of "Pools"	Chevron Notch Toughness MPa √m	SCG** Parameter N
				RT	1232 °C			
0	0	0	99.9	128	76	0.53	4.9	No SCG
+1	-1	+1	99.7	84	60	0.80	5.2	No SCG
-1	+1	-1	99.5	103	66	0.40	5.4	No SCG
+1	+1	+1	100.0	124	60	0.53	4.9	No SCG
-1	+1	+1	99.9	140	76	0.27	4.7	No SCG
0	0	0	99.9	115	72	0.53	4.9	No SCG
-1	-1	+1	99.3	105	62	0.33	4.4	No SCG
+1	-1	-1	98.0	79	54	0.66	4.6	No SCG
-1	-1	-1	97.7	80	57	0.33	4.3	No SCG
+1	+1	-1	98.2	84	58	0.73	5.5	No SCG

* Post Treatment

** Slow Crack Growth - No SCG means N is approaching infinity.



Figure 30. "Silicon-Rich Pool" as Strength-Limiting Volume Defect.
Flexural Strength = 1,020 MPa (148 ksi).

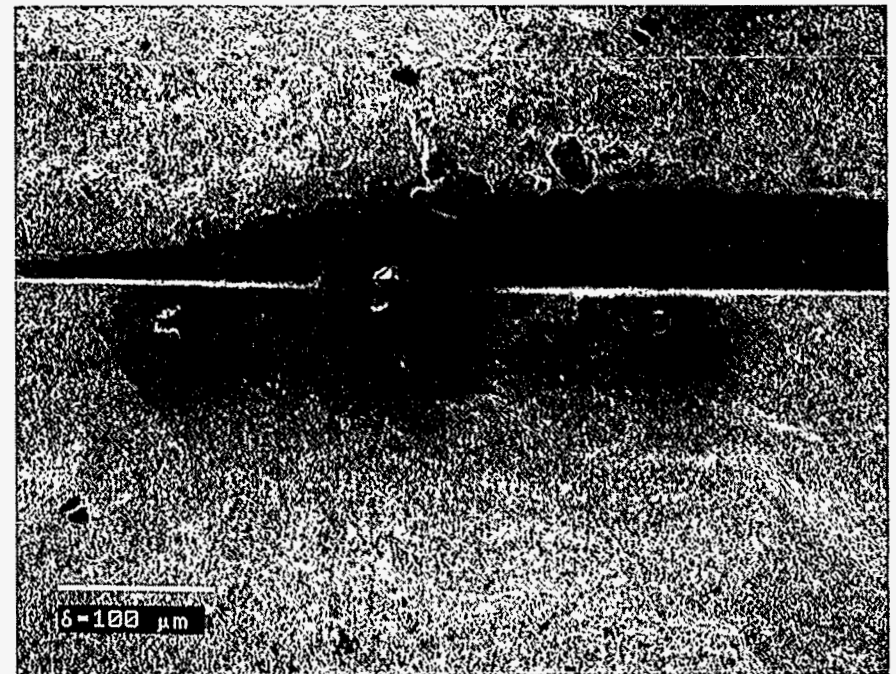
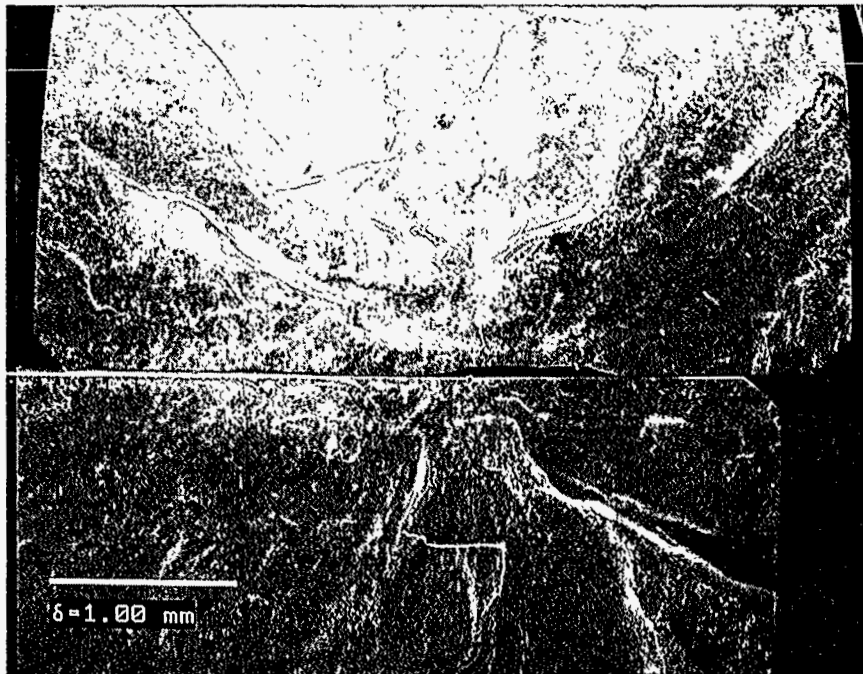


Figure 31. Machining Induced Surface Defect as the Fracture Origin.
Flexural Strength = 938 MPa (136 ksi).

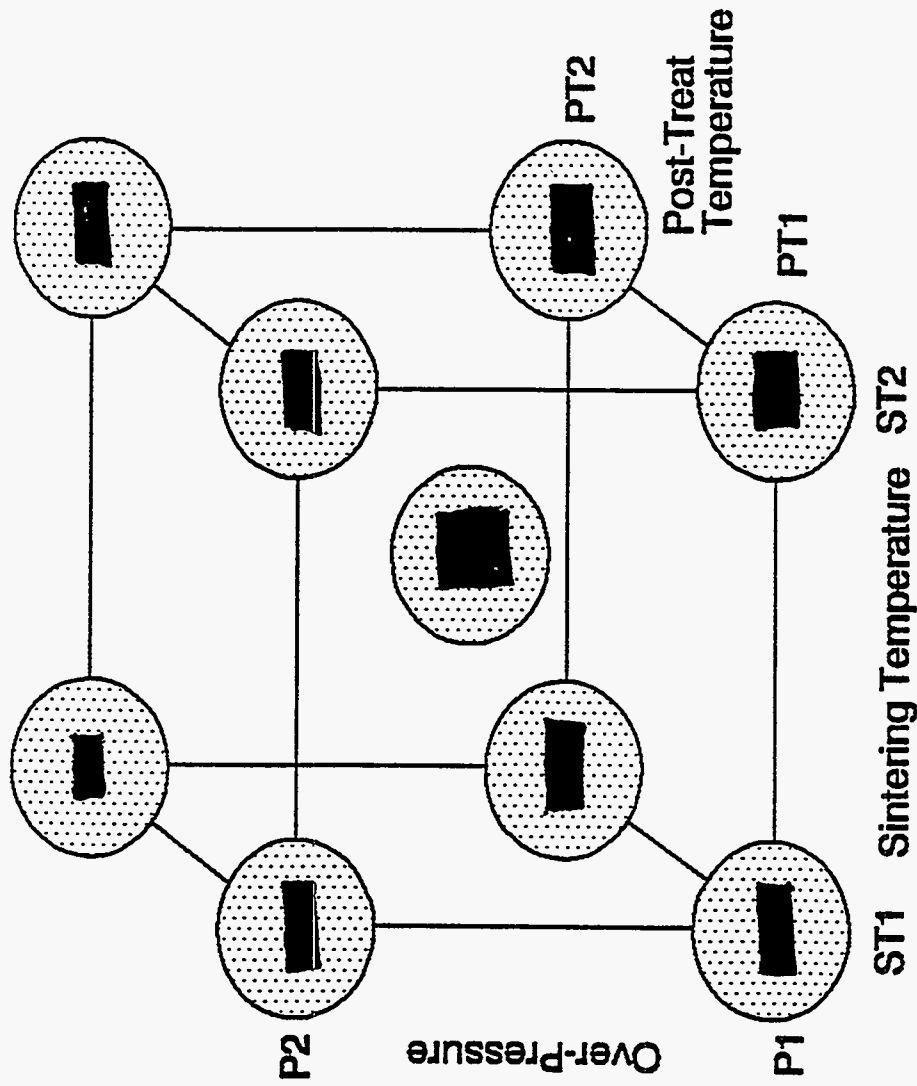


Figure 32. Room-Temperature Flexural Strength Corresponding to Various Densification Conditions in the Experimental Matrix.

statistical process design. The maximum room-temperature average flexural strength of 965 MPa (140 ksi) was observed for the densification conditions corresponding to the lowest sintering temperature, and higher post-treatment temperature and post-treatment pressure. Contour maps are shown in Figures 33, 34, and 35, illustrating the variation of strength with densification parameters.

It is interesting to note that a higher strength was observed with lower sintering temperatures and also corresponded to fewer volume flaws or "pools." The "pool" of second phase clusters appeared to form from the reaction of SiC with yttrium aluminate as suggested by Omori et al.[4], and from the SAM studies in Task 1. It is believed that at lower processing temperatures the extent of reaction was not as severe and thus a lesser number of smaller "pools" were formed.

It was clearly illustrated from the Task 4 experimental results that for the same corresponding post-treatment temperature and pressure, a lower sintering temperature leads to fewer "pools" and higher strength suggesting that sintering temperature was primarily responsible for the "pool" formation. The reaction between the Y-Al-O second phase and SiC matrix also involves the release of gaseous species such as CO and or CO₂. Under higher pressure the reactions would be thermodynamically less favorable. Hence, at higher pressures the reaction may be inhibited.

It was observed from the statistically designed experiments that the highest flexure strength obtained at room temperature was 965 MPa (140 ksi). This value was more than 20% higher than that obtained in the earlier Task 1 studies of 780 MPa (113 ksi). Also, fewer failures were due to volume defects and more failures were from the surface due to machining-induced defects. The higher fraction of surface defects will result in better reliability. Contour plots generated suggested that lower sintering temperatures combined with higher post-treatment temperatures and pressures would lead to improved flexure strengths. In fact, the optimum post-treatment conditions might fall outside the experimental cube indicating that the mechanical properties might be further improved with additional experimental work.

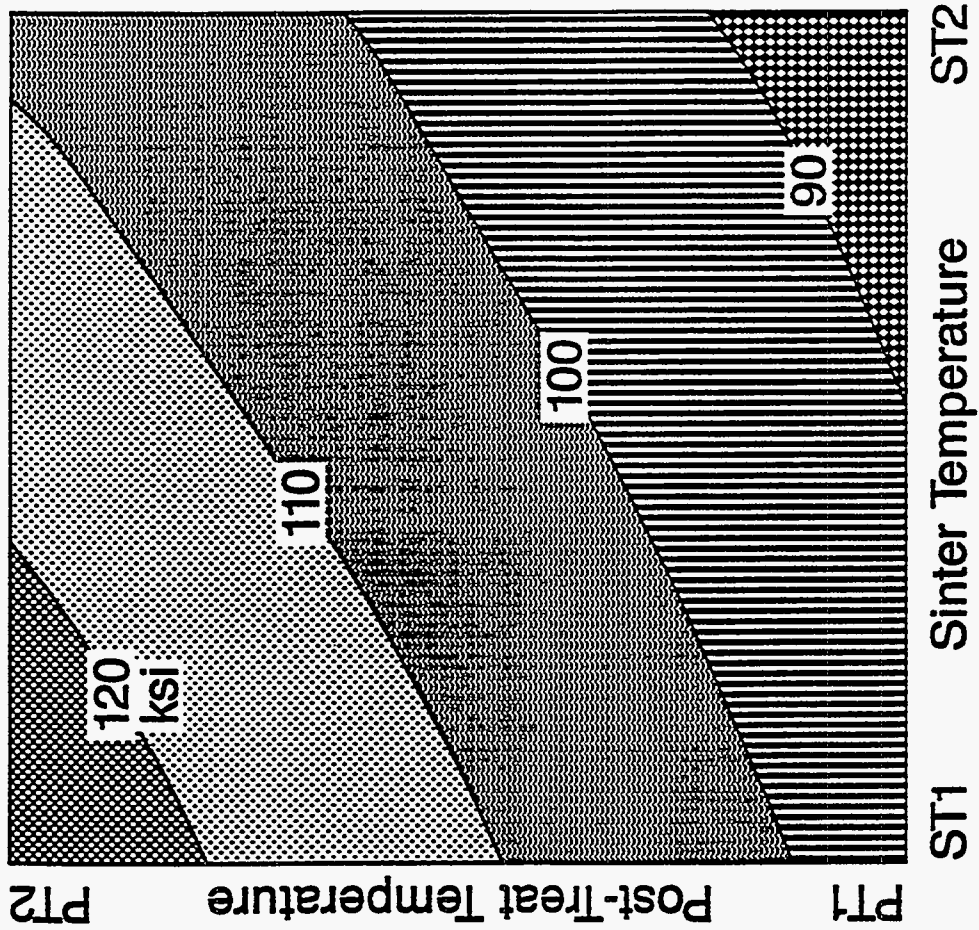


Figure 33. Contour Map of Room-Temperature Flexural Strength as a Function of Sintering Temperature and Post-Treatment Temperature

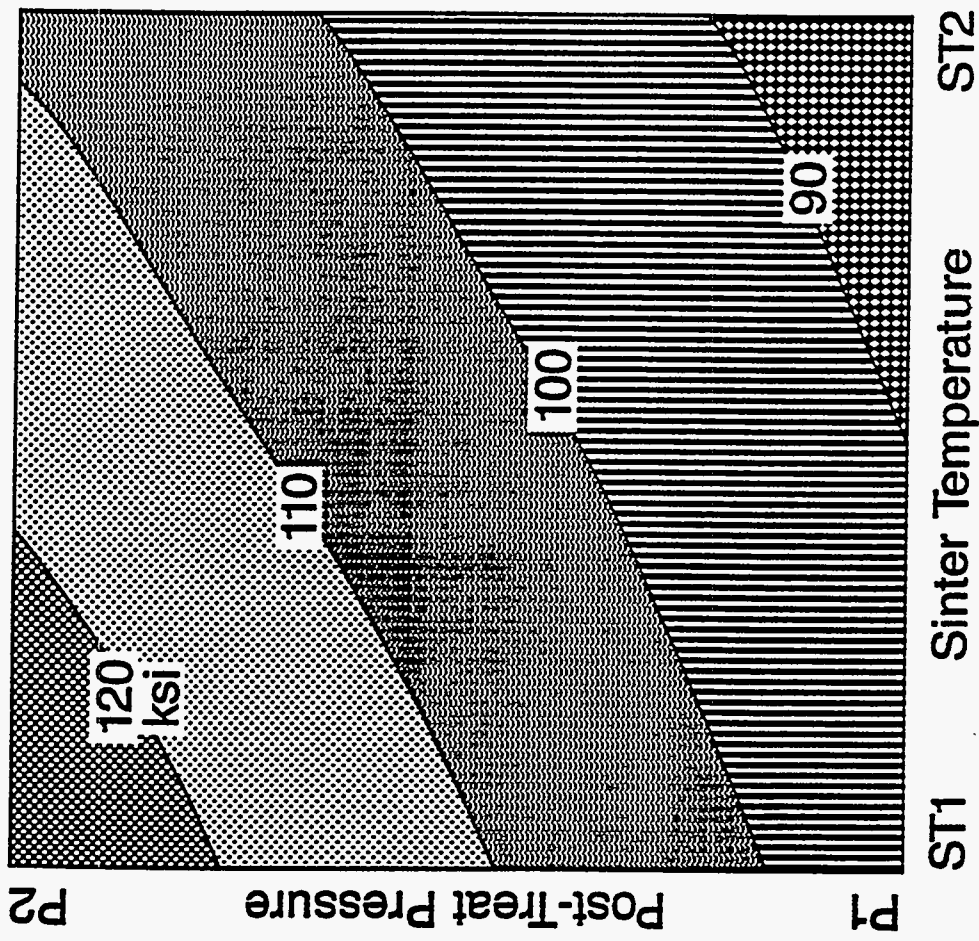


Figure 34. Contour Map of Room-Temperature Flexural Strength as a Function of Sintering Temperature and Post-Treatment Pressure.

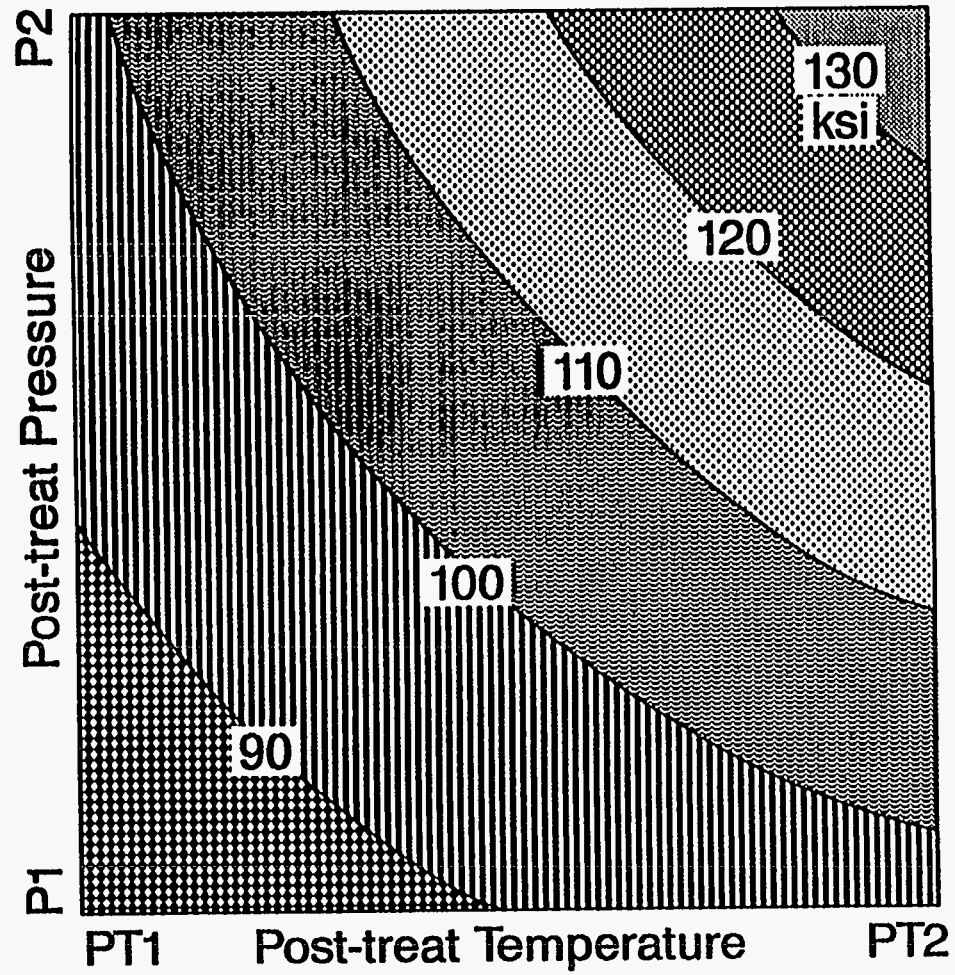


Figure 35. Contour Map of Room-Temperature Flexural Strength as a Function of Post-Treatment Temperature and Post-Treatment Pressure

Task 5a: Further Optimization of SX-G1.

Experimental Procedure and Results

The original objective of Task 5 was to optimize and fully characterize a second generation SX material. Prior to the start of Task 5 under a Carborundum in-house sponsored program, efforts to develop a second generation SX composition (SX-G2) as well as improve the processing conditions of turbomilling were conducted. Results obtained revealed that although there were several compositions identified to possess wider processing windows, the SX-G1 composition developed previously, after several years of intensive work, still provided the best room-temperature and high-temperature strength.

Based on these considerations, the technical approach for Task 5 was modified to conduct a second series of design experiments to further improve SX-G1 using the results described above and those reported under Task 4. The proposed experimental conditions were:

Powder Processing Techniques:	Improved Turbomilling Process
Sinter Temperature:	ST3 to ST4
Post-Treat Temperature:	PT3 to PT4
Post-Treat Pressure:	P3 to P4

The upper and lower limits for each of the furnacing parameters were selected based on the findings described earlier as well as previous Carborundum in-house research data. For example, although it was found that lower sintering temperatures and higher post-treatment temperatures were preferred, Carborundum in-house data has shown that SX-G1 could not be sintered below ST3 to achieve >99% post-treatment density. This defined the lower temperature limit. On the other hand, above T4 excessive silicon pool formation would occur, which defined the upper temperature limit. Regarding the post-treatment pressure, preliminary in-house data revealed that at or above P4 lower mechanical properties were obtained. Similar observations on Si_3N_4 furnacing indicated that too high a gas pressure could have the effect of "pumping" gaseous species into the material microstructure and retarding the sintering cycle. The upper limit for the post-treatment pressure was, therefore, set at P4.

It was estimated that 11 experiments were needed to complete the experimental matrix. Optimum furnacing conditions were to be selected after the evaluation of the resulting mechanical data, including MOR at room temperature and 1232°C, toughness at room temperature and 1232°C, and dynamic fatigue at 1232°C.

After an initial series of experiments to define the optimum turbomilling processing conditions, turbomilling was carried out in several batches at Southern Illinois University to yield 40 pounds of premix. These powder batches were then further processed at Carborundum. The particle size analysis and BET surface area measurements were consistent from batch to batch. The surface area increased from about 15 m²/g to about 22 m²/g after this milling process. The powder was then spray dried. Green plates were pressed and baked out. Prior to the start of the designed experiment, two plates were sintered at temperature ST3 since the sintering had never been attempted at this temperature. An acceptable density of 94% T.D. was obtained after pressureless sintering. Post treatment at temperature PT3 and pressure P4 resulted in >99% densification. Flexure bars were machined and an average MOR of 855 MPa (124 ksi) (from 18 samples) was obtained, which was about the order of strength expected from the previous design experiments. It was then decided to use this temperature in the design matrix.

Since a larger quantity of bars was needed for additional characterization and delivery, eight plates per crucible were used during the sintering runs, compared to two plates/crucible for the screening runs, and the sintering temperature was held constant. The density and mechanical property information are summarized in Table 6. The room-temperature MOR is schematically shown in Figure 36. It is surprising to note that plates sintered at temperature ST3 did not achieve density and mechanical property levels expected from the screening trials. For example, an average MOR of 965 MPa (140 ksi) was expected for the center point of the experiment. However, in two trials with a higher furnace loading, the MOR values were 806 MPa (117 ksi) and 813 MPa (118 ksi). The lower strength was attributed to an increased frequency of "pools."

The differences in densification and mechanical properties are believed to be due to the different number of plates used in the crucible for sintering (Table 7). It is possible that the partial pressures of gases are different under the two conditions leading to differences in densification and reaction of second phase(s) with SX SiC. It is realized here that the optimum densification condition is also a function of ratio of mass of green parts to volume of the crucible or, in general, furnacing configuration. This type of furnacing variation is not observed in the processing of HEXOLOY® SA SiC, and is therefore related to the presence of a second phase.

TABLE 6

Density and Mechanical Properties Determined at Specific Densification Conditions in the Expanded Experimental Design Matrix

					MOR, ksi		Toughness MPA \sqrt{m}		
Sin. Temp	Post Temp	Post Press	Sint. Density %	Post Density %	RT	1232 °C	RT	1232 °C	SCG* Parameter at 1232 °C
-1	-1	-1	85	91.5	57		3.1	2.5	No SCG
-1	-1	1	85	89.9	56		3.1	2.7	No SCG
-1	1	-1	85	93.7	79		4.0	2.7	No SCG
-1	1	1	85	97.4	75		4.0	2.8	No SCG
0	0	0	95.6	99.9	119	78	4.5	3.3	No SCG
0	0	0	94.8	99.8	114	71	4.5	3.1	No SCG
1	-1	-1	97	99.7	95		4.3	3.0	No SCG
1	-1	1	97	99.9	128	69	4.9	3.2	No SCG
1	1	-1	97.8	99.7	104	56	5.0	3.7	No SCG
1	1	1	97.8	99.8	100	55	5.2	4.0	No SCG

* Slow Crack Growth - No SCG means N is approaching infinity.

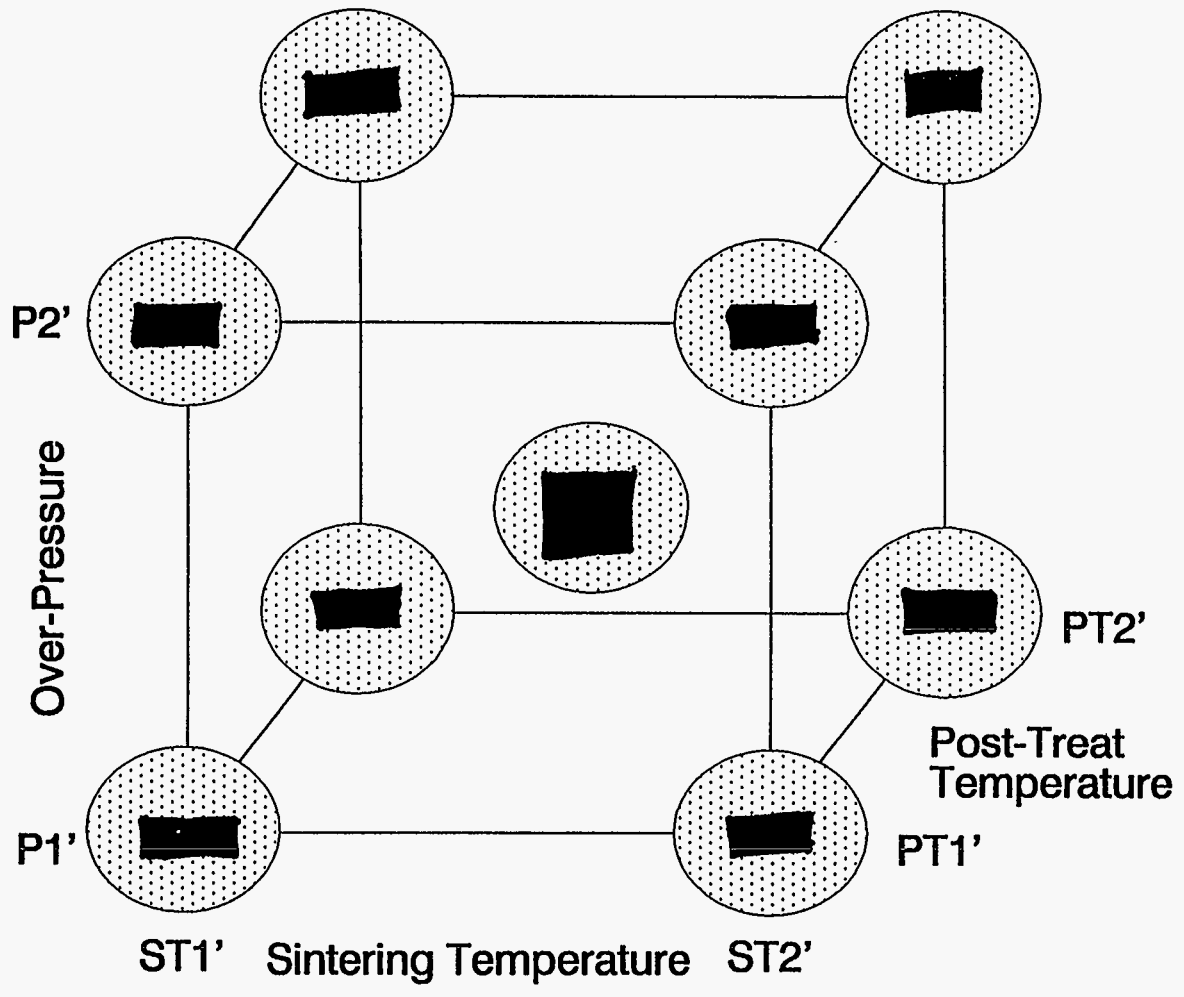


Figure 36. Room-Temperature Flexural Strength Corresponding to Various Densification Conditions in the Expanded Experimental Matrix.

TABLE 7

Summary of Strength and Flaw Data from Task 1, 4 and 5

Task	Fraction of "Pools" as Defects	MOR at RT MPa (ksi)
1	0.7	780 (113)
4	0.27	965 (140)
5	0.3	896 (130)

Task 5b: Complete Characterization of Optimized SX-G1 Composition.

Results

Based on the results obtained in Task 5a, it was determined that the optimum furnacing conditions corresponded to a sintering temperature of ST1 and a post-treatment temperature of PT1. It was realized from both Task 4 and 5 that higher post-pressures were favored. The optimum densification condition was then identified to correspond to a sintering temperature of ST1, post-treatment temperature of PT1, and a pressure of P4, which was higher than the maximum pressure P2 used in Task 3.

The premix powder was compacted into plates and rods. The rods were 216 mm in length and 21 mm in diameter. When densified under the above mentioned processing conditions, the plates resulted in >99% T.D. and rods resulted in 92% T.D. In Task 1 the rods also required a higher sintering temperature than plates for adequate densification. The rods were densified to >99% T.D. using the same conditions described in Task 1.

The stress rupture (static fatigue) and creep tests were not conducted because these properties were not expected to change since the chemistry and microstructure (grain size) were not different from the Task 1 material. However, flexural and tensile strength were evaluated at both room temperature and high temperatures. Dynamic fatigue experiments on flexural samples were conducted as in Task 1 for comparison.

The average room-temperature flexural strength for the optimized SX-G1 was determined to be 896 MPa (130 ksi). This strength is higher than the 780 MPa (113 ksi) obtained for SX-G1 from Task 1, and very close to 965 MPa (140 ksi) obtained from Task 4. The major strength-limiting defect was due to surface defects possibly introduced from grinding. The strength-limiting defects from Tasks 1, 4, and 5b are shown in Table 7 for comparison. It is clear that when densified under the optimum conditions as identified from Task 4, fewer "pools" were observed leading to higher strengths. Acceptable reproducibility in strength was also observed if the furnacing configuration (i.e., number of plates per crucible) was kept the same.

The flexural and tensile strengths determined at elevated temperatures are shown in Figure 37 and compared with the strength measured in Task 1. The strength at elevated temperatures is about the same for starting SX-G1 from Task 1 and optimized SX-G1 from Task 4 and 5 as expected. The dynamic fatigue response is shown in Figure 38 for both Task 1 and Task 5 materials. Again, no difference in slow crack growth characteristics was observed as expected. The uniaxial tensile strengths obtained from Task 1 and Task 5 are also about the same as seen in Figure 37. No

strengths obtained from Task 1 and Task 5 are also about the same as seen in Figure 37. No difference in strength was expected as the tensile rods were densified under the same sintering conditions.

The above characterization study reinforces the fact that sintering conditions, including the furnacing configurations, are very important in obtaining reproducible and improved mechanical properties.

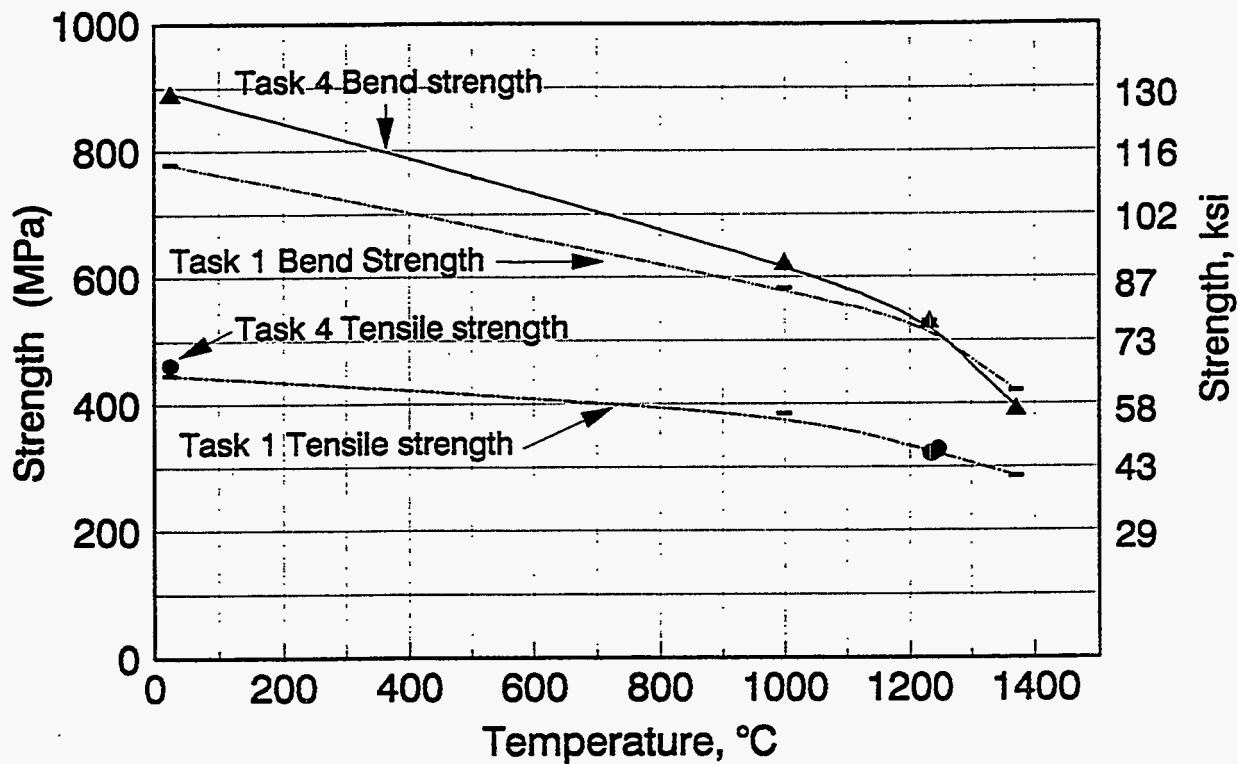


Figure 37. Flexural and Tensile Strength Determined in Tasks 1 and 5b at Various Temperatures.

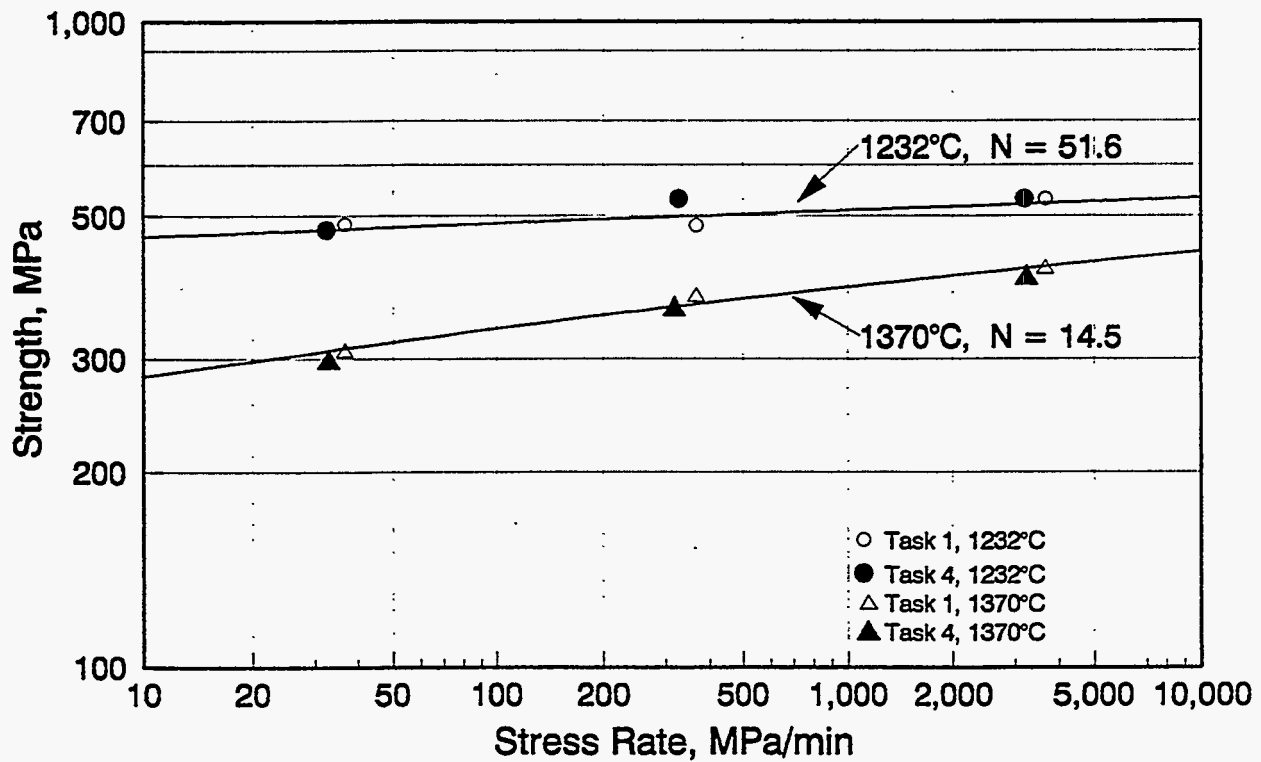


Figure 38. Dynamic Fatigue Response Measured from Tasks 1 and 5b.

SUMMARY

- A complete mechanical property database and structure–property relationship was established for the SX-G1 starting composition.
- From room temperature to 1232°C, the predominant strength-controlling defect was the silicon-rich pool of second phase clusters resulting from the reaction of yttrium aluminates with SiC.
- At elevated temperatures the decrease in strength was primarily due to the decrease in fracture toughness.
- Slow crack growth occurs at temperatures above 1300°C in air because of oxidation and subsequent glass-phase formation.
- The material possesses excellent creep resistance at all temperatures tested (up to 1450°C).
- Reduction in toughness and slow crack growth at elevated temperatures were inherent limitations of this material because of its chemistry.
- Turbomilling provides excellent mixing and dispersion but suffers from reproducibility due to excess wear of grinding media.
- Sintering-condition optimization lead to a reduction in reactivity of second phase and enhancement in room-temperature strength. Average flexural strength as high as 965 MPa (140 ksi) has been obtained.
- However, the optimum densification conditions and reactivity of second phase with SiC also depended upon furnacing configuration.

CONCLUSIONS

The results show that SiC materials sintered with the addition of yttrium and aluminum compounds can achieve the high level of mechanical properties required for their use in heat engine applications. Average MOR values up to 965 MPa (140 ksi) were demonstrated with a room-temperature fracture toughness up to two times that of boron and carbon sintered SiC. However, the reaction of the second phase with the SiC leading to strength-limiting pools results in increased variability in material properties. This variability was observed with both different sample sizes (i.e., plates vs tensile rods) and furnacing loads. If this variability can be eliminated or controlled, the relatively low cost of raw materials and processing for HEXOLOY® SX SiC manufacture would make these materials attractive candidates for commercialization for both low- and high-temperature engine applications.

ACKNOWLEDGMENTS

The authors gratefully acknowledge the support of HTML User Facility and the staffs, Drs. M.K. Ferber, M.G. Jenkins, and A.A. Wereszczak in conducting tensile tests and stress rupture experiments.

Research sponsored by the U.S. Department of Energy, Assistant Secretary for Energy Efficiency and Renewable Energy, Office of Transportation Technologies, as part of the Ceramic Technology Project of the Materials Development Program, under contract DE-AC05-84OR21400 with Martin Marietta Energy Systems, Inc.

REFERENCES

1. Chia, K. Y. and S. K. Lau, "High Toughness SiC," *Ceramic Eng. Sci. Proc.*, 12[9-10], 1845-61 (1991).
2. Srinivasan, G. V., K. Y. Chia, S. K. Lau, R. S. Storm, M. K. Ferber and M. G. Jenkins, "Mechanical Properties Evaluation of Generation I SX-SiC," Presented at the International Gas Turbine and Aeroengine Congress and Exposition, Cologne, Germany, June 1992. ASME/IGTI Proceedings, Publication # 92-GT-410.
3. Evans, A. G., Presentation at 92nd Annual Meeting of the Am. Ceram. Soc., Dallas, 1990.
4. Omori, M. and H. Takei, "Preparation of Pressureless-Sintered SiC-Y₂O₃-Al₂O₃," *J. Mater. Sci.*, 23, 3744-49 (1988).
5. Weber, C. and A. G. Evans, University of California, Santa Barbara, unpublished work.
6. Nixon, R. D. and R. F. Davis, "Diffusion Accommodated Grain Boundary Sliding and Dislocation Glide in the Creep of Sintered Alpha Silicon Carbide," *J. Am. Ceram. Soc.*, 75[7], 1786-1795 (1992).
7. Doehlert, D. H., *Experiment Strategies*, Seattle, WA.
8. Srinivasan, G. V., S. K. Lau, R. S. Storm, M. K. Ferber and M. G. Jenkins, "Process Optimization of HEXOLOY® SX-SiC Towards Improved Mechanical Properties," Presented at the International Gas Turbine and Aeroengine Congress and Exposition, Cincinnati, OH, May 24-27, 1992. ASME/IGTI Proceedings, Publication # 93-GT-415.

INTERNAL DISTRIBUTION

Central Research Library (2)
Document Reference Section
Laboratory Records Department (2)
Laboratory Records, ORNL RC
ORNL Patent Section
M&C Records Office (3)
L. F. Allard, Jr.
L. D. Armstrong
D. L. Balltrip
R. L. Beatty
P. F. Becher
T. M. Besmann
P. J. Blau
E. E. Bloom
K. W. Boling
R. A. Bradley
C. R. Brinkman
V. R. Bullington
R. S. Carlsmith
P. T. Carlson
G. M. Caton
S. J. Chang
D. D. Conger
R. H. Cooper, Jr.
S. A. David
J. H. DeVan
J. L. Ding
M. K. Ferber
W. Fulkerson
R. L. Graves
D. L. Greene
H. W. Hayden, Jr.
E. E. Hoffman
C. R. Hubbard

M. A. Janney
D. R. Johnson (5)
F. W. Jones
R. R. Judkins
M. A. Karnitz
B. L. Keyes
H. D. Kimrey, Jr.
T. G. Kollie
K. C. Liu
E. L. Long, Jr.
W. D. Manly
R. W. McClung
D. J. McGuire
J. R. Merriman
T. A. Nolan
A. E. Pasto
M. H. Rawlins
J. L. Rich
C. R. Richmond
J. M. Robbins
G. V. Rogers, Jr.
M. L. Santella
A. C. Schaffhauser
S. Scott
E. J. Soderstrom
D. P. Stinton
R. W. Swindeman
M. C. Tate
V. J. Tennery
T. N. Tiegs
J. R. Weir, Jr.
B. H. West
S. G. Winslow
J. M. Wyrick
C. S. Yust

EXTERNAL DISTRIBUTION

Pioneering Research Info. Ctr. E.I. Dupont de Nemours & Co. Inc. Experimental Station P.O. Box 80302 Wilmington DE 19880-0302	Joseph E. Amaral Instron Corporation Corporate Engineering Office 100 Royale Street Canton MA 02021
Jeffrey Abboud U.S. Advanced Ceramics Assoc. 1600 Wilson Blvd., Suite 1008 Arlington VA 22209	Edward M. Anderson Aluminum Company of America N. American Industrial Chemical P.O. Box 300 Bauxite AR 72011
James H. Adair University of Florida Materials Science & Engineering 317 MAE Bldg. Gainesville FL 32611-2066	Norman C. Anderson Ceradyne, Inc. Ceramic-to-Metal Division 3169 Redhill Avenue Costa Mesa CA 92626
Donald F. Adams University of Wyoming Mechanical Engineering Department P.O. Box 3295 Laramie WY 82071	Don Anson BCL Thermal Power Systems 505 King Avenue Columbus OH 43201-2693
Jalees Ahmad AdTech Systems Research Inc. Solid Mechanics 1342 N. Fairfield Road Dayton OH 45432-2698	Thomas Arbanas G.B.C. Materials Corporation 580 Monastery Drive Latrobe PA 15650-2698
Yoshio Akimune NISSAN Motor Co., Ltd. Materials Research Laboratory 1 Natsushima-Cho Yokosuka 237 JAPAN	Frank Armatiss 3M Company Building 60-1N-01 St. Paul MN 55144-1000
Mufit Akinc Iowa State University 322 Spedding Hall Ames IA 50011	Everett B. Arnold Detroit Diesel Corporation Mechanical Systems Technology 13400 Outer Drive West Detroit MI 48239-4001
Ilhan A. Aksay Princeton University A313 Engineering Quadrangle Princeton NJ 08544-5263	Bertil Aronsson Sandvik AB S-12680 Stockholm Lerkrogsvagen 19 SWEDEN
Richard L. Allor Ford Motor Company Materials Systems Reliability P.O. Box 2053, Room S-2031 Dearborn MI 48121-2053	Dennis Assanis University of Illinois Dept. of Mechanical Engineering 1206 W. Green Street Urbana IL 61801

V. S. Avva
North Carolina A&T State Univ.
Dept. of Mechanical Engineering
Greensboro NC 27411

Patrick Badgley
Sky Technologies, Inc.
2815 Franklin Drive
Columbus IN 47201

Sunggi Baik
Pohang Institute of Sci. & Tech.
P.O. Box 125
Pohang 790-600
KOREA

John M. Bailey
Consultant
Caterpillar, Inc.
P.O. Box 1875
Peoria IL 61656-1875

Bob Baker
Ceradyne, Inc.
3169 Redhill Avenue
Costa Mesa CA 92626

Frank Baker
Aluminum Company of America
Alcoa Technical Center
Alcoa Center PA 15069

Clifford P. Ballard
AlliedSignal Aerospace Company
Ceramics Program
P.O. Box 1021
Morristown NJ 07962-1021

B. P. Bandyopadhyay
ELID Team
Wako Campus
2-1 Hirosawa Wako-shi
Saitama 351-01
JAPAN.

P. M. Barnard
Ruston Gas Turbines Limited
P.O. Box 1
Lincoln LN2 5DJ
ENGLAND

Harold N. Barr
Hittman Corporation
9190 Red Branch Road
Columbia MD 21045

Renald D. Bartoe
Vesuvius McDanel
510 Ninth Avenue
Box 560
Beaver Falls PA 15010-0560

David L. Baty
Babcock & Wilcox - LRC
P.O. Box 11165
Lynchburg VA 24506-1165

Donald F. Baxter, Jr.
ASM International
Advanced Materials & Processes
Materials Park OH 44073-0002

M. Brad Beardsley
Caterpillar Inc.
Technical Center Bldg. E
P.O. Box 1875
Peoria IL 61656-1875

John C. Bell
Shell Research Limited
Thornton Research Centre
P.O. Box 1
Chester CH1 3SH
ENGLAND

M. Bentele
Xamag, Inc.
259 Melville Avenue
Fairfield CT 06430

Larry D. Bentsen
BFGoodrich Company
R&D Center
9921 Brecksville Road
Brecksville OH 44141

Louis Beregszazi
Defiance Precision Products
P.O. Drawer 428
Defiance OH 43512

Tom Bernecki
Northwestern University
1801 Maple Avenue
Evanston IL 60201-3135

Charles F. Bersch
Institute for Defense Analyses
1801 N. Beauregard Street
Alexandria VA 22311

Ram Bhatt
NASA Lewis Research Center
21000 Brookpark Road
Cleveland OH 44135

Deane I. Biehler
Caterpillar Inc.
Engineering Research Materials
P.O. Box 1875, Bldg. E
Peoria IL 61656-1875

John W. Bjerklie
Consolidated Natural Gas Service
Co. Inc.
Research Department
Pittsburgh PA 15222-3199

William D. Björndahl
TRW, Inc.
One Space Park, MS:R6-2188
Building 01, Room 2040
Redondo Beach CA 90278

Keith A. Blakely
Advanced Refractory Technologies,
Inc.
699 Hertel Avenue
Buffalo NY 14207

Edward G. Blanchard
Netzsch Inc.
119 Pickering Way
Exton PA 19341

Bruce Boardman
Deere and Company Technical Ctr.
3300 River Drive
Moline IL 61265

Hoechst Celanese Corporation
Short Hills NJ 07078

Russell Bockstedt
Hoechst Celanese Corporation
150 JFK Parkway
Short Hills NJ 07078

M. Boehmer
DLR German Aerospace Research
Estab.
Postfach 90 60 58
D-5000 Köln 90
GERMANY

Lawrence P. Boesch
EER Systems Corp.
1593 Spring Hill Road
Vienna VA 22182-2239

Donald H. Boone
Boone & Associates
2412 Cascade Drive
Walnut Creek CA 94598-4313

Tom Booth
AlliedSignal, Inc.
AiResearch Los Angeles Division
2525 West 190th Street
Torrance CA 90509-2960

Tibor Bornemisza
Sundstrand Power Systems
4400 Ruffin Road
San Diego CA 92186-5757

J.A.M. Boulet
University of Tennessee
Engineering Science and Mechanics
Knoxville TN 37996-2030

H. Kent Bowen
Massachusetts Institute of
Technology
77 Massachusetts Ave., Rm E40-434
Cambridge MA 02139

Leslie J. Bowen
Materials Systems
53 Hillcrest Road
Concord MA 01742

Steven C. Boyce
Air Force Office of Scientific
Research
AFOSR/NA Bldg. 410
Boiling AFB DC 20332-6448

Gary L. Boyd
Ceramic Engineering Consulting
328 Sneath Way
Alpine CA 91901

Steve Bradley
UOP Research Center
50 E. Algonquin Road
Des Plaines IL 60017-6187

Michael C. Brands
Cummins Engine Company, Inc.
P.O. Box 3005, Mail Code 50179
Columbus IN 47201

Raymond J. Bratton
Westinghouse Science & Technology
1310 Beulah Road
Pittsburgh PA 15235

John J. Brennan
United Technologies Corporation
Silver Lane, MS:24
East Hartford CT 06108

Terrence K. Brog
Golden Technologies Company
4545 McIntyre Street
Golden CO 80403

Gunnar Broman
317 Fairlane Drive
Spartanburg SC 29302

Al Brown
High-Tech Materials Alert
P.O. Box 882
Dayton NJ 08810

Jesse J. Brown
VPI & SU
Ctr. for Advanced Ceram Materials
Blacksburg VA 24061-0256

Sherman D. Brown
University of Illinois
Materials Science and Engineering
105 South Goodwin Avenue
Urbana IL 61801

S. L. Bruner
Ceramatec, Inc.
2425 South 900 West
Salt Lake City UT 84119

Walter Bryzik
U.S. Army Tank Automotive Command
R&D Center, Propulsion Systems
Warren MI 48397-5000

S. J. Burden
2572 Devonwood
Troy MI 48098

Curt V. Burkland
AMERCOM, Inc.
8928 Fullbright Avenue
Chatsworth CA 91311

Bill Bustamante
AMERCOM, Inc.
8928 Fullbright Avenue
Chatsworth CA 91311

Oral Buyukozturk
Massachusetts Institute of
Technology
77 Massachusetts Ave., Room 1-280
Cambridge MA 02139

David A. Caillet
Ethyl Corporation
451 Florida Street
Baton Rouge La 70801

Frederick J. Calnan
Heany Industries, Inc.
249 Briarwood Lane
Scottsville NY 14546

Roger Cannon
Rutgers University
P.O. Box 909
Piscataway NJ 08855-0909

Scott Cannon
P.O. Box 567254
Atlanta GA 30356

Harry W. Carpenter
1844 Fuerte Street
Fallbrook CA 92028

David Carruthers
Kyocera Industrial Ceramics
Company
P.O. Box 2279
Vancouver WA 98668-2279

Calvin H. Carter, Jr.
Cree Research, Inc.
2810 Meridian Parkway
Durham NC 27713

J. David Casey
35 Atlantis Street
West Roxbury MA 02132

Jere G. Castor
J. C. Enterprise
5078 N. 83rd Street
Scottsdale AZ 85250

James D. Cawley
Case Western Reserve University
Materials Science & Engineering
Cleveland OH 44106

Thomas C. Chadwick
Den-Mat Corporation
P.O. Box 1729
Santa Maria CA 93456

Ronald H. Chand
Chand Kare Technical Ceramics
2 Coppage Drive
Worcester MA 01603-1252

Robert E. Chaney
EG&G Idaho, Inc.
Idaho National Engineering Lab
P.O. Box 1625
Idaho Falls ID 83415-3525

Frank C. Chang
U.S. Army Materials Technology
AMTL-EMM
405 Arsenal Street
Watertown MA 02172

Nam S. Chang
Chrysler Corporation
12000 Chrysler Drive
Highland Park MI 48288-0001

William Chapman
Williams International Corp.
2280 W. Maple Road
Walled Lake MI 48390-0200

Ching-Fong Chen
LECO Corporation
3000 Lakeview Avenue
St. Joseph MI 49085

Frank Childs
EG&G Idaho, Inc.
Idaho National Engineering Lab
P.O. Box 1625
Idaho Falls ID 83415-3527

William J. Chmura
Torrington Company
59 Field Street
Torrington CT 06790-4942

Tsu-Wei Chou
University of Delaware
201 Spencer Laboratory
Newark DE 19716

R. J. Christopher
Ricardo Consulting Engineers
Bridge Works
Shoreham-By-Sea W. Sussex BN435FG
ENGLAND

Joel P. Clark
Massachusetts Institute of
Technology
Room 8-409
Cambridge MA 02139

Giorgio Clarotti
 Commission of the European Comm
 DGXII-C3, M075, 1-53;
 200 Rue de la Loi
 B-1049 Brussels
 BELGIUM

W. J. Clegg
 ICI Advanced Materials
 P.O. Box 11, The Heath
 Runcorn Cheshire WA7 4QE
 ENGLAND

Joseph Cleveland
 GTE Products Corporation
 Hawes Street
 Towanda PA 18848-0504

William S. Coblenz
 Adv. Research Projects Agency
 3701 N. Fairfax Drive
 Arlington VA 22203

Gloria M. Collins
 ASTM
 1916 Race Street
 Philadelphia PA 19103

William C. Connors
 Sundstrand Aviation Operations
 Materials Science & Engineering
 4747 Harrison Avenue
 Rockford IL 61125-7002

John A. Coppola
 Carborundum Company
 Niagara Falls R&D Center
 P.O. Box 832
 Niagara Falls NY 14302

Normand D. Corbin
 Norton Company
 SGNICC/NRDC
 Goddard Road
 Northboro MA 01532-1545

Douglas Corey
 AlliedSignal, Inc.
 2525 West 190th Street, MS:T52
 Torrance CA 90504-6099

Keith P. Costello
 Chand/Kare Technical Ceramics
 2 Coppage Drive
 Worcester MA 01603-1252

Ed L. Courtright
 Pacific Northwest Laboratory
 MS:K3-59
 Richland WA 99352

Anna Cox
 Mitchell Market Reports
 P.O. Box 23
 Monmouth Gwent NP5 4YG
 UNITED KINGDOM

J. Wesley Cox
 BIRL
 1801 Maple Avenue
 Evanston IL 60201-3135

Art Cozens
 Instron Corporation
 3414 Snowden Avenue
 Long Beach CA 90808

Mark Crawford
 New Technology Week
 4604 Monterey Drive
 Annandale VA 22003

Richard A. Cree
 Markets & Products, Inc.
 P.O. Box 14328
 Columbus OH 43214-0328

Les Crittenden
 Vesuvius McDanel
 Box 560
 Beaver Falls PA 15010

William J. Croft
 U.S. Army Materials Technology
 405 Arsenal Street
 Watertown MA 02172

M. J. Cronin
 Mechanical Technology, Inc.
 968 Albany-Shaker Road
 Latham NY 12110

Gary M. Crosbie
 Ford Motor Company
 20000 Rotunda Drive
 MD-2313, SRL Building
 Dearborn MI 48121-2053

Floyd W. Crouse, Jr.
 U.S. Department of Energy
 Morgantown Energy Technology Ctr
 P.O. Box 880
 Morgantown WV 26505

John Cuccio
 AlliedSignal Engines
 P.O. Box 52180, MS:1302-2Q
 Phoenix AZ 85072-2180

Raymond A. Cutler
 Ceramatec, Inc.
 2425 South 900 West
 Salt Lake City UT 84119

Stephen C. Danforth
 Rutgers University
 P.O. Box 909
 Piscataway NJ 08855-0909

Sankar Das Gupta
 Electrofuel Manufacturing Co.
 9 Hanna Avenue
 Toronto Ontario MGK-1W8
 CANADA

Frank Davis
 AlliedSignal Aerospace Company
 7550 Lucerne Drive, #203
 Middleburg Heights OH 44130

Robert F. Davis
 North Carolina State University
 Materials Engineering Department
 P.O. Box 7907
 Raleigh NC 27695

Thomas DeAngelis
 Carborundum Company
 Niagara Falls R&D Center
 P.O. Box 832
 Niagara Falls NY 14302

Michael DeLuca
 RSA Research Group
 1534 Claas Ave.
 Holbrook NY 11741

Gerald L. DePoorter
 Colorado School of Mines
 Metallurgical & Materials Engr
 Golden CO 80401

J. F. DeRidder
 Omni Electro Motive, Inc.
 12 Seely Hill Road
 Newfield NY 14867

Nick C. Dellow
 Materials Technology Publications
 40 Sotheron Road
 Watford Herts WD1 2QA
 UNITED KINGDOM

L. R. Dharani
 University of Missouri-Rolla
 224 M.E.
 Rolla MO 65401

Douglas A. Dickerson
 Union Carbide Specialty Powders
 1555 Main Street
 Indianapolis IN 46224

John Dodsworth
 Vesuvius Research & Development
 Technical Ceramics Group
 Box 560
 Beaver Falls PA 15010

B. Dogan
 Institut fur Werkstofforschung
 GKSS-Forschungszentrum Geesthacht
 Max-Planck-Strasse
 D-2054 Geesthacht
 GERMANY

Alan Dragoo
 U.S. Department of Energy
 ER-131, MS:F-240
 Washington DC 20817

Jean-Marie Drapier
 FN Moteurs S.A.
 Material and Processing
 B-4041 Milmort (Herstal)
 BELGIUM

Kenneth C. Dreitlein
 United Technologies Research Ctr
 Silver Lane
 East Hartford CT 06108

Robin A.L. Drew
 McGill University
 3450 University Street
 Montreal Quebec H3A 2A7
 CANADA

Winston H. Duckworth
 BCL
 Columbus Division
 505 King Avenue
 Columbus OH 43201-2693

Bill Durako
 Sundstrand Aviation Operations
 P.O. Box 7002
 Rockford IL 61125-7002

Ernest J. Duwell
 3M Abrasive Systems Division
 3M Center
 St. Paul MN 55144-1000

Chuck J. Dziedzic
 GTC Process Forming Systems
 4545 McIntyre Street
 Golden CO 80403

Robert J. Eagan
 Sandia National Laboratories
 Engineered Materials & Processes
 P.O. Box 5800
 Albuquerque NM 87185-5800

Jeffrey Eagleson
 Lanxide Corporation
 1001 Connecticut Avenue, N.W.
 Washington DC 20036

Harry E. Eaton
 United Technologies Corporation
 Silver Lane
 East Hartford CT 06108

Harvill C. Eaton
 Louisiana State University
 240 Thomas Boyd Hall
 Baton Rouge LA 70803

Christopher A. Ebel
 Carborundum Company
 Technology Division
 P.O. Box 832
 Niagara Falls NY 14302-0832

J. J. Eberhardt
 U.S. Department of Energy
 Office of Transportation Matrl's
 CE-34, Forrestal Building
 Washington DC 20585

Jim Edler
 Eaton Corporation
 26201 Northwestern Highway
 P.O. Box 766
 Southfield MI 48037

G. A. Eisman
 Dow Chemical Company
 Ceramics and Advanced Materials
 52 Building
 Midland MI 48667

William A. Ellingson
 Argonne National Laboratory
 Energy Technology Division
 9700 S. Cass Avenue
 Argonne IL 60439

Anita Kaye M. Ellis
 Machined Ceramics
 629 N. Graham Street
 Bowling Green KY 42101

Glen B. Engle
 Nuclear & Aerospace Materials
 16716 Martincoit Road
 Poway CA 92064

Jeff Epstein
Ceramic Technologies, Inc.
12739 Ashford Knoll
Houston TX 77082

Kenneth A. Epstein
Dow Chemical Company
2030 Building
Midland MI 48674

Art Erdemir
Argonne National Laboratory
9700 S. Cass Avenue
Argonne IL 60439

E. M. Erwin
Lubrizol Corporation
1819 East 225th Street
Euclid OH 44117

John N. Eustis
U.S. Department of Energy
Industrial Energy Efficiency Div
CE-221, Forrestal Building
Washington DC 20585

W. L. Everitt
Kyocera International, Inc.
8611 Balboa Avenue
San Diego CA 92123

Gordon Q. Evison
332 S. Michigan Avenue
Suite 1730
Chicago IL 60604

John W. Fairbanks
U.S. Department of Energy
Office of Propulsion Systems
CE-322, Forrestal Building
Washington DC 20585

Tim Fawcett
Dow Chemical Company
Advanced Ceramics Laboratory
1776 Building
Midland MI 48674

Robert W. Fawley
Sundstrand Power Systems
Div. of Sundstrand Corporation
P.O. Box 85757
San Diego CA 92186-5757

John J. Fedorchak
GTE Products Corporation
Hawes Street
Towanda PA 18848-0504

Jeff T. Fenton
Vista Chemical Company
900 Threadneedle
Houston TX 77079

Larry Ferrell
Babcock & Wilcox
Old Forest Road
Lynchburg VA 24505

Raymond R. Fessler
BIRL
1801 Maple Avenue
Evanston IL 60201

Ross F. Firestone
Ross Firestone Company
188 Mary Street
Winnetka IL 60093-1520

Sharon L. Fletcher
Arthur D. Little, Inc.
15 Acorn Park
Cambridge MA 02140-2390

Thomas F. Foltz
Textron Specialty Materials
2 Industrial Avenue
Lowell MA 01851

Renee G. Ford
Materials and Processing Report
P.O. Box 72
Harrison NY 10528

John Formica
Supermaterials
2020 Lakeside Avenue
Cleveland OH 44114

Edwin Frame
Southwest Research Institute
P.O. Drawer 28510
San Antonio TX 78284

Armanet Francois
French Scientific Mission
4101 Reservoir Road, N.W.
Washington DC 20007-2176

R. G. Frank
Technology Assessment Group
10793 Bentley Pass Lane
Loveland OH 45140

David J. Franus
Forecast International
22 Commerce Road
Newtown CT 06470

Marc R. Freedman
NASA Lewis Research Center
21000 Brookpark Road, MS:49-3
Cleveland OH 44135

Douglas Freitag
Bayside Materials Technology
17 Rocky Glen Court
Brookeville MD 20833

Brian R.T. Frost
Argonne National Laboratory
9700 S. Cass Avenue, Bldg. 900
Argonne IL 60439

Lawrence R. Frost
Instron Corporation
100 Royall Street
Canton MA 02021

Xiren Fu
Shanghai Institute of Ceramics
1295 Ding-xi Road
Shanghai 200050
CHINA

J. P. Gallagher
University of Dayton Research
Institute
300 College Park, JPC-250
Dayton OH 45469-0120

Garry Garvey
Golden Technologies Company Inc.
4545 McIntyre Street
Golden CO 80403

Richard Gates
NIST
Materials Bldg., A-256
Gaithersburg MD 20899

L. J. Gauckler
ETH-Zurich
Sonneggstrasse 5
CH-8092 Zurich 8092
SWITZERLAND

George E. Gazza
U.S. Army Materials Technology
Ceramics Research Division
405 Arsenal Street
Watertown MA 02172-0001

D. Gerster
CEA-DCOM
33 Rue De La Federation
Paris 75015
FRANCE

John Ghinazzi
Coors Technical Ceramics Company
1100 Commerce Park Drive
Oak Ridge TN 37830

Robert Giddings
General Electric Company
P.O. Box 8
Schenectady NY 12301

A. M. Glaeser
University of California
Lawrence Berkeley Laboratory
Hearst Mining Building
Berkeley CA 94720

Joseph W. Glatz
Naval Air Propulsion Center
Systems Engineering Division
510 Rocksville Road
Holland PA 18966

W. M. Goldberger
 Superior Graphite Company
 R&D
 2175 E. Broad Street
 Columbus OH 43209

Allan E. Goldman
 U.S. Graphite, Inc.
 907 W. Outer Drive
 Oak Ridge TN 37830

Stephen T. Gonczy
 Allied Signal Research
 P.O. Box 5016
 Des Plaines IL 60017

Jeffrey M. Gonzales
 GTE Products Corporation
 Hawes Street
 Towanda PA 18848-0504

Robert J. Gottschall
 U.S. Department of Energy
 ER-131, MS:G-236
 Washington DC 20585

Earl Graham
 Cleveland State University
 Dept. of Chemical Engineering
 Euclid Avenue at East 24th Street
 Cleveland OH 44115

John W. Graham
 Astro Met, Inc.
 9974 Springfield Pike
 Cincinnati OH 45215

G. A. Graves
 U. of Dayton Research Institute
 300 College Park
 Dayton OH 45469-0001

Robert E. Green, Jr.
 Johns Hopkins University
 Materials Science and Engineering
 Baltimore MD 21218

Alex A. Greiner
 Plint & Partners
 Oaklands Park
 Wokingham Berkshire RG11 2FD
 UNITED KINGDOM

Lance Groseclose
 General Motors Corporation
 Allison Gas Turbine Division
 P.O. Box 420, MS:W-5
 Indianapolis IN 46206

Thomas J. Gross
 U.S. Department of Energy
 Transportation Technologies
 CE-30, Forrestal Building
 Washington DC 20585

Mark F. Gruninger
 Union Carbide Corporation
 Specialty Powder Business
 1555 Main Street
 Indianapolis IN 46224

Ernst Gugel
 Cremer Forschungsinstitut
 GmbH&Co.KG
 Oeslauer Strasse 35
 D-8633 Roedental 8633
 GERMANY

John P. Gyekenyesi
 NASA Lewis Research Center
 21000 Brookpark Road, MS:6-1
 Cleveland OH 44135

Nabil S. Hakim
 Detroit Diesel Corporation
 13400 Outer Drive West
 Detroit MI 48239

Philip J. Haley
 General Motors Corporation
 P.O. Box 420, MS:T12A
 Indianapolis IN 46236

Judith Hall
 Fiber Materials, Inc.
 Biddeford Industrial Park
 5 Morin Street
 Biddeford ME 04005

Y. Hamano
Kyocera Industrial Ceramics Corp.
5713 E. Fourth Plain Blvd.
Vancouver WA 98661-6857

Y. Harada
IIT Research Institute
10 West 35th Street
Chicago IL 60616

R. A. Harmon
25 Schalren Drive
Latham NY 12110

Norman H. Harris
Hughes Aircraft Company
P.O. Box 800520
Saugus CA 91380-0520

Alan M. Hart
Dow Chemical Company
1776 Building
Midland MI 48674

Pat E. Hart
Battelle Pacific Northwest Labs
Ceramics and Polymers Development
P.O. Box 999
Richland WA 99352

Michael H. Haselkorn
Caterpillar In.
Technical Center, Building E
P.O. Box 1875
Peoria IL 61656-1875

Debbie Haught
U.S. Department of Energy
Off. of Transportation Materials
EE-34, Forrestal Bldg.
Washington DC 20585

N. B. Havewala
Corning Inc.
SP-PR-11
Corning NY 14831

John Haygarth
Teledyne WAA Chang Albany
P.O. Box 460
Albany OR 97321

Norman L. Hecht
U. of Dayton Research Institute
300 College Park
Dayton OH 45469-0172

Peter W. Heitman
General Motors Corporation
P.O. Box 420, MS:W-5
Indianapolis IN 46206-0420

Robert W. Hendricks
VPI & SU
210 Holden Hall
Blacksburg VA 24061-0237

Thomas L. Henson
GTE Products Corporation
Chemical & Metallurgical Division
Hawes Street
Towanda PA 18848

Thomas P. Herbell
NASA Lewis Research Center
21000 Brookpark Road, MS:49-3
Cleveland OH 44135

Marlene Heroux
Rolls-Royce, Inc.
2849 Paces Ferry Road, Suite 450
Atlanta GA 30339-3769

Robert L. Hershey
Science Management Corporation
1255 New Hampshire Ave., N.W.
Suite 1033
Washington DC 20036

Hendrik Heystek
Bureau of Mines
Tuscaloosa Research Center
P.O. Box L
University AL 35486

Robert V. Hillery
GE Aircraft Engines
One Neumann Way, M.D. H85
Cincinnati OH 45215

Arthur Hindman
Instron Corporation
100 Royall Street
Canton MA 02021

Hans Erich Hintermann
CSEM
Rue Breguet 2
Neuchatel 2000
SWITZERLAND

Shinichi Hirano
Mazda R&D of North America, Inc.
1203 Woodridge Avenue
Ann Arbor MI 48105

Tommy Hiraoka
NGK Locke, Inc.
1000 Town Center
Southfield MI 48075

Fu H. Ho
General Atomics
P.O. Box 85608
San Diego CA 92186-9784

John M. Hobday
U.S. Department of Energy
Morgantown Energy Technology Ctr
P.O. Box 880
Morgantown WV 26507

Clarence Hoenig
Lawrence Livermore National Lab
P.O. Box 808, Mail Code L-369
Livermore CA 94550

Thomas Hollstein
Fraunhofer-Institut fur
Werkstoffmechanik
Wohlerstrasse 11
79108 Freiburg
GERMANY

Richard Holt
National Research Council Canada
Structures and Materials Lab
Ottawa Ontario K1A 0R6
CANADA

Woodie Howe
Coors Technical Ceramics Company
1100 Commerce Park Drive
Oak Ridge TN 37830

Stephen M. Hsu
NIST
Gaithersburg MD 20899

Hann S. Huang
Argonne National Laboratory
9700 S. Cass Avenue
Argonne IL 60439-4815

Gene Huber
Precision Ferrites & Ceramics
5576 Corporate Drive
Cypress CA 90630

Harold A. Huckins
Princeton Advanced Technology
4 Bertram Place
Hilton Head SC 29928

Fred R. Huettig
Advanced Magnetics Inc.
45 Corey Lane
Mendham NJ 07945

Brian K. Humphrey
Lubrizol Petroleum Chemicals Co.
3000 Town Center, Suite 1340
Southfield MI 48075-1201

Robert M. Humrick
Dylon Ceramic Technologies
3100 Edgemoor Road
Cleveland Heights OH 44118

Lorretta Inglehart
National Science Foundation
Division of Materials Research
1800 "G" Street, N.W., Room 408
Washington DC 20550

Michael S. Inoue
Kyocera International, Inc.
8611 Balboa Avenue
San Diego CA 92123-1580

Joseph C. Jackson
U.S. Advanced Ceramics Assoc.
1600 Wilson Blvd., Suite 1008
Arlington VA 22209

Osama Jadaan
U. of Wisconsin-Platteville
1 University Plaza
Platteville WI 53818

Said Jahanmir
NIST
Materials Bldg., Room A-237
Gaithersburg MD 20899

Curtis A. Johnson
General Electric Company
P.O. Box 8
Schenectady NY 12301

Sylvia Johnson
SRI International
333 Ravenswood Avenue
Menlo Park CA 94025

Thomas A. Johnson
Lanxide Corporation
P.O. Box 6077
Newark DE 19714-6077

W. S. Johnson
Indiana University
One City Centre, Suite 200
Bloomington IN 47405

Walter F. Jones
AFOSR/NA
110 Duncan Ave., Ste. B115
Washington DC 20332-0001

Jill E. Jonkouski
U.S. Department of Energy
9800 S. Cass Avenue
Argonne IL 60439-4899

L. A. Joo
Great Lakes Research Corporation
P.O. Box 1031
Elizabethton TN 37643

A. David Joseph
SPX Corporation
700 Terrace Point
Muskegon MI 49443

Adam Jostsons
Australian Nuclear Science &
Technology
New Illawarra Road
Lucas Heights New South Wales
AUSTRALIA

Matthew K. Juneau
Ethyl Corporation
451 Florida Street
Baton Rouge LA 70801

Tom Kalamasz
Norton/TRW Ceramics
7A-4 Raymond Avenue
Salem NH 03079

Lyle R. Kallenbach
Phillips Petroleum
Mail Drop:123AL
Bartlesville OK 74004

Nick Kamiya
Kyocera Industrial Ceramics Corp.
25 Northwest Point Blvd., #450
Elk Grove Village IL 60007

Roy Kamo
Adiabatics, Inc.
3385 Commerce Park Drive
Columbus IN 47201

Chih-Chun Kao
Industrial Technology Research
Institute
195 Chung-Hsing Road, Sec. 4
Chutung Hsinchu 31015 R.O.C.
TAIWAN

Keith R. Karasek
AlliedSignal Aerospace Company
50 E. Algonquin Road
Des Plaines IL 60017-5016

Martha R. Kass
 U.S. Department of Energy
 Oak Ridge Operations
 Building 4500N, MS:6269
 Oak Ridge TN 37831-6269

Robert E. Kassel
 Ceradyne, Inc.
 3169 Redhill Avenue
 Costa Mesa CA 92626

Allan Katz
 Wright Laboratory
 Metals and Ceramics Division
 Wright-Patterson AFB OH 45433

R. Nathan Katz
 Worcester Polytechnic Institute
 100 Institute Road
 Worcester MA 01609

Tony Kaushal
 Detroit Diesel Corporation
 13400 Outer Drive, West
 Detroit MI 48239-4001

Ted Kawaguchi
 Tokai Carbon America, Inc.
 375 Park Avenue, Suite 3802
 New York NY 10152.

Noritsugu Kawashima
 TOSHIBA Corporation
 4-1 Ukishima-Cho
 Kawasaki-Ku Kawasaki 210
 JAPAN

Lisa Kempfer
 Penton Publishing
 1100 Superior Avenue
 Cleveland OH 44114-2543

Frederick L. Kennard, III
 AC Rochester
 1300 N. Dort Highway
 Flint MI 48556

David O. Kennedy
 Lester B. Knight Cast Metals Inc.
 549 W. Randolph Street
 Chicago IL 60661

George Keros
 Photon Physics
 3175 Penobscot Building
 Detroit MI 48226

Thomas Ketcham
 Corning, Inc.
 SP-DV-1-9
 Corning NY 14831

Pramod K. Khandelwal
 General Motors Corporation
 Allison Gas Turbine Division
 P.O. Box 420, MS:W05
 Indianapolis IN 46206

Jim R. Kidwell
 AlliedSignal Engines
 P.O. Box 52180
 Phoenix AZ 85072-2180

Shin Kim
 The E-Land Group
 19-8 ChangJeon-dong
 Mapo-gu, Seoul 121-190
 KOREA

W. C. King
 Mack Truck, Z-41
 1999 Pennsylvania Avenue
 Hagerstown MD 21740

Carol Kirkpatrick
 MSE, Inc.
 P.O. Box 3767
 Butte MT 59702

Tony Kirn
 Caterpillar Inc.
 Defense Products Department, JB7
 Peoria IL 61629

James D. Kiser
 NASA Lewis Research Center
 21000 Brookpark Road, MS:49-3
 Cleveland OH 44135

Max Klein
 900 24th Street, N.W., Unit G
 Washington DC 20037

Richard N. Kleiner
Golden Technologies Company
4545 McIntyre Street
Golden CO 80403

Stanley J. Klima
NASA Lewis Research Center
21000 Brookpark Road, MS:6-1
Cleveland OH 44135

Albert S. Kobayashi
University of Washington
Mechanical Engineering Department
Mail Stop:FU10
Seattle WA 98195

Shigeki Kobayashi
Toyota Central Research Labs
Nagakute Aichi 480-11
JAPAN

Richard A. Kole
Z-Tech Corporation
8 Dow Road
Bow NH 03304

Joseph A. Kovach
Eaton Corporation
32500 Chardon Road
Willoughby Hills OH 44094

Kenneth A. Kovaly
Technical Insights Inc.
P.O. Box 1304
Fort Lee NJ 07024-9967

Ralph G. Kraft
Spraying Systems Company
North Avenue at Schmale Road
Wheaton IL 60189-7900

Arthur Kranish
Trends Publishing Inc.
1079 National Press Building
Washington DC 20045

A. S. Krieger
Radiation Science, Inc.
P.O. Box 293
Belmont MA 02178

Pieter Krijgsman
Ceramic Design International
Holding B.V.
P.O. Box 68
Hattem 8050-AB
THE NETHERLANDS

Waltraud M. Kriven
University of Illinois
105 S. Goodwin Avenue
Urbana IL 61801

Edward J. Kubel, Jr.
ASM International
Advanced Materials & Processes
Materials Park OH 44073

Dave Kupperman
Argonne National Laboratory
9700 S. Cass Avenue
Argonne IL 60439

Oh-Hun Kwon
North Company
SGNICC/NRDC
Goddard Road
Northboro MA 01532-1545

W. J. Lackey
GTRI
Materials Science and Tech. Lab
Atlanta GA 30332

Jai Lal
Tenmat Ltd.
40 Somers Road
Rugby Warwickshire CV22 7DH
ENGLAND

Hari S. Lamba
General Motors Corporation
9301 West 55th Street
LaGrange IL 60525

Richard L. Landingham
Lawrence Livermore National Lab
P.O. Box 808, L-369
Livermore CA 94550

James Lankford
Southwest Research Institute
6220 Culebra Road
San Antonio TX 78228-0510

Stanley B. Lasday
Business News Publishing Co.
1910 Cochran Road, Suite 630
Pittsburgh PA 15220

S. K. Lau
Carborundum Company
Technology Division
P.O. Box 832, B-100
Niagara Falls NY 14302

J. Lawrence Lauderdale
Babcock & Wilcox
1850 "K" Street, Suite 950
Washington DC 20006

Jean F. LeCostaouec
Textron Specialty Materials
2 Industrial Avenue
Lowell MA 01851

Benson P. Lee
Technology Management, Inc.
4440 Warrensville Rd., Suite A
Cleveland OH 44128

Burtrand I. Lee
Clemson University
Olin Hall
Clemson SC 29634-0907

June-Gunn Lee
KIST
P.O. Box 131, Cheong-Ryang
Seoul 130-650
KOREA

Ran-Rong Lee
Ceramics Process Systems
Corporation
155 Fortune Boulevard
Mildford MA 01757

Stan Levine
NASA Lewis Research Center
21000 Brookpark Road, MS:49-3
Cleveland OH 44135

David Lewis, III
Naval Research Laboratory
Code 6370
Washington DC 20375-5343

Ai-Kang Li
Materials Research Labs., ITRI
195-5 Chung-Hsing Road, Sec. 4
Chutung Hsinchu 31015 R.O.C.
TAIWAN

Winston W. Liang
Hong Kong Industrial Technology
Centre
78 Tat Chee Avenue
4/F, HKPC Building -- Kowloon
HONG KONG

Robert Licht
Norton Company
SGNICC/NRDC
Goddard Road
Northboro MA 01532-1545

E. Lilley
Norton Company
SGNICC/NRDC
Goddard Road
Northboro MA 01532-1545

Chih-Kuang Lin
National Central University
Dept. of Mechanical Engineering
Chung-Li 32054
TAIWAN

Laura J. Lindberg
AlliedSignal Aerospace Company
Garrett Fluid Systems Division
P.O. Box 22200
Tempe AZ 85284-2200

Hans A. Lindner
 Cremer Forschungsinstitut
 GmbH&Co.KG
 Oeslauer Strasse 35
 D-8633 Rodental 8866
 GERMANY

Ronald E. Loehman
 Sandia National Laboratories
 Chemistry & Ceramics Dept. 1840
 P.O. Box 5800
 Albuquerque NM 87185

Jeffrey C. Logas
 Winona State University
 115 Pasteur Hall
 Winona MN 55987

Bill Long
 Babcock & Wilcox
 P.O. Box 11165
 Lynchburg VA 24506

L. A. Lott
 EG&G Idaho, Inc.
 Idaho National Engineering Lab
 P.O. Box 1625
 Idaho Falls ID 83415-2209

Raouf O. Loutfy
 MER Corporation
 7960 S. Kolb Road
 Tucson AZ 85706

Gordon R. Love
 Aluminum Company of America
 Alcoa Technical Center
 Alcoa Center PA 15960

Lydia Luckevich
 Ortech International
 2395 Speakman Drive
 Mississauga Ontario L5K 1B3
 CANADA

James W. MacBeth
 Carborundum Company
 Structural Ceramics Division
 P.O. Box 1054
 Niagara Falls NY 14302

George Maczura
 Aluminum Company of America
 3450 Park Lane Drive
 Pittsburgh PA 15275-1119

David Maginnis
 Tinker AFB
 OC-ALC/LIIRE
 Tinker AFB OK 73145-5989

Frank Maginnis
 Aspen Research, Inc.
 220 Industrial Boulevard
 Moore OK 73160

Tai-il Mah
 Universal Energy Systems, Inc.
 4401 Dayton-Xenia Road
 Dayton OH 45432

Kenneth M. Maillar
 Barbour Stockwell Company
 83 Linskey Way
 Cambridge MA 02142

S. G. Malghan
 NIST
 I-270 & Clopper Road
 Gaithersburg MD 20899

Lars Malrup
 United Turbine AB
 Box 13027
 Malmo S-200 44
 SWEDEN

John Mangels
 Ceradyne, Inc.
 3169 Redhill Avenue
 Costa Mesa CA 92626

Murli Manghnani
 University of Hawaii
 2525 Correa Road
 Honolulu HI 96822

Russell V. Mann
 Matec Applied Sciences, Inc.
 75 South Street
 Hopkinton MA 01748

William R. Manning
 Champion Aviation Products Div
 P.O. Box 686
 Liberty SC 29657

Ken Marnoch
 Amercom, Inc.
 8928 Fullbright Avenue
 Chatsworth CA 91311

Robert A. Marra
 Aluminum Company of America
 Alcoa Technical Center
 Alcoa Center PA 15069

Chauncey L. Martin
 3M Company
 3M Center, Building 60-1N-01
 St. Paul MN 55144

Steve C. Martin
 Advanced Refractory Technologies
 699 Hertel Avenue
 Buffalo NY 14207

Kelly J. Mather
 William International Corporation
 2280 W. Maple Road
 Walled Lake MI 48088

James P. Mathers
 3M Company
 3M Center, Bldg. 201-3N-06
 St. Paul MN 55144

Ron Mayville
 Arthur D. Little, Inc.
 15-163 Acorn Park
 Cambridge MA 02140

F. N. Mazadarany
 General Electric Company
 Bldg. K-1, Room MB-159
 P.O. Box 8
 Schenectady NY 12301

James W. McCauley
 Alfred University
 Binns-Merrill Hall
 Alfred NY 14802

Louis R. McCreight
 2763 San Ramon Drive
 Rancho Palos Verdes CA 90274

Colin F. McDonald
 McDonald Thermal Engineering
 1730 Castellana Road
 La Jolla CA 92037

B. J. McEntire
 Norton Company
 10 Airport Park Road
 East Granby CT 06026

Chuck McFadden
 Coors Ceramics Company
 600 9th Street
 Golden CO 80401

Thomas D. McGee
 Iowa State University
 110 Engineering Annex
 Ames IA 50011

Carol McGill
 Corning Inc.
 Sullivan Park, FR-02-08
 Corning NY 14831

James McLaughlin
 Sundstrand Power Systems
 4400 Ruffin Road
 P.O. Box 85757
 San Diego CA 92186-5757

Matt McMonigle
 U.S. Department of Energy
 Improved Energy Productivity
 CE-231, Forrestal Building
 Washington DC 20585

J. C. McVickers
 AlliedSignal Engines
 P.O. Box 52180, MS:9317-2
 Phoenix AZ 85072-2180

D. B. Meadowcroft
 "Jura," The Ridgeway
 Oxshott
 Leatherhead Surrey KT22 OLG
 UNITED KINGDOM

Joseph J. Meindl
Reynolds International, Inc.
6603 W. Broad Street
P.O. Box 27002
Richmond VA 23261-7003

Michael D. Meiser
AlliedSignal, Inc.
Ceramic Components
P.O. Box 2960, MS:T21
Torrance CA 90509-2960

George Messenger
National Research Council of
Canada
Building M-7
Ottawa Ontario K1A 0R6
CANADA

D. Messier
U.S. Army Materials Technology
SLCMT-EMC
405 Arsenal Street
Watertown MA 02172-0001

Arthur G. Metcalfe
Arthur G. Metcalfe and
Associates, Inc.
2108 East 24th Street
National City CA 91950

R. Metselaar
Eindhoven University
P.O. Box 513
Eindhoven 5600 MB
THE NETHERLANDS

David J. Michael
Harbison-Walker Refractories Co.
P.O. Box 98037
Pittsburgh PA 15227

Ken Michaels
Chrysler Motors Corporation
P.O. Box 1118, CIMS:418-17-09
Detroit MI 48288

Bernd Michel
Institute of Mechanics
P.O. Box 408
D-9010 Chemnitz
GERMANY

D. E. Miles
Commission of the European Comm.
rue de la Loi 200
B-1049 Brussels
BELGIUM

Carl E. Miller
AC Rochester
1300 N. Dort Highway, MS:32-31
Flint MI 48556

Charles W. Miller, Jr.
Centorr Furnaces/Vacuum
Industries
542 Amherst Street
Nashua NH 03063

R. Minimmi
Enichem America
2000 Cornwall Road
Monmouth Junction NJ 08852

Michele V. Mitchell
AlliedSignal, Inc.
Ceramic Components
P.O. Box 2960, MS:T21
Torrance CA 90509-2960

Howard Mizuhara
WESGO
477 Harbor Boulevard
Belmont CA 94002

Helen Moeller
Babcock & Wilcox
P.O. Box 11165
Lynchburg VA 24506-1165

Francois R. Mollard
Concurrent Technologies Corp.
1450 Scalp Avenue
Johnstown PA 15904-3374

Phil Mooney
Panametrics
221 Crescent Street
Waltham MA 02254

Geoffrey P. Morris
3M Company
3M Traffic Control Materials
Bldg. 209-BW-10, 3M Center
St. Paul MN 55144-1000

Jay A. Morrison
Rolls-Royce, Inc.
2849 Paces Ferry Road, Suite 450
Atlanta GA 30339-3769

Joel P. Moskowitz
Ceradyne, Inc.
3169 Redhill Avenue
Costa Mesa CA 92626

Brij Moudgil
University of Florida
Material Science & Engineering
Gainesville FL 32611

Christoph J. Mueller
Sprechsaa1 Publishing Group
P.O. Box 2962, Mauer 2
D-8630 Coburg
GERMANY

Thomas W. Mullan
Vapor Technologies Inc.
345 Route 17 South
Upper Saddle River NJ 07458

Theresa A. Mursick-Meyer
Norton Company
SGNICC/NRDC
Goddard Road
Northboro MA 01532-1545

M. K. Murthy
MkM Consultants International
10 Avoca Avenue, Unit 1906
Toronto Ontario M4T 2B7
CANADA

David L. Mustoe
Custom Technical Ceramics
8041 West I-70 Service Rd. Unit 6
Arvada CO 80002

Curtis V. Nakaishi
U.S. Department of Energy
Morgantown Energy Technology Ctr.
P.O. Box 880
Morgantown WV 26507-0880

Yoshio Nakamura
Faicera Research Institute
3-11-12 Misono
Sagamihara, Tokyo
JAPAN

Stefan Nann
Roland Berger & Partner GmbH
Georg-Glock-Str. 3
40474 Dusseldorf
GERMANY

K. S. Narasimhan
Hoeganaes Corporation
River Road
Riverton NJ 08077

Robert Naum
Applied Resources, Inc.
P.O. Box 241
Pittsford NY 14534

Malcolm Naylor
Cummins Engine Company, Inc.
P.O. Box 3005, Mail Code 50183
Columbus IN 47202-3005

Fred A. Nichols
Argonne National Laboratory
9700 S. Cass Avenue
Argonne IL 60439

H. Nickel
Forschungszentrum Juelich (KFA)
Postfach 1913
D-52425 Juelich
GERMANY

Dale E. Niesz
Rutgers University
Center for Ceramic Research
P.O. Box 909
Piscataway NJ 08855-0909

Paul W. Niskanen
Lanxide Corporation
P.O. Box 6077
Newark DE 19714-6077

David M. Nissley
United Technologies Corporation
Pratt & Whitney Aircraft
400 Main Street, MS:163-10
East Hartford CT 06108

Bruce E. Novich
Ceramics Process Systems Corp.
155 Fortune Boulevard
Milford MA 01757

Daniel Oblas
50 Meadowbrook Drive
Bedford MA 01730

Don Ohanehi
Magnetic Bearings, Inc.
1908 Sussex Road
Blacksburg VA 24060

Hitoshi Ohmori
ELID Team
Itabashi Branch
1-7 13 Kaga Itabashi
Tokyo 173
JAPAN

Robert Orenstein
General Electric Company
55-112, River Road
Schenectady NY 12345

Norb Osborn
Aerodyne Dallas
151 Regal Row, Suite 120
Dallas TX 75247

Richard Palicka
Cercom, Inc.
1960 Watson Way
Vista CA 92083

Muktesh Paliwal
GTE Products Corporation
Hawes Street
Towanda PA 18848

Joseph N. Panzarino
Norton Company
SGNICC/NRDC
Goddard Road
Northboro MA 01532-1545

Pellegrino Papa
Corning Inc.
MP-WX-02-1
Corning NY 14831

Terry Paquet
Boride Products Inc.
2879 Aero Park Drive
Traverse City MI 49684

E. Beth Pardue
MPC
8297 Williams Ferry Road
Lenior City TN 37771

Soon C. Park
3M Company
Building 142-4N-02
P.O. Box 2963
St. Paul MN 55144

Vijay M. Parthasarathy
Caterpillar/Solar Turbines
2200 Pacific Highway
P.O. Box 85376
San Diego CA 92186-5376

Harmut Paschke
Schott Glaswerke
Christoph-Dorner-Strasse 29
D-8300 Landshut
GERMANY

James W. Patten
 Cummins Engine Company, Inc.
 P.O. Box 3005, Mail Code 50183
 Columbus IN 47202-3005

Robert A. Penty
 Eastman Kodak Company
 Kodak Park
 Bldg., 326, 3rd Floor
 Rochester NY 14652-5120

Robert W. Pepper
 Textron Specialty Materials
 2 Industrial Avenue
 Lowell MA 01851

Peter Perdue
 Detroit Diesel Corporation
 13400 Outer Drive West,
 Speed Code L-04
 Detroit MI 48239-4001

John J. Petrovic
 Los Alamos National Laboratory
 Group MST-4, MS:G771
 Los Alamos NM 87545

Frederick S. Pettit
 University of Pittsburgh
 Pittsburgh PA 15261

Ben A. Phillips
 Phillips Engineering Company
 721 Pleasant Street
 St. Joseph MI 49085

Richard C. Phoenix
 Ohmtek, Inc.
 2160 Liberty Drive
 Niagara Falls NY 14302

Bruce J. Pletka
 Michigan Technological University
 Metallurgical & Materials Engr.
 Houghton MI 49931

John P. Pollinger
 AlliedSignal, Inc.
 Ceramic Components
 P.O. Box 2960, MS:T21
 Torrance CA 90509-2960

P. Popper
 High Tech Ceramics International
 Journal
 22 Pembroke Drive - Westlands
 Newcastle-under-Lyme
 Staffs ST5 2JN
 ENGLAND

F. Porz
 Universitat Karlsruhe
 Institut für Keramik im
 Maschinendau
 Postfach 6980
 D-76128 Karlsruhe
 GERMANY

Harry L. Potma
 Royal Netherlands Embassy
 Science and Technology
 4200 Linnean Avenue, N.W.
 Washington DC 20008

Bob R. Powell
 North American Operations
 Metallurgy Department
 Box 9055
 Warren MI 48090-9055

Stephen C. Pred
 ICD Group, Inc.
 1100 Valley Brook Avenue
 Lyndhurst NJ 07071

Karl M. Prewo
 United Technologies Research Ctr.
 411 Silver Lane, MS:24
 East Hartford CT 06108

Vimal K. Pujari
 Norton Company
 SGNICC/NRDC
 Goddard Road
 Northboro MA 01532-1545

George Quinn
 NIST
 Ceramics Division, Bldg. 223
 Gaithersburg MD 20899

Ramas V. Raman
Ceracon, Inc.
1101 N. Market Boulevard, Suite 9
Sacramento CA 95834

Charles F. Rapp
Owens Corning Fiberglass
2790 Columbus Road
Granville OH 43023-1200

Dennis W. Readey
Colorado School of Mines
Metallurgy and Materials Engr.
Golden CO 80401

Wilfred J. Rebello
PAR Enterprises, Inc.
12601 Clifton Hunt Lane
Clifton VA 22024

Harold Rechter
Chicago Fire Brick Company
7531 S. Ashland Avenue
Chicago IL 60620

Robert R. Reeber
U.S. Army Research Office
P.O. Box 12211
Research Triangle Park NC
27709-2211

K. L. Reifsnider
VPI & SU
Engineering Science and Mechanics
Blacksburg VA 24061

Paul E. Rempes
McDonnell Douglas Aircraft Co.
P.O. Box 516, Mail Code:0642263
St. Louis MO 63166-0516

Gopal S. Revankar
John Deere Company
3300 River Drive
Moline IL 61265

K. Y. Rhee
Rutgers University
P.O. Box 909
Piscataway NJ 08854

James Rhodes
Advanced Composite Materials Corp
1525 S. Buncombe Road
Greer SC 29651

Roy W. Rice
W. R. Grace and Company
7379 Route 32
Columbia MD 21044

David W. Richerson
2093 E. Delmont Drive
Salt Lake City UT 84117

Tomas Richter
J. H. France Refractories
1944 Clarence Road
Snow Shoe PA 16874

Michel Rigaud
Ecole Polytechnique
Campus Universite De Montreal
P.O. Box 6079, Station A
Montreal, P.Q. Quebec H3C 3A7
CANADA

John E. Ritter
University of Massachusetts
Mechanical Engineering Department
Amherst MA 01003

Frank L. Roberge
AlliedSignal Engines
P.O. Box 52180
Phoenix AZ 85072-2180

W. Eric Roberts
Advanced Ceramic Technology, Inc.
990 "F" Enterprise Street
Orange CA 92667

Y. G. Roman
TNO TPD Keramick
P.O. Box 595
Eindhoven 5600 AN
HOLLAND

Michael Rossetti
Arthur D. Little, Inc.
15 Acorn Park
Cambridge MA 01240

Barry Rossing
Lanxide Corporation
P.O. Box 6077
Newark DE 19714-6077

Steven L. Rotz
Lubrizol Corporation
29400 Lakeland Boulevard
Wickliffe OH 44092

Robert Ruh
Wright Laboratory
WL/MLLM
Wright-Patterson AFB OH 45433

Robert J. Russell
17 Highgate Road
Framingham MA 01701

Jon A. Salem
NASA Lewis Research Center
21000 Brookpark Road
Cleveland OH 44135

W. A. Sanders
NASA Lewis Research Center
21000 Brookpark Road, MS:49-3
Cleveland OH 44135

J. Sankar
North Carolina A&T State Univ.
Dept. of Mechanical Engineering
Greensboro NC 27406

Yasushi Sato
NGK Spark Plugs (U.S.A.), Inc.
1200 Business Center Drive, #300
Mt. Prospect IL 60056

Maxine L. Savitz
AlliedSignal, Inc.
Ceramic Components
P.O. Box 2960, MS:T21
Torrance CA 90509-2960

Ashok Saxena
GTRI
Materials Engineering
Atlanta GA 30332-0245

David W. Scanlon
Instron Corporation
100 Royall Street
Canton MA 02021

Charles A. Schacht
Schacht Consulting Services
12 Holland Road
Pittsburgh PA 15235

Robert E. Schafrik
National Materials Advisory Board
2101 Constitution Ave., N.W.
Washington DC 20418

James Schienle
AlliedSignal Engines
P.O. Box 52180, MS:1302-2P
Phoenix AZ 85072-2180

John C. Schneider
San Juan Technologies, Inc.
3210 Arena Road
Colorado Springs CO 80921-1503

Gary Schnittgrund
Rocketdyne, BA05
6633 Canoga Avenue
Canoga Park CA 91303

Mark Schomp
Lonza, Inc.
17-17 Route 208
Fair Lann NJ 07410

Joop Schoonman
Delft University of Technology
P.O. Box 5045
2600 GA Delft
THE NETHERLANDS

Robert B. Schulz
U.S. Department of Energy
Office of Transportation Matrls.
CE-34, Forrestal Building
Washington DC 20585

Murray A. Schwartz
Materials Technology Consulting
30 Orchard Way, North
Potomac MD 20854

Peter Schwarzkopf
SRI International
333 Ravenswood Avenue
Menlo Park CA 94025

William T. Schwessinger
Multi-Arc Scientific Coatings
1064 Chicago Road
Troy MI 48083-4297

W. D. Scott
University of Washington
Materials Science Department
Mail Stop:FB10
Seattle WA 98195

Nancy Scoville
Thermo Electron Technologies
P.O. Box 9046
Waltham MA 02254-9046

Thomas M. Sebestyen
U.S. Department of Energy
Advanced Propulsion Division
CE-322, Forrestal Building
Washington DC 20585

Brian Seegmiller
Coors Ceramics Company
600 9th Street
Golden CO 80401

T. B. SeLover
AICRE/DIPPR
3575 Traver Road
Shaker Heights OH 44122

Charles E. Semler
Semler Materials Services
4160 Mumford Court
Columbus OH 43220

Thomas Service
Service Engineering Laboratory
324 Wells Street
Greenfield MA 01301

Kish Seth
Ethyl Corporation
P.O. Box 341
Baton Rouge LA 70821

William J. Shack
Argonne National Laboratory
9700 S. Cass Avenue, Bldg. 212
Argonne IL 60439

Peter T.B. Shaffer
Technical Ceramics Laboratories,
4045 Nine/McFarland Drive
Alpharetta GA 30201

Richard K. Shaltens
NASA Lewis Research Center
21000 Brookpark Road, MS:302-2
Cleveland OH 44135

Robert S. Shane
1904 NW 22nd Street
Stuart FL 34994-9270

Ravi Shankar
Chromalloy
Research and Technology Division
Blaisdell Road
Orangeburg NY 10962

Terence Sheehan
Alpex Wheel Company
727 Berkley Street
New Milford NJ 07646

Dinesh K. Shetty
University of Utah
Materials Science and Engineering
Salt Lake City UT 84112

Masahide Shimizu
New Ceramics Association
Shirasagi 2-13-1-208, Nakano-ku
Tokyo 165
JAPAN

Thomas Shreves
American Ceramic Society, Inc.
735 Ceramic Place
Westerville OH 43081-8720

Jack D. Sibold
Coors Ceramics Company
4545 McIntyre Street
Golden CO 80403

Johann Siebels
Volkswagen AG
Werkstofftechnologie
Postfach 3180
Wolfsburg 1
GERMANY

George H. Siegel
Point North Associates, Inc.
P.O. Box 907
Madison NJ 07940

Richard Silberglitt
FM Technologies, Inc.
10529-B Braddock Road
Fairfax VA 22032

Mary Silverberg
Norton Company
SGNICC/NRDC
Goddard Road
Northboro MA 01532-1545

Gurpreet Singh
Department of the Navy
Code 56X31
Washington DC 20362-5101

Maurice J. Sinnott
University of Michigan
5106 IST Building
Ann Arbor MI 48109-2099

John Skildum
3M Company
3M Center
Building 224-2S-25
St. Paul MN 55144

Richard H. Smoak
Smoak & Associates
3554 Hollystone Road
Altadena CA 91001-3923

Jay R. Smyth
AlliedSignal Engines
111 S. 34th Street, MS:503-412
Phoenix AZ 85034

Rafal A. Sobotowski
British Petroleum Company

Technical Center, Broadway
3092 Broadway Avenue
Cleveland OH 44115

S. Somiya
Nishi Tokyo University
3-7-19 Seijo, Setagaya
Tokyo 157
JAPAN

Boyd W. Sorenson
DuPont Lanxide Composites
1300 Marrows Road
Newark DE 19711

Charles A. Sorrell
U.S. Department of Energy
Advanced Industrial Concepts
CE-232, Forrestal Building
Washington DC 20585

C. Spencer
EA Technology
Capenhurst Chester CH1 6ES
UNITED KINGDOM

Allen Spizzo
Hercules Inc.
Hercules Plaza
Wilmington DE 19894

Richard M. Spriggs
Alfred University
Center for Advanced Ceramic
Technology
Alfred NY 14802

Charles Spuckler
NASA Lewis Research Center
21000 Brookpark Road, MS:5-11
Cleveland OH 44135-3191

G. V. Srinivasan
The Carborundum Company
P.O. Box 832, B-100
Niagara Falls, NY 14302

M. Srinivasan
Material Solutions
P.O. Box 663
Grand Island NY 14702-0663

Gordon L. Starr
Cummins Engine Company, Inc.
P.O. Box 3005, Mail Code:50182
Columbus IN 47202-3005

Tom Stillwagon
AlliedSignal, Inc.
Ceramic Components
P.O. Box 2960, MS:T21
Torrance CA 90509-2960

H. M. Stoller
TPL Inc.
3754 Hawkins, N.E.
Albuquerque NM 87109

Paul D. Stone
Dow Chemical USA
1776 "Eye" Street, N.W., #575
Washington DC 20006

R. S. Storm
The Carborundum Company
P.O. Box 832, B-100
Niagara Falls, NY 14302

F. W. Stringer
Aero & Industrial Technology Ltd.
P.O. Box 46, Wood Top
Burnley Lancashire BB11 4BX
UNITED KINGDOM

Thomas N. Strom
NASA Lewis Research Center
21000 Brookpark Road, MS:86-6
Cleveland OH 44135

M. F. Stroosnijder
Institute for Advanced Materials
Joint Research Centre
21020 Ispra (VA)
ITALY

Karsten Styhr
30604 Ganado Drive
Rancho Palos Verdes CA 90274

T. S. Sudarshan
Materials Modification, Inc.
2929-P1 Eskridge Center
Fairfax VA 22031

M. J. Sundaresan
University of Miami
P.O. Box 248294
Coral Gables FL 33124

Patrick L. Sutton
U.S. Department of Energy
Office of Propulsion Systems
CE-322, Forrestal Building
Washington DC 20585

Willard H. Sutton
United Technologies Corporation
Silver Lane, MS:24
East Hartford CT 06108

J. J. Swab
U.S. Army Materials Technology
Ceramics Research Division,
SLCMT-EMC
405 Arsenal Street
Watertown MA 02172

Robert E. Swanson
Metalworking Technology, Inc.
1450 Scalp Avenue
Johnstown PA 15904

Steve Szaruga
Air Force Wright Aeronautical Lab
WL/MLBC
Wright-Patterson AFB OH
45433-6533

Yo Tajima
NGK Spark Plug Company
2808 Iwasaki
Komaki-shi Aichi-ken 485
JAPAN

Fred Teeter
5 Tralee Terrace
East Amherst NY 14051

Monika O. Ten Eyck
Carborundum Microelectronics
P.O. Box 2467
Niagara Falls NY 14302-2467

David F. Thompson
 Corning Glass Works
 SP-DV-02-1
 Corning NY 14831
 Merle L. Thorpe
 Hobart Tafa Technologies, Inc.
 20 Ridge Road
 Concord NH 03301-3010

T. Y. Tien
 University of Michigan
 Materials Science and Engineering
 Dow Building
 Ann Arbor MI 48103

D. M. Tracey
 Norton Company
 SGNICC/NRDC
 Goddard Road
 Northboro MA 01532-1545

L. J. Trostel, Jr.
 Box 199
 Princeton MA 01541

W. T. Tucker
 General Electric Company
 P.O. Box 8, Bldg. K1-4C35
 Schenectady NY 12301

Masanori Ueki
 Nippon Steel Corporation
 1618 Ida
 Nakahara-Ku Kawasaki 211
 JAPAN

Filippo M. Ugolini
 ATA Studio
 Via Degli Scipioni, 268A
 ROMA, 00192
 ITALY

Donald L. Vaccari
 General Motors Corporation
 Allison Gas Turbines
 P.O. Box 420, Speed Code S49
 Indianapolis IN 46206-0420

Carl F. Van Conant
 Boride Products, Inc.
 2879 Aero Park Drive
 Traverse City MI 49684

Marcel H. Van De Voorde
 Commission of the European Comm.
 P.O. Box 2
 1755 ZG Petten
 THE NETHERLANDS

O. Van Der Biest
 Katholieke Universiteit Leuven
 Dept. Metaalkunde en Toegepaste
 de Croylaan 2
 B-3030 Leuven
 BELGIUM

Michael Vannier
 Washington University, St. Louis
 510 S. Kings Highway
 St. Louis MO 63110

Stan Venkatesan
 Southern Coke & Coal Corporation
 P.O. Box 52383
 Knoxville TN 37950

V. Venkateswaran
 Carborundum Company
 Niagara Falls R&D Center
 P.O. Box 832
 Niagara Falls NY 14302

Dennis Viechnicki
 U.S. Army Materials Technology
 405 Arsenal Street
 Watertown MA 02172-0001

Ted Vojnovich
 U.S. Department of Energy, ST-311
 Office of Energy Research, 3F077P
 Washington DC 20585

John D. Volt
 E.I. Dupont de Nemours & Co. Inc.
 P.O. Box 80262
 Wilmington DE 19880

John B. Wachtman
 Rutgers University
 P.O. Box 909
 Piscataway NJ 08855

Shigetaka Wada
Toyota Central Research Labs
Nagakute Aichi 480-11
JAPAN

Robert M. Washburn
ASMT
11203 Colima Road
Whittier CA 90604

Janet Wade
AlliedSignal Engines
P.O. Box 52180, MS:1303-2
Phoenix AZ 85072-2180

Gerald Q. Weaver
Carborundum Specialty Products
42 Linus Allain Avenue
Gardner MA 01440-2478

Richard L. Wagner
Ceramic Technologies, Inc.
537 Turtle Creek South Dr., #24D
Indianapolis IN 46227

Kevin Webber
Toyota Technical Center, U.S.A.
1410 Woodridge, RR7
Ann Arbor MI 48105

J. Bruce Wagner, Jr.
Arizona State University
Center for Solid State Science
Tempe AZ 85287-1704

Karen E. Weber
Detroit Diesel Corporation
13400 Outer Drive West
Detroit MI 48239-4001

Daniel J. Wahlen
Kohler, Co.
444 Highland Drive
Kohler WI 53044

James K. Weddell
Du Pont Lanxide Composites Inc.
P.O. Box 6100
Newark DE 19714-6100

Ingrid Wahlgren
Royal Institute of Technology
Studsvik Library
S-611 82 Nykoping
SWEDEN

R. W. Weeks
Argonne National Laboratory
MCT-212
9700 S. Cass Avenue
Argonne IL 60439

Ron H. Walecki
AlliedSignal, Inc.
Ceramic Components
P.O. Box 2960, MS:T21
Torrance CA 90509-2960

Ludwig Weiler
ASEA Brown Boveri AG
Eppelheimer Str. 82
D-6900 Heidelberg
GERMANY

Michael S. Walsh
Vapor Technologies Inc.
6300 Gunpark Drive
Boulder CO 80301

James Wessel
Dow Corning Corporation
1800 "M" Street, N.W., #325 South
Washington DC 20036

Chien-Min Wang
Industrial Technology Research
Institute
195 Chung-Hsing Road, Sec. 4
Chutung Hsinchu 31015 R.O.C.
TAIWAN

Robert D. West
Therm Advanced Ceramics
P.O. Box 220
Ithaca NY 14851

Thomas J. Whalen
 Ford Motor Company
 SRL Bldg., Mail Drop 2313
 P.O. Box 2053
 Dearborn MI 48121-2053

Ian A. White
 Hoeganaes Corporation
 River Road
 Riverton NJ 08077

Sheldon M. Wiederhorn
 NIST
 Building 223, Room A329
 Gaithersburg MD 20899

John F. Wight
 Alfred University
 McMahon Building
 Alfred NY 14802

D. S. Wilkinson
 McMaster University
 1280 Main Street, West
 Hamilton Ontario L8S 4L7
 CANADA

James C. Williams
 General Electric Company
 Engineering Materials Technology
 One Neumann Way, Mail Drop:H85
 Cincinnati OH 45215-6301

Steve J. Williams
 RCG Hagler Bailly, Inc.
 1530 Wilson Boulevard, Suite 900
 Arlington VA 22209-2406

Thomas A. Williams
 National Renewable Energy Lab
 1617 Cole Boulevard
 Golden CO 80401

Craig A. Willkens
 Norton Company
 SGNICC/NRDC
 Goddard Road
 Northboro MA 01532-1545

Roger R. Wills
 TRW, Inc.
 Valve Division
 1455 East 185th Street
 Cleveland OH 44110

David Gordon Wilson
 Massachusetts Institute of
 Technology
 77 Massachusetts Ave., Room 3-455
 Cambridge MA 02139

Matthew F. Winkler
 Seaworthy Systems, Inc.
 P.O. Box 965
 Essex CT 06426

Gerhard Winter
 Hermann C. Starck Berlin GmbH
 P.O. Box 25 40
 D-3380 Goslar 3380
 GERMANY

William T. Wintucky
 NASA Lewis Research Center
 Terrestrial Propulsion Office
 21000 Brookpark Road, MS:86-6
 Cleveland, OH 44135

Thomas J. Wissing
 Eaton Corporation
 Engineering and Research Center
 P.O. Box 766
 Southfield MI 48037

James C. Withers
 MER Corporation
 7960 S. Kolb Road
 Building F
 Tucson AZ 85706

Dale E. Wittmer
 Southern Illinois University
 Mechanical Engineering Department
 Carbondale IL 62901

Warren W. Wolf
 Owens Corning Fiberglass
 2790 Columbus Road, Route 16
 Granville OH 43023

Egon E. Wolff
Caterpillar Inc.
Technical Center
P.O. Box 1875
Peoria IL 61656-1875

George W. Wolter
Howmet Turbine Components Corp.
Technical Center
699 Benston Road
Whitehall MI 49461

James C. Wood
NASA Lewis Research Center
21000 Brookpark Road, MS:86-6
Cleveland OH 44135

Marrill Wood
LECO Corporation
P.O. Box 211688
Augusta GA 30917-1688

Wayne L. Worrell
University of Pennsylvania
3231 Walnut Street
Philadelphia PA 19104

John F. Wosinski
Corning Inc.
ME-2 E-5 H8
Corning NY 14830

Ian G. Wright
BCL
505 King Avenue
Columbus OH 43201

Ruth Wroe
ERDC
Capenhurst Chester CH1 6ES
ENGLAND

Bernard J. Wrona
Advanced Composite Materials Corp
1525 S. Buncombe Road
Greer SC 29651

Carl C. M. Wu
Naval Research Laboratory
Ceramic Branch, Code 6373
Washington DC 20375

John C. Wurst
U. of Dayton Research Institute
300 College Park
Dayton OH 45469-0101

Neil Wyant
ARCH Development Corp.
9700 S. Cass Avenue, Bldg. 202
Argonne IL 60439

Roy Yamamoto
Texaco Inc.
P.O. Box 509
Beacon NY 12508-0509

John Yamanis
AlliedSignal Aerospace Company
P.O. Box 1021
Morristown NJ 07962-1021

Harry C. Yeh
AlliedSignal, Inc.
Ceramic Components
P.O. Box 2960, MS:T21
Torrance CA 90509-2960

Hiroshi Yokoyama
Hitachi Research Lab
4026 Kuji-Cho
Hitachi-shi Ibaraki 319-12
JAPAN

Thomas M. Yonushonis
Cummins Engine Company, Inc.
P.O. Box 3005, Mail Code 50183
Columbus IN 47202-3005

Thomas J. Yost
Corning Inc.
Technical Products Div., 21-1-2
Corning NY 14831

Jong Yung
Sundstrand Aviation Operations
4747 Harrison Avenue
Rockford IL 61125

A. L. Zadoks
Caterpillar Inc.
Technical Center, Building L
P.O. Box 1875
Peoria IL 61656-1875

Avi Zangvil
University of Illinois
104 S. Goodwin Avenue
Urbana IL 61801

Charles H. Zenuk
Transtech
6662 E. Paseo San Andres
Tucson AZ 85710-2106

Carl Zweben
General Electric Company
P.O. Box 8555, VFSC/V4019
Philadelphia PA 19101

Department of Energy
Oak Ridge Operations Office
Assistant Manager for Energy
Research and Development
P.O. Box 2001
Oak Ridge, TN 37831-8600

Department of Energy (2)
Office of Scientific and
Technical
Information
Office of Information Services
P.O. Box 62
Oak Ridge, TN 37831

For distribution by microfiche
as shown in DOE/OSTI-4500,
Distribution Category UC-332
(Ceramics/Advanced Materials).